



**UNIVERSITÀ DEGLI STUDI DI PARMA**

Department of Pharmacy

PhD course in "Drugs, Biomolecules and Health Products"

XXIX Cycle

**Toward Innovative Therapeutics for the Eradication of  
Mycobacterial Infections**

Coordinator: Prof. Marco Mor

Supervisor: Prof. Gabriele Costantino

PhD student: Elisa Azzali



*“Da chimico un giorno avevo il potere  
di sposare gli elementi e di farli reagire,  
ma gli uomini mai mi riuscì di capire  
perché si combinassero attraverso l'amore.  
Affidando ad un gioco la gioia e il dolore.*

*Ma guardate l'idrogeno tacere nel mare  
guardate l'ossigeno al suo fianco dormire:  
soltanto una legge che io riesco a capire  
ha potuto sposarli senza farli scoppiare.  
Soltanto la legge che io riesco a capire.”*

Fabrizio De Andrè



## List of abbreviations

AMK	Amikacin
CFZ	Clofazimine
CM	Capreomycin
CPZ	Chlorpromazine
DCE	Dichloroethane
DCS	Cycloserine
DMF	Dimethylformamide
DMSO	Dimethyl sulfoxide
DOTS	Direct Observed Treatment Short-course
EMB	Ethambutol
EtBr	Ethidium bromide
EP	Efflux pump
EPI	Efflux pump inhibitor
ETO	Ethionamide
FDA	Food and Drug Administration
FIC	Fractional inhibitory concentration
GFX	Gatifloxacin
HIV	Human immunodeficiency virus
HPLC	High performance liquid chromatography
Hz	Hertz
IC <sub>50</sub>	Inhibitory concentration 50
INH	Isoniazid
<i>J</i>	Coupling constant
KM	Kanamycin
LFX	Levofloxacin

MABA	Microplate Alamar Blue Assay
MDR-TB	Multi drug-resistant tuberculosis
MHz	Mega hertz
MIC	Minimum inhibitory concentration
MXF	Moxifloxacin
Mtb	<i>Mycobacterium tuberculosis</i>
MTBC	Mycobacterium tuberculosis complex
NBS	N-bromosuccinimide
NCS	N-chlorosuccinimide
NMI	N-methylimidazole
NMP	N-methyl-2-pyrrolidone
OFX	Ofloxacin
μW	Microwave
PAS	p-aminosalicylic acid
Ppm	Parts per million
PTO	Prothionamide
PZA	Pyrazinamide
RFF	Relative final fluorescence
RIF	Rifampicin
SAR	Structure-activity relationship
SI	Selectivity index
STM	Streptomycin
TB	Tuberculosis
TDR-TB	Totally drug-resistant tuberculosis
TDZ	Thioridazine
TEA	Triethylamine

THF	Tetrahydrofuran
TLC	Thin layer chromatography
WHO	World health organization
XDR-TB	Extensively drug-resistant tuberculosis
VER	Verapamil





## List of publications

1. Pieroni, M.; Annunziato, G.; **Azzali, E.**; Dessanti, P.; Mercurio, C.; Meroni, G.; Trifirò, P.; Vianello, P.; Villa, M.; Beato, C.; Varasi, M.; Costantino, G.; Further insights into the SAR of  $\alpha$ -substituted cyclopropylamine derivative as inhibitors of histone demethylase KDM1A; *European Journal of Medicinal Chemistry*; **2015**; 377-386.
2. Pieroni, M.; Machado, D.; **Azzali, E.**; Santos Costa, S.; Couto, I.; Costantino, G.; Viveiros, M.; Rational Design and Synthesis of Thioridazine Analogues as Enhancers of the Antituberculosis Therapy; *Journal of Medicinal Chemistry*; **2015**; 5842-5853.
3. Vucicevic, J.; Srdic-Rajic, T.; Pieroni, M.; Laurila, J.M.M.; Perovic, V.; Tassini, S.; **Azzali, E.**; Costantino, G.; Glisic, S.; Agbaba, D.; Scheinin, M.; Nikolic, K.; Radi, M.; Veljkovic, N.; A combined ligand- and structure-based approach for the identification of rilmenidine-derived compounds which synergize the antitumor effects of doxorubicin; *Bioorganic & Medicinal Chemistry*; **2016**; 24; 3174-3183.
4. Santos Costa, S.; Lopes, E.; **Azzali, E.**; Machado, D.; Coelho, T.; Eduardo Almeida da Silva, E.; Viveiros, M.; Pieroni, M.; Couto, I.; An Experimental Model for the Rapid Screening of Compounds with Potential Use Against Mycobacteria; *Assay and Drug Development Technologies*; **2016**; 14; 524-534.
5. Pieroni, M.; **Azzali, E.**; Basilico, N.; Parapini, S.; Zolkiewski, M; Beato, C.; Annunziato, G.; Bruno, A.; Vacondio, F.; Costantino, G.; Accepting the Invitation to Open Innovation in Malaria Drug Discovery: Synthesis, Biological Evaluation and Investigation on the Structure–Activity Relationships of Benzo[*b*]thiophene-2-carboxamides as Antimalarial Agents; *Journal of Medicinal Chemistry*; Just Accepted Manuscript.



## Summary

<b>1. Introduction</b>	<b>15</b>
<b>1.1 Tuberculosis</b>	<b>15</b>
<b>1.2 Epidemiology</b>	<b>16</b>
<b>1.3 Pathogenesis</b>	<b>19</b>
<b>1.4 Current drug therapy</b>	<b>22</b>
<b>1.5 Classification of anti-TB drugs</b>	<b>24</b>
1.5.1 First-line anti-TB drugs	24
1.5.2 Second-line anti-TB drugs	28
<b>1.6 Current anti-TB pipeline</b>	<b>31</b>
1.6.1 Clinical candidates: an overview	32
1.6.2 Preclinical candidates: an overview	35
<b>1.7 Resistance in Mtb</b>	<b>42</b>
<b>1.8 Outline of the project</b>	<b>47</b>
<b>2. Development of new chemical entities that inhibit the growth of Mtb, active also against resistant strains</b>	<b>49</b>
<b>2.1 Introduction</b>	<b>49</b>
<b>2.2 Evolution of a series of 2-aminothiazoles</b>	<b>54</b>
2.2.1 Rational design, results and discussion	54
2.2.2 Chemistry	65
2.2.3 Conclusion	69
<b>2.3 Novel and efficient synthesis of 2-aminooxazoles</b>	<b>70</b>
2.3.1 Rationale	70
2.3.2 Synthetic strategy	73
2.3.3 Antitubercular activity	83

2.3.4 Conclusion	84
<b>3. Development of efflux pump inhibitors that will increase the concentration of antibacterial agents into the Mtb</b>	<b>85</b>
<b>3.1 Introduction</b>	<b>85</b>
3.1.1 Efflux pumps inhibitors (EPIs)	86
<b>3.2 Rational design and synthesis of Thioridazine analogues as enhancers of the antituberculosis therapy</b>	<b>90</b>
3.2.1 Rational design	90
3.2.2 Chemistry	93
3.2.3 Results and discussion	95
3.2.4 Structure-Activity Relationships (SAR)	108
3.2.5 Conclusion	109
<b>3.3 Development of new chemotypes as inhibitors of efflux</b>	<b>111</b>
<b>4. Microwave-assisted synthesis of nucleotide phosphoroamidates</b>	<b>114</b>
<b>4.1 Introduction</b>	<b>114</b>
<b>4.2 ProTide Approach</b>	<b>116</b>
<b>4.3 ProTide preparation</b>	<b>119</b>
<b>4.4 Aim of the work</b>	<b>121</b>
<b>4.5 Results</b>	<b>122</b>
<b>4.6 Conclusion</b>	<b>129</b>
<b>5. Experimental section</b>	<b>130</b>
<b>5.1 Chemistry</b>	<b>130</b>
5.1.1 Evolution of a series of 2-aminothiazoles	131
5.1.2 Novel and efficient synthesis of 2-aminooxazoles	151

5.1.3 Rational design and synthesis of Thioridazine analogues as enhancers of the antituberculosis therapy	163
5.1.4 Microwave-assisted synthesis of nucleotide phosphoramidates	171
<b>5.2 Biology</b>	<b>173</b>
5.2.1 Evolution of a series of 2-aminothiazoles	173
5.2.2 Novel and efficient synthesis of 2-aminooxazoles	176
5.2.3 Rational design and synthesis of Thioridazine analogues as enhancers of the antituberculosis therapy	178
<b>6. Acknowledgements</b>	<b>186</b>
<b>7. References</b>	<b>187</b>



# 1. Introduction

## 1.1 Tuberculosis

Tuberculosis (TB) is a highly contagious airborne disease and, according to a number of epidemiological data, it is the second cause of death in the world from an infectious disease after human immunodeficiency virus (HIV). It is mostly caused by *M. Tuberculosis* (Mtb), an obligate<sup>1</sup> pathogenic bacterial species of the family *Mycobacteriaceae*, belonging to the genus *Mycobacterium*<sup>2</sup>, described by Robert Koch in 1882.

The term Mycobacteria<sup>3</sup> has a Greek fount (“myco” means “fungus”) and it has been referred to the peculiar way these microorganisms grow in a mold-like manner on the surface of cultures, as fungi do.

They can be classified into several major groups according to their treatment and diagnosis; along with the above-mentioned Mtb, also *M. bovis*, *M. africanum*, *M. bovis*, *M. caprae*, *M. canetti* and *M. microti* belong to the Mycobacterium tuberculosis complex (MTBC), and may cause TB infections in humans and animals.

Mtb, like all Mycobacteria, has a coating mostly constituted by mycolic acids, which makes the cell surface particularly waxy and therefore resistant to Gram staining, disinfectants and various antibiotics. As such, this protective envelope represents a mechanism of intrinsic resistance, that makes Mtb particularly harsh to treat and may predisposes the emergence of resistance.<sup>4</sup>

TB generally affects the lungs, but it can also affect other organs throughout the body. Differently from other bacteria, TB infection might be active or latent. In general, symptoms of active TB are represented by a chronic cough with blood-containing sputum, fever, night sweats and weight loss. In

addition, when the infection is active, the patient is highly contagious and can infect other people by coughing, spitting, speaking, or sneezing. On the other hand, latent TB does not present any evident symptom, and cannot be transmitted to other people. However, latent infections might reactivate and become active after particular events that may compromise the immune system.<sup>5</sup>



**Figure 1:** Mtb culture revealing the organism foam-like growth.

## **1.2 Epidemiology**

TB causes ill-health among millions of people each year and ranks alongside the HIV as a leading cause of death worldwide. In 2015, there were an estimated 10.4 millions new TB cases: 5.9 were men, 3.5 women and 1.0 children. Also, it has been estimated that over two billions of the world population has been latently infected with TB.

The distribution of TB is not uniform across the globe, as in 2015 most of the cases occurred in Asia (61%) and in the African Regions (26%); smaller



figures are recorded in the Eastern Mediterranean Region (7%), the European Region (3%) and in America (3%).<sup>6</sup>

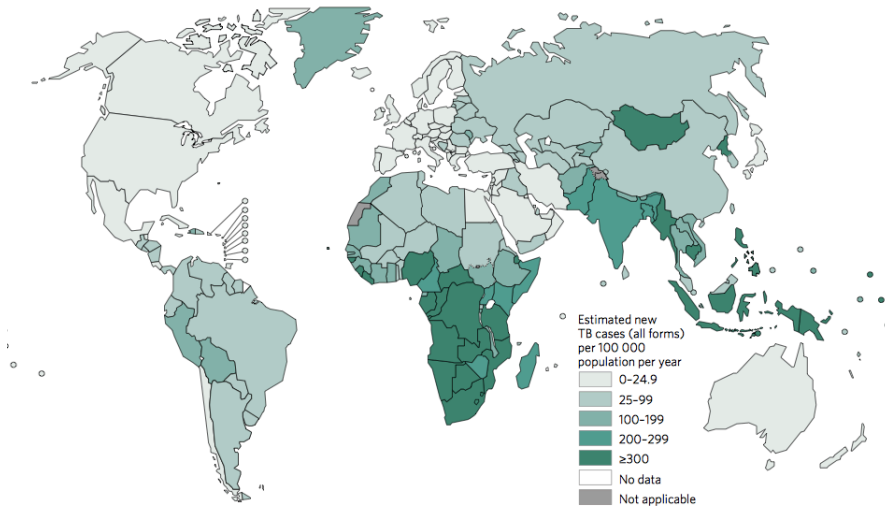


**Figure 2:** Estimated TB incidence rates in 2015.

In 2015, the six countries with highest number of cases were India, Indonesia, China, Nigeria, Pakistan and South Africa. It is worthwhile to notice that three of the above mentioned countries belong to the so called BRICS (Brazil, Russia, India, China, South Africa): since these countries are the most involved in the flow of goods and people with the EU, it is quite obvious that TB has also a deep and not underestimate socio-economic impact.

Of the 10.4 millions new TB cases in 2015, 1.2 million (12%) occurred in HIV patients, with a considerably higher rate in the African Region, where TB-HIV co-morbidity was reported in more than 50% of cases.<sup>7</sup>

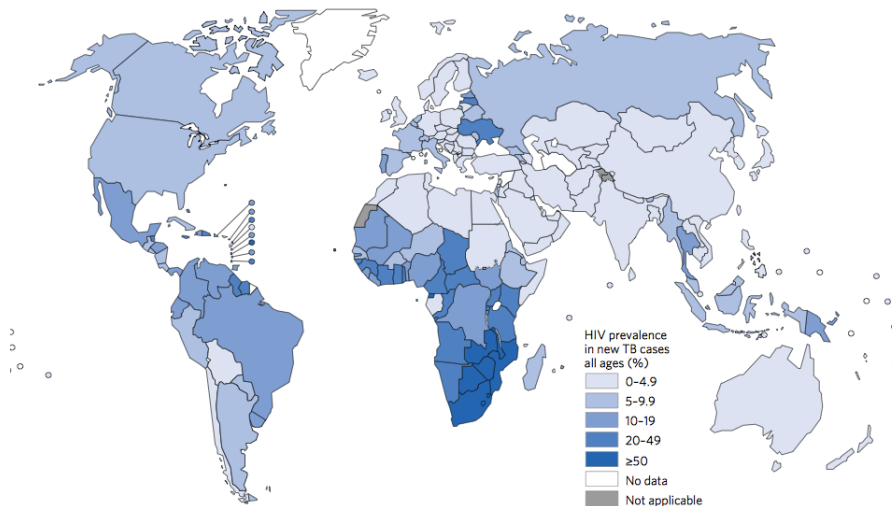


**Figure 3:** Estimated HIV prevalence in new and relapse TB cases in 2015.

The co-infection with HIV is not the only worrying feature related to TB infection. Indeed, it is a widely accepted belief that resistant strains represent the most challenging menace nowadays for the treatment of TB. Resistant TB can be divided into three main categories: multi drug-resistant TB (**MDR-TB**), extensively drug-resistant TB (**XDR-TB**) and totally drug-resistant TB (**TDR-TB**).

By definition, **MDR-TB** is referred to a strain that is resistant to at least two of the first-line drugs, *i.e.* isoniazid (INH) and rifampicin (RIF). While rates of MDR-TB infections are relatively low in North America and Western Europe, they are steadily increasing worldwide, particularly in Asia. According to recent reports, in 2015, 480000 people worldwide developed MDR-TB. Moreover, MDR-TB infection may be divided into primary or acquired. Primary infection occurs when patients are exposed to MDR-TB strains, contracting the disease; on the other hand, acquired infection occurs when

TB patients are treated with a drug regimen that eventually is not effective at eradicating the infection, leading to the selection of multi-drug resistant strains.<sup>6</sup>

**XDR-TB** shows a similar behaviour as the MDR-TB, but it additionally fails to respond to any fluoroquinolone and at least one of three injectable second line drugs (*i.e.* amikacin, capreomycin or kanamycin).

Lately, the isolation of a pan-resistant Mtb strain (**TDR-TB**) threatens the rise of a virtually incurable pathogen. Indeed, these strains cannot be cured by any of the currently used anti-TB chemotherapeutics. However, due to issues in the biological characterization of these strains, such as reliability and reproducibility of testing, this kind of infection is not yet recognised by the World Health Organization.<sup>6</sup>

These resistant phenotypes are spreading at a fast rate, are more difficult to eradicate than the susceptible ones and need more toxic and poorly tolerated drugs for their treatment.<sup>8,9</sup>

### **1.3 Pathogenesis**

TB is a multicomponent disease that primarily affects the lungs in discrete consolidated foci known as granulomas. As mentioned before, TB patients can have “active” or “latent” disease: from a merely diagnostic viewpoint, the active form is characterized by the microscopic observation of viable bacteria in the sputum, whereas the latent one is recognized by a delayed-type hypersensitivity reaction when the patient is subcutaneously challenged with purified protein derivative (PPD).

Infection with Mtb follows a well-defined sequence of events. The infectious bacilli are inhaled as droplets from the air.

Once in the lung, Mtb is phagocytised by alveolar macrophages (AV) and this event induces a proinflammatory response that leads to recruitment of mononuclear cells from the blood vessel.

These cells are the building block of the granuloma, or tubercle, that defines the pathology. The granuloma has an internal core of infected macrophages, surrounded by foamy giant cells (giant and multinucleate macrophages loaded with lipid) and other macrophages with a mantle of lymphocyte, a type of leukocyte with specific functions in specific immunity. The main role of granuloma is to contain the infectious particles, and indeed during this phase there are not any symptoms of the disease, neither patients are contagious.<sup>10</sup> Radiographically, this infection stage is usually characterized by the presence of an apparently healed granulomatous structure in the mid-region of the lung and the draining hilar lymphnode.

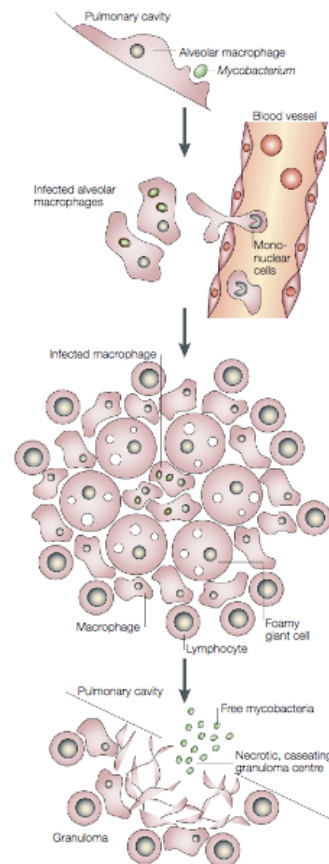


**Figure 4:** The pathogenesis of TB.<sup>9</sup>

This primary infection site is the base from which bacteria diffuse to the bloodstream through the draining lymphatic system, where reinfection of the apical regions of the lungs occurs and secondary lesions are formed.<sup>11</sup> In these lesions, dormant bacilli are thought to reside, and their replication

and dissemination is controlled by the host immune system, that prevent the risk of TB reactivation.<sup>11</sup>

However, due to immunosuppression (as in the case of HIV infected patients or after administration of immunosuppressive drugs), the containments fail and approximately 5% of latently infected individuals will subsequently develop active TB.<sup>11</sup> The centre of the granuloma undergoes caseation, a form of necrosis in which tissue is changed into a dry and amorphous mass resembling cheese. Finally, infectious bacilli are released into the airways and this stimulates the production of cough, that accelerates aerosol spread of infectious bacilli and the diffusion of the disease.<sup>12</sup>

Since the multifaceted aspects of TB infection, a specific combined drug therapy is nowadays recognized as the gold standard for the treatment. Also, the treatment must be prolonged up to a maximum of seven months, multidrug therapy in TB patients leads to a relatively rapid sterilization of bacteria in the sputum; typically, after eight weeks, viable bacteria are not anymore present in the sputum. However, several events (such as discontinuation of treatment before its completion and/or overexpression of efflux pumps) are strongly associated with relapse to active disease. For what concern the prolongation of therapy, it has been reported that 16 weeks are usually needed to eradicate the bacteria from other types of lesions, like those located in the necrotic or caseous regions that are remote from the cavity surface and where the availability of oxygen, nutrients and drugs is likely to be most restricted.

During granuloma development, oxygen depletion represent the main event leading to a change in the metabolic state of the bacteria and

therefore to a state of dormancy. Indeed, an *in vitro* model for the metabolic alterations that are associated with oxygen depletion has shown that replication is dependent on the presence of oxygen.<sup>13, 14</sup>

#### **1.4 Current drug therapy**

The current anti-TB chemotherapy, an unusual long-term treatment with a combination of drugs, is administered as Direct Observed Treatment, Short-course (DOTS).<sup>15</sup>

The DOTS is the major point in the WHO Global Plan to Stop TB and it can be divided in two phases:

- 1) Intensive Phase
- 2) Continuation Phase

In the intensive phase patients are treated, generally for a period of two months, with a combination of rifampicin (RIF), isoniazid (INH), pyrazinamide (PZA), and ethambutol (EMB).<sup>16</sup> This treatment is studied to kill all of the actively replicating bacteria, so as to contain the infection and the spread of the disease.

In the second phase, usually from a minimum of four up to seven months, a combination of RIF and INH is used to treat the patients. As above-mentioned, in this phase bacilli are in slow-growing persistent form, and this is the reason why the treatment must be prolonged for such a long time, somehow impairing the compliance of the patients.

Ideally, according to this short-course strategy, the actively replicating strains are killed in the initial phase whereas the dormant bacilli in the second one.<sup>17</sup>

The above-mentioned drugs represent the current standard of basic TB treatment and, as such, INH, RIF, EMB, and PZA are considered first-line

anti-TB drugs. With the exception of the US, also streptomycin (STM) is considered a first-line drug, especially in those countries where the cost of the treatment must be contained. The correct use of these molecules, administered under the DOTS protocol, is useful in the treatment of susceptible TB. However, this ideal situation seldom occurs, and most of the times the standard therapy must be emended depending on the needs.

This long protocol (usually between six-nine months) may show several and severe side effects, leading to unsatisfactory patient compliance. This makes extremely difficult the proper administration of the therapy, and, on turn, this leads to the raise of drug-resistant forms, that WHO has recently declared a global threat. Treatment of resistant forms requires a set molecules that are different from the first-line therapeutics, and that belong to the so called second-line anti-TB drugs: they are normally less efficacious than the first-line drugs on non-resistant strains, more toxic or anyway less tolerated, expensive and requires a longer period of therapy compared to the first-line anti-TB drugs.<sup>16</sup> Moreover, since the unique characteristics of each resistant strain, sometimes also second-line drugs fail in eradicating the infections, leading to further selection of resistant mutants.

As such, many efforts have been devoted to the search of novel therapeutic approach, that can be made either shortening the length of the therapy or using innovative drugs or drug delivery strategies with the aim of enhancing the patient compliance and, consequently, reduce the emergence of resistant strains.<sup>18</sup>

## 1.5 Classification of anti-TB drugs

As above-mentioned, anti-TB drugs can be subdivided in two classes:<sup>8</sup>

- **First-line anti-TB drugs:** INH, RIF, PZA, EMB and STM.
- **Second-line anti-TB drugs:** aminoglycosides (amikacin (AMK) and kanamycin (KM)), polypeptides (capreomycin (CM) and viomycin), fluoroquinolones (moxifloxacin (MXF), levofloxacin (LFX) and ofloxacin (OFX)), thioamides (ethionamide (ETO), prothionamide (PTO)), cycloserine (DCS) and p-aminosalicylic acid (PAS).

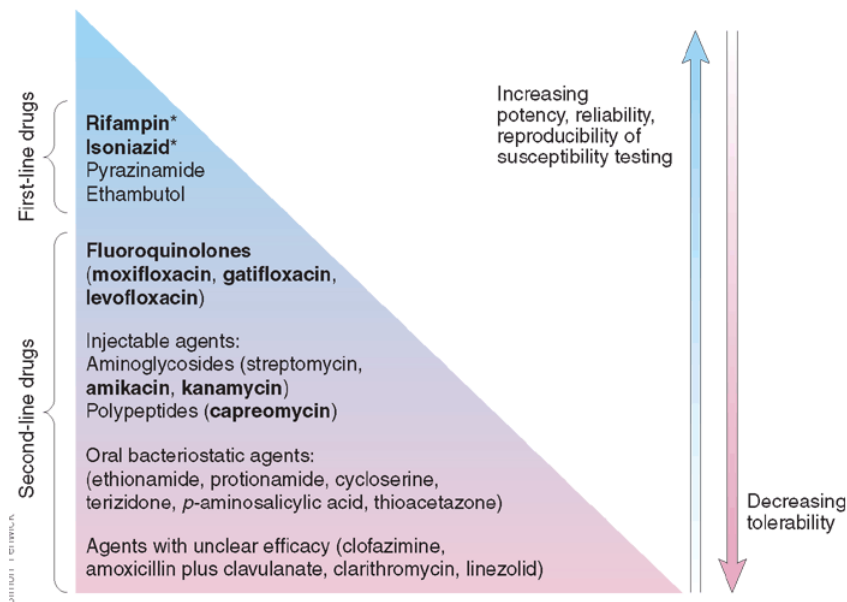


**Figure 5:** Classification of anti-TB drugs.<sup>19</sup>

### 1.5.1 First-line anti-TB drugs

- **INH**, also called isonicotinylnhydrazide, is one of the most effective and specific anti-TB drugs, which has been a key to treatment since its introduction in 1952.<sup>20</sup> It has a dual role against Mtb: it is a bactericidal agent toward rapidly-dividing Mtb, but it is bacteriostatic if the



mycobacteria are slow-growing. It is a pro-drug activated by a peroxidase enzyme called KatG. Once activated, it inactivate the NADH-dependent enoyl-acyl carrier protein reductase, preventing the synthesis of mycolic acids, that are essential component in the cell wall.<sup>21</sup> The introduction of INH is considered a milestone in the treatment of TB on a global scale, as it is available worldwide, inexpensive, and generally well tolerated.

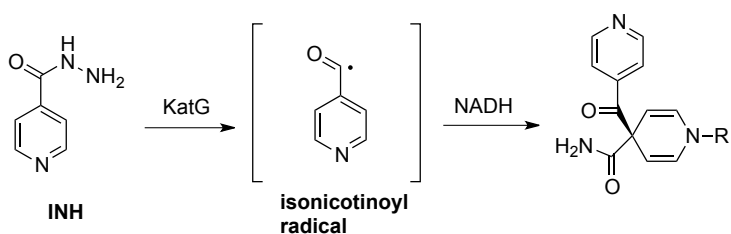


**Figure 6:** Mechanism of activation and action of INH.<sup>21</sup>

- **RIF**, also known as rifampin in US, is an antibiotic used for different kind of infections.<sup>22</sup> It was introduced in 1972 as an anti-TB drug and has excellent sterilizing activity.<sup>23</sup>

The group of rifamycins, and RIF in particular, were discovered in 1959 in the Lepetit laboratories in Milan. The bacteria present in the soil were analysed by the team of Italian researchers led by Hermes Pagani, Piero Sensi and Maria Teresa Timbal. The researchers of the Lepetit used to call each soil sample collected with the name of a movie, in this case Rififi.

It acts by binding to the  $\beta$ -subunit of RNA polymerase<sup>24</sup>, the enzyme responsible for transcription and expression of mycobacterial genes, resulting in inhibition of the bacterial transcription activity and thereby

killing the organism. Like INH, RIF is active against actively growing and slowly metabolizing bacilli.

- **PZA** has remarkable sterilising activity, and when added to regimens containing RMP, it is responsible for the killing of persisting bacilli during the initial intensive phase of chemotherapy, allowing treatment to be shortened from 9 months to 6 months. The notable point is that the activity of PZA was discovered because its chemical synthesis was followed immediately by *vivo* efficacy testing in mice, without the practice of screening *in vitro*. The next equally remarkable aspect of the development of PZA was that, without further investigation, it was immediately tested in the treatment of TB infected patients and found to be effective. Despite its *in vivo* activity, PZA is not active against Mtb under usual culture conditions at close to neutral pH,<sup>25</sup> whereas it inhibits those bacilli living in acidic environments (pH 5-6), that is the pH usually recorded in the highly pro-inflammatory environment at the TB infection site. From the structural point of view, it is an analogue of nicotinamide and is a pro-drug that needs to be converted into its active form, pyrazinoic acid, by the enzyme pyrazinamidase/nicotinamidase.<sup>25</sup> Pyrazinoic acid was thought to inhibit the enzyme fatty acid synthase (FAS), which is required by Mtb to synthesise fatty acids.<sup>26</sup> According to another hypothesis, it was also suggested that the accumulation of pyrazinoic acid disrupts membrane potential and interferes with the production of energy.<sup>27</sup> However, the actual mechanism(s) of action has not been completely elucidated.

- **EMB** is a bacteriostatic agent that targets the cell wall synthesis in a similar fashion as INH, but with a different mechanism of action. EMB interferes with an essential mechanism for the cell wall production, the biosynthesis of arabinogalactan by targeting arabinosyl transferase. Disruption of the arabinogalactan synthesis inhibits the formation of this complex and leads to increased permeability of the cell wall. However, It caused different severe adverse reaction such as hepatotoxicity, problem with vision, allergies.<sup>28</sup>

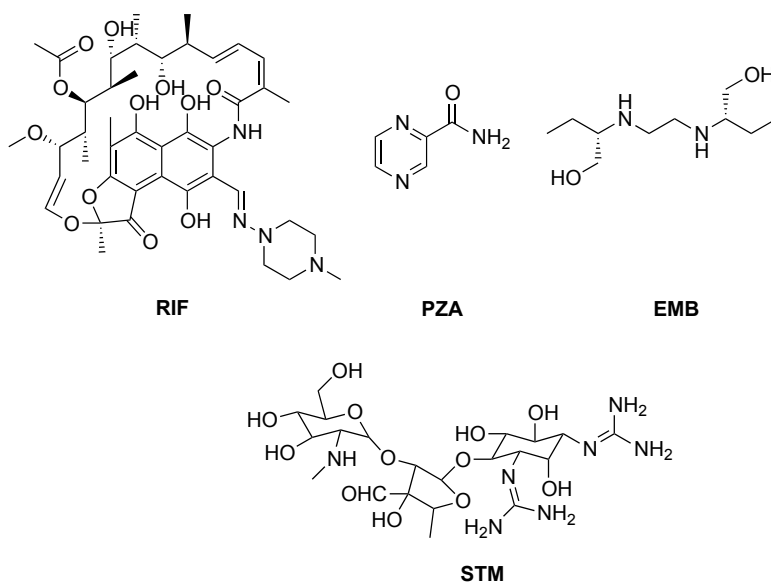


**Figure 7:** First-line drugs.

- **STM** was the first aminoglycoside developed. It is a natural compound derived from the actinobacterium *Streptomyces griseus* and has bactericidal activity.<sup>29</sup> It is used for the treatment of several diseases like infective endocarditis, plague and TB. For the TB treatment, it is not considered a first-line drug, because it lead several adverse effects,

except in medically under-served populations where the cost of more expensive treatments is prohibitive.<sup>30</sup>

It acts by inhibiting the protein synthesis. It binds to the small 16S rRNA of the 30S subunit of the bacterial ribosome, interfering with the binding of formyl-methionyl-tRNA to the 30S subunit.<sup>31</sup> This leads to codon misreading, eventual inhibition of protein synthesis and ultimately death of microbial cells through mechanisms that are still not understood. Speculation on this mechanism indicates that the binding of the molecule to the 30S subunit interferes with 50S subunit association with the m-RNA strand. This results in an unstable ribosomal-mRNA complex, leading to a mutations and defective protein synthesis; leading to cell death. Humans have ribosomes which are structurally different from those in bacteria, so the drug does not have this effect in human cells.

### **1.5.2 Second-line anti-TB drugs**

Among the anti-TB drugs, there are 3 reasons for which a drug may belong to the second line class:

- It may be less effective than the first line drugs in susceptible wild-type strains (p-aminosalicylic acid)
- It may have toxic side effects (cycloserine)
- It may be effective, but unavailable in many developing countries (fluoroquinolones)

Although several clinical studies have assessed the efficacy of these compounds, they are used only to treat infections that are resistant to the first-line therapy, for example **XDR-TB** or **MDR-TB**.<sup>32</sup>

According to WHO there are six classes of second line drugs that are used in the treatment of TB:<sup>33</sup>

- **Aminoglycosides** are molecules embodying an amino sugar moiety. They inhibit protein synthesis and are conventionally used to treat infections.<sup>34</sup> Aminoglycoside antibiotics display bactericidal activity against aerobes gram-negative and some anaerobic bacilli where resistance has not yet arisen, but generally their use is not recommended against Gram-positive and anaerobic Gram-negative bacteria.<sup>35</sup>
- **Polypeptides** are peptide, non-ribosomal secondary metabolites usually produced by microorganism like bacteria and fungi,<sup>36</sup> exhibiting anti-TB properties. *Viomycin* and *capreomycin*, belonging to the tuberactinomycins family, are essential components in the drug cocktail currently used to fight infections from resistant Mtb strains. *Viomycin* was the first member of the polypeptides class to be isolated and identified, and was used to treat TB until it was replaced by the less toxic, structurally related, *capreomycin*. The tuberactinomycins act on bacterial ribosomes, binding RNA and disrupting bacterial protein biosynthesis.<sup>37</sup>
- **Fluoroquinolones** are broad-spectrum antibiotics with a significant role in the treatment of many bacterial infections, amongst which TB. Fluoroquinolones have *in vitro* activity against Mtb and they have also been shown to penetrate into macrophages and kill intracellular

bacteria. In particular, the gatifloxacin and moxifloxacin showed to have lower minimum inhibitory concentrations (MICs) than second-generation fluoroquinolones. Moreover, they show bactericidal activity against RIF-tolerant persistent bacilli that survive despite chemotherapy,<sup>37</sup> for this reason fluoroquinolones are currently approved as second-line agents for the treatment of MDR-TB by the WHO.

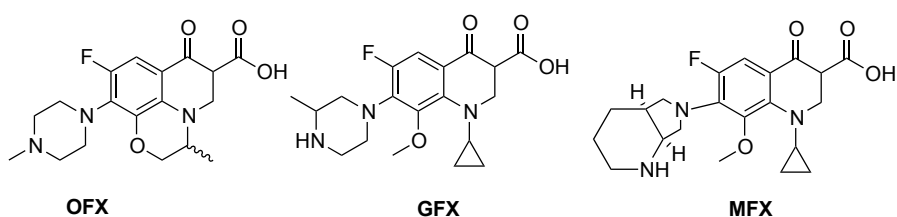


**Figure 8:** Fluoroquinolones.

- **Thioamides** (Ethionamide and Prothionamide). Thioamides drugs seem to inhibit mycolic acid biosynthesis, but their precise mechanism of action has not been completely elucidated yet. They are generally well tolerated, apart from gastric adverse effects and they are frequently source of cross-resistance with other drugs.<sup>8</sup>
- **Cycloserine** is a bacteriostatic agent that competitively blocks the enzymes incorporating alanine into the alanyl-alanine dipeptide, an essential component of the mycobacterial cell wall. The advantages of using cycloserine consist in its high gastric tolerance (compared with the other drugs in this group) and the absence of cross-resistance with other compounds. However, it also possesses adverse side effects such as the short shelf-life (24 months)<sup>8</sup> and the psychiatric adverse events (mainly psychotic reactions with suicidal

tendencies), that makes necessary a psychiatric evaluation before starting the treatment.

- **p-aminosalicylic acid** has a very low effectiveness, is poorly tolerated, and is expensive, which make it the last resort drug among the second-line group. Moreover it needs to be kept refrigerated (at 4°C), therefore requiring a cold chain, which is not always available in developing countries. However, despite its drawbacks, p-aminosalicylic acid has a main role for the treatment of MDR-TB and most patients with XDR-TB.<sup>8</sup>

PAS has been shown to be a pro-drug and it is incorporated into the folate pathway by dihydropteroate synthase (DHPS) and dihydrofolate synthase (DHFS) to generate a hydroxyl dihydrofolate antimetabolite, which in turn inhibits dihydrofolate reductase enzymatic activity.<sup>38</sup>

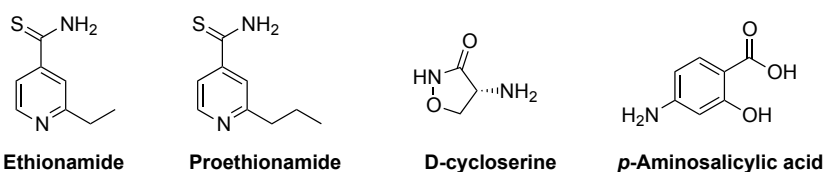


**Figure 9:** Second-line drugs.

## 1.6 Current anti-TB pipeline

Information compiled by [www.newtbdrugs.com](http://www.newtbdrugs.com) has shown an encouraging increase in the global TB drug pipeline. There are approximately 30 projects and 18 compounds in the pipeline, among which 10 compounds are in clinical development and 8 are in the preclinical stages. Moreover, since polipharmacology represent the standard of treatment for TB, there are also a number of drug combinations under evaluation.

# Global TB Drug Pipeline <sup>1</sup>

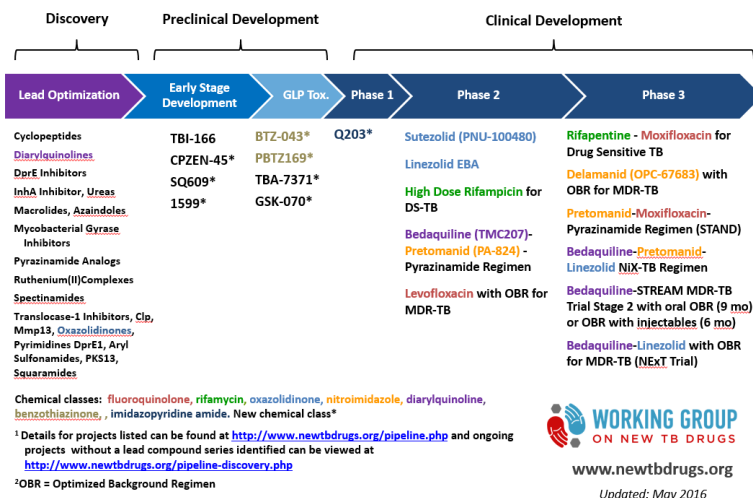


Figure 10: Global TB drug pipeline.

## 1.6.1 Clinical candidates: an overview

Several compounds, either alone or in combination, are spread through the various phases of clinical development:

- Q-203 (Phase I)
- Sutezolid, Linezolid, Bedaquiline in combination with Pretomanid, high-dose Rifampicin and LFX (Phase II)
- Delamanid, Moxifloxacin and Rifapentine (Phase III)

**Q-203** is a new chemical entity developed for TB treatment. It has an imidazopyridine core and it is the only one compound in phase I. Q-203 is active against Mtb strain H37Rv at a MIC<sub>50</sub> of 2.7 nM in culture broth medium and at a MIC<sub>50</sub> of 0.28 nM inside macrophages.<sup>39</sup> The metabolic stability of Q-203 in microsomes and cryopreserved hepatocytes from human, monkey, rat and dog origin is high, suggesting that Q-203 may



achieve good blood exposure in humans. All new anti-TB drugs are studied to be administered in combination with other medications so the absence of drug-drug interactions is a highly desirable property. Q203 does not inhibit any of the cytochrome P450 (CYP450) isoenzymes tested. In addition, it is not a substrate or an inhibitor for the P-glycoprotein, indicating that it has low potential for drug-drug interaction. Moreover, the pharmacokinetic profile of Q203 in mice is quite good; it has a bioavailability of 90% and a terminal half-life of 23.4 h. The volume of distribution was moderate (5.27 l per kg body weight), and the systemic clearance is low (4.03 ml min<sup>-1</sup> kg<sup>-1</sup>). The compound is also really effective in an acute mouse model of TB, in fact it promote a reduction in bacterial load of more than 90% at a dose of 10 mg per kg body weight, an effect comparable to that of bedaquiline or IHN. Furthermore in a mouse model of established TB, it showed, after 4 weeks of treatment, a reduction of 90%, 99% and 99.9% in Mtb H37Rv bacterial load in the groups treated with Q203 at 0.4, 2 and 10 mg per kg body weight, respectively.<sup>39</sup>

**Sutezolid** or **PNU-100480** is an oxazolidinone that was identified contemporaneously with Linezolid, a compound widely used for severe infections caused by Gram-positive, even resistant.<sup>40,41</sup> However, compared to Linezolid, Sutezolid has better antimycobacterial activity both *in vitro* and *in vivo*, has an improved safety profile and shows better time dependent killing in an *ex vivo* whole blood culture test.<sup>42</sup> In addition, it has activity against both drug-susceptible and drug-resistant TB.<sup>43</sup>

**Pretomanid** (formerly PA-824) and **Delamanid** or OPC-67683 belong to the class of nitroimidazoles. Pretomanid has many attractive characteristics, especially its novel mechanism of action, its activity *in vitro* against drug-resistant clinical isolates, and its potent bactericidal and sterilizing properties *in vivo*. In addition, the compound shows no evidence of mutagenicity, no significant cytochrome P450 interactions, and no significant activity against a broad range of Gram-positive and Gram-negative bacteria. It is currently in phase II and phase III in combination with other anti-TB drugs.<sup>44</sup> Delamanid was approved in 2014 in several countries, including Japan and EU, to be used as part of a specific combination regimen in patients with **MDR-TB**, when an effective treatment regimen cannot otherwise be composed due to resistance or tolerability. It is not associated with clinically relevant drug-drug interactions, including those with antiretroviral drugs. Moreover, it is generally well tolerated in patients, although the incidence of QT interval prolongation is higher with delamanid-based therapy but, fortunately, it is not associated with clinical symptoms such as syncope and arrhythmia.<sup>45</sup>

**Bedaquiline** (formerly TMC-207, marketed as Sirturo®), is an ATP synthase inhibitor discovered from a whole-cell high-throughput screening against *Mycobacterium smegmatis* (*M. smegmatis*). It resulted highly potent against drug-susceptible and drug-resistant strains of Mtb (MIC  $\leq 0.063$   $\mu\text{g/mL}$ ). After its approval by FDA on the 28<sup>th</sup> December 2012, it was the first new drug specifically developed for TB treatment in more than forty years. Bedaquiline should not be co-administered with other drugs that are strong inducers or inhibitors of CYP3A4, such as rifampin, as it results in a

52% decrease in the AUC of the drug. This reduces the exposure of the drug to the body and might generate resistant strains. Along with being marketed for the purpose of treating resistant infections, bedaquiline is also in phase II in combination with pretomanid and in phase III in combination with pretomanid and linezolid or only linezolid for the treatment of **MDR-TB**.<sup>46</sup>

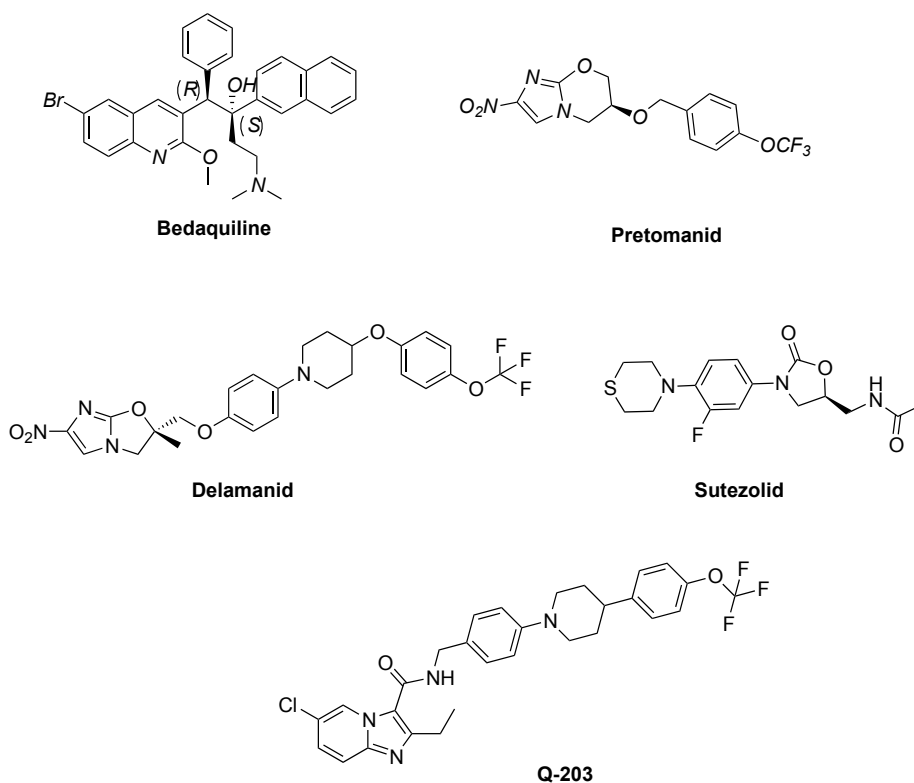


**Figure 11:** Clinical candidates.

### 1.6.2 Preclinical candidates: an overview

A promising anti-TB candidate is selected to advance into preclinical development to determine if the agent is likely to be safe and effective for use in human.<sup>47</sup>

At this stage, candidates must be tested for:<sup>47</sup>

- Animal model of efficacy
- GLP and non GLP animal pharmacology
- Safety
- Pharmacokinetics and pharmacodynamics
- Toxicity studies in two animal species
- Long term and short term exposition
- Process development chemistry
- Stability assays

**TBI-166** is a synthetic analogue of Clofazimine (CFM). CFM, an antimycobacterial agent introduced in 1962 for the treatment of leprosy, has demonstrated excellent activity against various drug-resistant Mtb strains and is currently used as a component of new regimens for the treatment of MDR-TB. Unfortunately there is a rapid development of drug resistance for CFM and it is highly lipophilic and it accumulates extensively in fat and skin tissues, leading to an extremely long half-life (over 70 days in humans) and undesirable side effects such as skin discoloration. The undesirable properties of CFM preclude its widespread use in the treatment of TB.<sup>48</sup>

A structure–activity study of more than 500 CFM analogues for anti-TB activity was conducted and TBI-166 emerged as one of the finest synthetic analogues of CFM. It demonstrated enhanced *in vitro* potency compared to CFM against actively replicating Mtb, it exhibited greater activity compared to CFM against intracellular Mtb and, in addition, it was active against non-replicating strains. TBI-166 is less lipophilic and has a shorter plasma half-life than CFM *in vivo*, suggesting its lesser tendency to accumulate. Most

importantly, the new compound demonstrated inhibition of bacterial growth in the lungs that is superior to the activity of an equivalent dose of CFM in efficacy testing *in vivo*. The efficacy of this compound, along with its decreased potential for accumulation and tissue discoloration, make TBI-166 a promising candidate for the treatment of TB.<sup>48</sup>

**CPZEN-45** Caprazene (CPZEN), a core structure of the caprazamycins, is known to be a good precursor of anti-TB antibiotics.<sup>49</sup> Structure–activity relationships studies on different CPZEN derivatives against Mtb showed excellent activity. CPZEN-45 is the most promising because of its activity against Mtb strains *in vitro* in fact its MIC is 1.56 µg/ml for Mtb (H37Rv) and 6.25 µg/ml for MDR-TB. It may be a good candidate for treatment of MDR-TB and XDR-TB since it has never been used in therapy but it shows a solubility of approximately 10 mg/ml in water and has a very low oral bioavailability as a result of poor absorption from the gastrointestinal (GI) tract. Despite its attractive features, development of an oral formulation for CPZEN-45 may not be possible. Parenteral formulation of this compound may be possible but the daily injections for TB treatment are unattractive and would decrease the compliance by patients.<sup>50</sup> Therefore, alternative drug delivery strategies should be studied for this new drug. Since the lungs are the primary sites of TB infection, formulation of CPZEN-45 as powder for inhalation can potentially enhance the efficacy of TB treatment with this new agent and this is the crucial point to overcome the preclinical phase.<sup>50</sup>

**SQ-609** An interesting class of new anti-TB compounds was identified by Sequella Incorporated, that has already licensed SQ-109. This class derived

from a screening of compounds library based on commercially available amino acids and containing a dipiperidine pharmacophore.<sup>51</sup> SQ-609 is the most promising compound of this class.<sup>52</sup> It has good *in vitro* activity against a broad range of clinical isolates of Mtb, including toward MDR strains, and it shows additive or synergistic activity with all of the first line TB drugs. In a mouse model of TB infection, SQ-609, prevented Mtb induced weight loss and, at the same time, improved survival if compared to mice treated with other anti-TB drugs (moxifloxacin or ethambutol).<sup>53</sup>

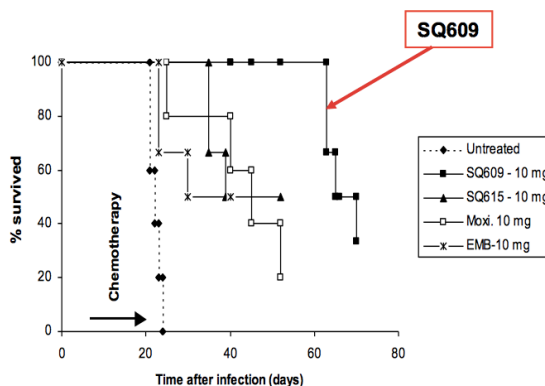


**Figure 12:** SQ-609 activity.

In addition, the compound has good aqueous solubility and is orally available. It has encouraging *in vitro* safety pharmacology and ADME profile, including: high metabolic stability in human liver microsomes, low inhibitory activity on cytochrome 450 enzymes, low potency of binding to the common of receptor and transporters and low activity on HERG channel.<sup>53</sup>

**Spectinamide 1599** is a spectinomycin derivative developed through a structure-based drug design approach. Spectinomycin has been used

previously as a second-line drug to treat gonorrhoeal infections. Although spectinomycin is chemically similar to aminoglycosides, it binds to a different site within the 16S bacterial ribosomal subunit and blocks ribosome translocation.<sup>54</sup> Unlike aminoglycosides, spectinomycin has a high safety margin, with only minimal side effects (injection site soreness, chills and nausea) and no nephrotoxicity or ototoxicity when administered for a short term at high therapeutic doses. Lee and co-workers developed a new anti-TB spectinamide series generated by chemical modification of spectinomycin. **1599** was the lead compound of this series, it demonstrated potent anti-TB activity *in vivo* in different TB infection mouse models and excellent anti-TB activity was observed in both acute and chronic TB models. Moreover, intrapulmonary administration of 1599 also provided excellent protection, reducing the bacterial load throughout the 4-week treatment period, suggesting sterilizing activity, whereas other drugs apparently did not show further killing beyond the first 2 weeks of treatment.<sup>54</sup>

*In vitro* studies demonstrated a lack of cross-resistance with existing anti-TB drugs and an excellent pharmacological profile. Moreover, it is active against MDR and XDR strains. Key to its potent anti-TB properties is the structural modification to evade the Rv1258c efflux pump, which is upregulated in MDR strains and is implicated in macrophage-induced drug tolerance. The anti-TB efficacy of spectinamides demonstrates that synthetic modifications to classical antibiotics can overcome the challenge of intrinsic efflux pump-mediated resistance.<sup>55</sup>

In conclusion this lead is an excellent preclinical drug candidate for TB with potent *in vivo* efficacy as well as a safe *in vitro* pharmacological profile.

**BTZ-043** and **PBTZ-169** A new class of anti-TB compounds having 3-benzothiazin-4-ones core (BTZs) has been recently disclosed.<sup>56</sup> Among all the derivatives, BTZ-043 is the most promising, as it proved to kill Mtb *in vitro*, *ex vivo*, and in a mouse models of TB infection. The MIC of BTZ043 was found to be 1 ng/mL against Mtb, which is considerably low compare to existing drugs such as INH and EMB. Moreover, the lead compound is active against all tested Mtb strains including clinical isolated from MDR and XDR patients. Its mechanism of action is highly selective for mycobacterial species and it is related with the inhibition of the Mtb cell wall synthesis by blocking the decaprenyl-phosphoribose-2'-epimerase (DprE1), necessary for the synthesis of D-Arabinofuranose, a component of arabinogalactan and arabinomannan.<sup>57</sup> More recently, additional SAR studies led to the development of PBTZs derivatives. PBTZ169 has several advantages compared to BTZ043, amongst which the more feasible chemical synthesis, the cost of goods and the better pharmacodynamics.<sup>58</sup> It also shows additive effects with many TB therapeutic agents, both marketed and in development, and has synergic effects with bedaquiline in preclinical models.<sup>58</sup>

**NITD-304** and **NITD-349** Indolcarboxamides are a valuable series of compounds having relatively low molecular weight and easily synthesized, disclosed for the first time by the group of Prof Kozikowski at the UIC<sup>59</sup> and developed simultaneously by Novartis. The 4,6-dichloro-N-(4,4-dimethylcyclohexyl)-1H-indole-2-carboxamide NITD-304 and the 4,6-difluoro analogue NITD-349 are promising compounds with high activity



against Mtb (15 and 23 nM respectively) and are superior to many existing TB drugs.<sup>60</sup> Indeed, these compounds are at least 10 times more potent than isoniazid (MIC<sub>50</sub>, 0.33 μM) and also PA-824 (MIC<sub>50</sub>, 0.4 μM)<sup>61</sup>, but are comparable to TMC-207 (MIC<sub>50</sub>, 50 nM).<sup>62</sup>

The lead candidates showed potent activity against both drug-sensitive and MDR clinical Mtb isolates, the MIC required to inhibit 99% growth of the diverse drug-resistant clinical isolates by NITD-304 and NITD-349 was in a similar range to that of wild-type Mtb H37Rv indicating a new mode of action for this series of compounds. Moreover, they were efficacious in mouse models of both acute and chronic infection and despite their low aqueous solubility and high lipophilicity, both compounds displayed favourable PK properties after oral administration in mouse, rat, and dog.

In addition, neither compound showed a risk for hERG-mediated cardiotoxicity and *in vitro* and *in vivo* safety assessment of both candidate compounds including two weeks of exploratory toxicology studies in rat demonstrated that the lead compounds are potential preclinical candidate.

Finally, both the molecules did not inhibit the major CYP450 isoenzyme 3A4 and also did not induce hPXR (human pregnane X receptor) activation, suggesting a low potential for drug- drug interactions.<sup>60</sup>

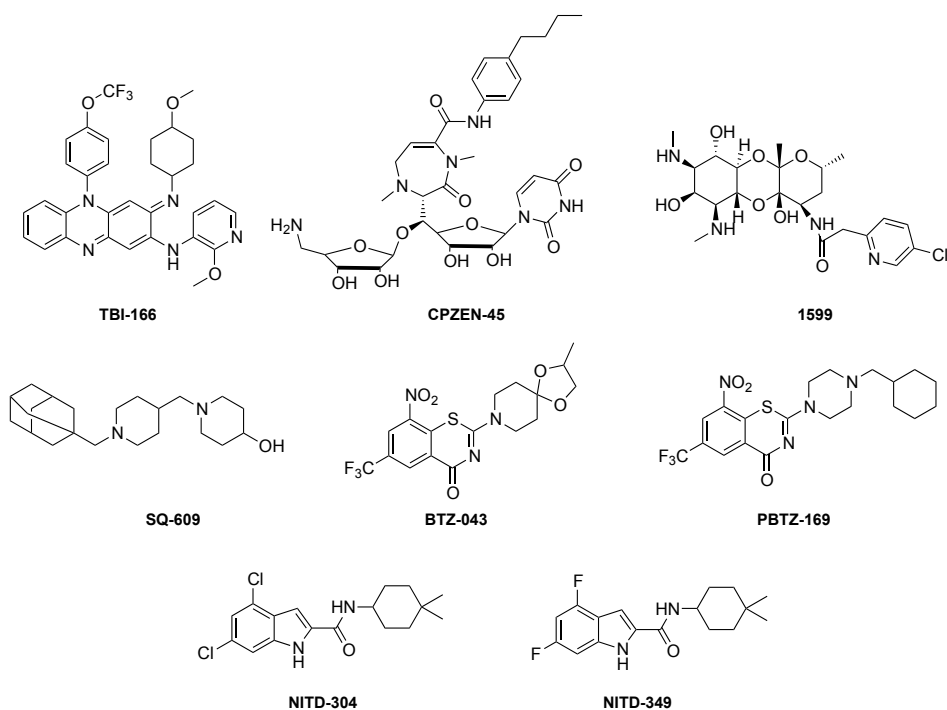


**Figure 13:** Main preclinical candidates.

## 1.7 Resistance in Mtb

Resistance to antituberculars may arise due to various mechanisms and can be grouped into three main categories: primary resistance, acquired resistance and mixed resistance.

**Primary resistance** is described as the infection of a patient with an Mtb strain that has already developed resistance. **Acquired resistance** develops in patients who originally were infected with a susceptible strain of TB, which eventually turns resistant. The cause of this infection resides for the most part in the inappropriate treatment protocols, non-compliance or incorrect dosing schedule. The third category of resistance, called **mixed resistance**, develops in individuals for which the clinical history cannot be

confirmed, therefore medication misuse is added to the uncertainty of the strain responsible for the infection.<sup>63</sup>

For what concerns the mechanisms of resistance, at least three have been reported to belong to Mtb:

- Target alterations
- Degradation/modification of the drug
- Efflux pumps

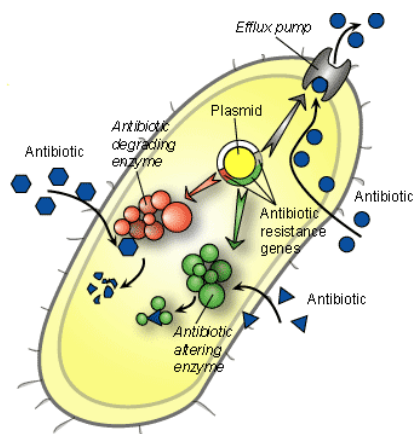


**Figure 14:** Mechanism of resistance in Mtb.

**Target alterations** are structural modifications of the target that interfere with the binding of the antimicrobial agents, reducing the susceptibility to different antibiotics. It is the most common mechanism of resistance throughout bacteria and it involves the acquisition of new genes that result in enzymatic modification of the native target.<sup>64</sup>

In the case of **RIF**, numerous single amino acid substitutions may provide large decreases in the affinity of the target for the antibiotic, leading to clinically significant levels of resistance. It has been proposed that resistance due to target alterations should occur less frequently for those antibiotics (**penicillin**, for example) that inactivate multiple targets

irreversibly by acting as close analogues of the natural substrate. Resistance to penicillin because of target changes has emerged only in a limited number of species. However, as reported below, inactivating enzymes commonly provide resistance to antibiotics that, like penicillin, are derived from natural products.<sup>64</sup>

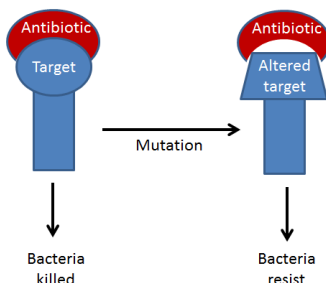


**Figure 15:** Target alteration.

**Degradation or modification of the drugs** are chemical strategies that lead to antibiotic inactivation; these include hydrolysis, group transfer, and redox mechanisms. While hydrolysis is especially important clinically, particularly as applied to  $\beta$  lactam antibiotics, the group transfer approaches are the most diverse and include the modification by acyltransfer, phosphorylation, glycosylation, nucleotidylation, ribosylation, and thiol transfer.<sup>65</sup>

Many antibiotics have hydrolytically susceptible chemical bonds (e.g., esters and amides), whose integrity is central to exert the biological activity. Not surprisingly then, there are several examples of enzymes that have evolved to target and cleave these vulnerable bonds and, as a result, provide a means of destroying antibiotic activity. For instance, a class of amidases cleave the  $\beta$ -lactam ring of the **penicillin** and **cephalosporin**, and their

inhibition may be a fruitful strategy to prolong the activity of these drugs. Moreover, degradation enzymes have targeted also the macrolide antibiotics such as **erythromycin**. Macrolides are cyclized via an ester bond that results from the final ring forming step catalysed by the thioesterase module of the polyketide synthase responsible for the ring closure step that generates 6-deoxyerythronolide B (for the 15-member erythromycin) macrocycle.<sup>66</sup> It is, therefore, not surprising that this key bond has been targeted by erythromycin esterase operating now in the reverse ring-opening mode.<sup>65</sup> It must be noticed, that such enzymes have not been found for synthetic antibacterial.

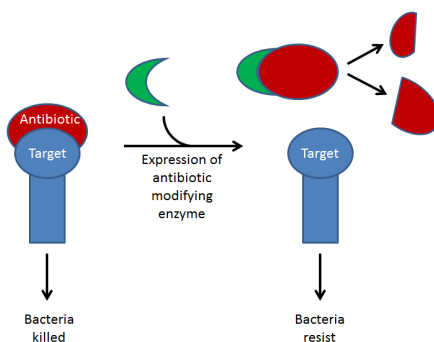


**Figure 16:** Degradation or modification of the drugs.

**Efflux pumps (EP)** are membrane-spanning proteins involved in the outward transport of a wide variety of substrates to the exterior of the cell in an energy-dependent manner. Moreover, they are part of the innate mechanism of antibiotic resistance of many microbes: in a not specifically fashion, they extrudes out of the cell toxins and every substance deemed dangerous for the microorganism.<sup>67</sup>

EP can be organized in several families according to their energy source.

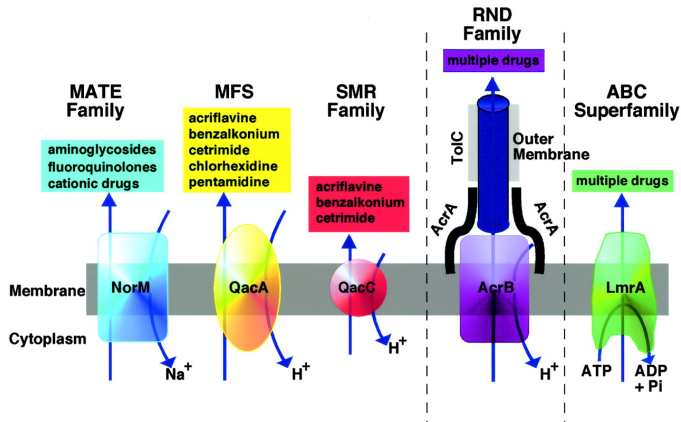


**Figure 17:** Efflux pumps families.<sup>68</sup>

Usually they confer low-to medium level of resistance, but the sustained pressure of subinhibitory concentrations of antibiotic triggered by the overexpression of efflux pumps, may result in the selection of spontaneous mutants. As such, efflux pumps have a prominent role in the raise of resistances.<sup>69</sup>

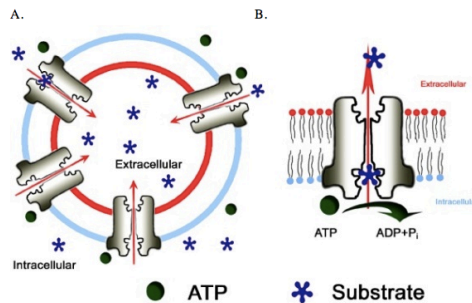


**Figure 18:** Efflux pumps.

## 1.8 Outline of the project

The high diffusion of TB throughout the world and the steadily growing number of resistant mutants to various anti-TB drugs highlight the fact that the development of new anti-TB agents remains a key priority. After many years without delivering any new anti-TB drug, the discovery of bedaquiline for the treatment of MDR-TB, and a nourished pipeline of compounds already in clinical trials, have renewed hope for the treatment of TB and especially MDR-TB. The discovery of bedaquiline and pretomanid has showed that the whole cell phenotypic assay of large libraries of compounds, and the wise medicinal chemistry efforts toward the improvement of these molecules, are reliable methodological approaches to drive the research towards novel anti-TB agents. While this approach has proved to be correct, it is nevertheless incomplete. It does not consider that, besides mutations, other mechanisms such as efflux play an important role in the development of resistance in Mtb. Indeed, although many recent anti-TB agents are active against resistant strains, targeting novel key proteins, the contribution of efflux systems to the selection of persistent strains is often unwisely neglected.

*A different idea is needed to face the disease at 360 degrees.* Taking into account the main causes of drug-resistance from Mtb (*i.e.* mutation of the target, increase of efflux, and drug-tolerance induced by intracellular Mtb) I herein propose in this PhD work a double-headed approach expressly planned to fight the resistant strains and shorten the therapy. This project presents a combination of two different, but converging, approaches:

**a) Development of new chemical entities that inhibit the growth of Mtb, active also against resistant strains**

- 1. Evolution of a series of 2-aminothiazoles*
- 2. Novel and efficient synthesis of 2-aminoxazoles*

**b) Development of efflux pump inhibitors that will increase the concentration of antibacterial agents into the Mtb**

- 1. Rational design and synthesis of Thioridazine analogues as enhancers of the antituberculosis therapy*
- 2. Development of new chemotypes as inhibitors of efflux*

The latter approach might bring new life to old drugs, preserve the new ones, and strike the intracellular strains, shortening the cure. As such, the anti-TB arsenal will be enriched of novel agents that aim at treating TB from a different standpoint, in particular limiting the raise and the spread of resistance.



## **2. Development of new chemical entities that inhibit the growth of Mtb, active also against resistant strains**

### **2.1 Introduction**

A considerable number of novel anti-TB agents are fueling the TB drug pipeline, however bedaquiline (Sirturo), former TMC207<sup>62</sup> is the only new chemical entity developed specifically for the treatment of tuberculosis that has reached the market since the introduction of RIF (1967).<sup>70</sup> With regard to anti-TB agents, and to antibacterials more in general, the whole cell phenotypic assay has demonstrated to be a profitable method to produce lead candidates for further development, especially if compared to the target-based approaches. Indeed, both the above-mentioned Bedaquiline and Pretomanid<sup>71</sup> were discovered following a cell phenotypic approach.

In the research group where I have conducted this PhD research, a phenotypic screening of an in-house chemical library was carried out in order to obtain novel anti-TB chemotypes. Despite the small amount of compounds tested, a number of hits bearing the 2-aminothiazole scaffold showed an encouraging activity, and derivative **2** (Figure 1) was taken under consideration for further investigation.

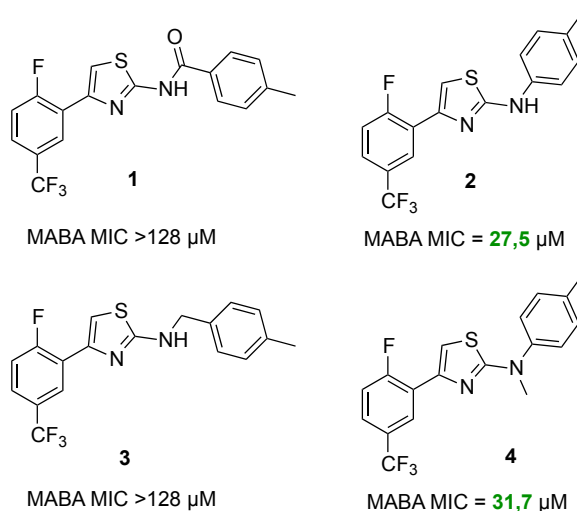


**Figure 1:** 2-aminothiazole derivatives preliminary tested as anti-TB agents.

In particular, the synthetic accessibility allowed for the possibility to expand the series and elucidate the anti-TB potential of these aminothiazole-based compounds. Keeping intact the aminothiazole core, which is suggested to act as the pharmacophore, it was investigated whether the appropriate substitutions at the aromatic rings of the hit compound **2** could lead to an improvement in the anti-TB activity and, also, in a reduction of the cytotoxicity (Figure 2).<sup>72</sup>

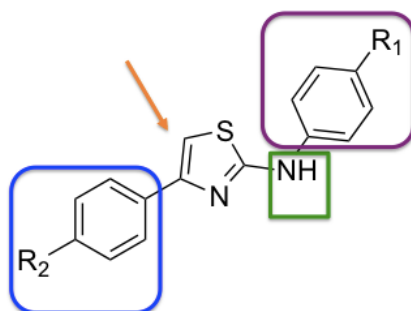


**Figure 2:** Sites for modifications of 2-aminothiazole derivatives.<sup>72</sup>

Among the compounds reported, some derivatives were found to be active not only toward the actively replicating mycobacterial strain, but also toward the non-replicating persistent phenotype in low oxygen conditions (LORA Assay). Moreover, when tested against a panel of single-drug resistant Mtb strains, these derivatives maintained the same activity as for the wild type, indicating a mechanism of action different from those of the currently used drugs. In particular, it could be noticed that, at the 4-phenyl ring, lipophilic substituents of various size as well as more polar group, such as the methoxy moiety, are important in order to confer certain anti-TB activity, however the methoxy group couples the good killing activity with an ameliorated cytotoxic profile.<sup>72</sup> Although the inhibitory activity toward Mtb of some aminothiazoles and benzothiazoles was already reported,<sup>73</sup> the detailed SAR disclosed for this new series has set the background for the studies reported in this thesis.

Therefore, compounds **5** and **6** (Figure 3) were chosen as starting points to set the design of improved analogues.

As reported, the SAR explored gave a number of valuable hints for the design of ameliorated analogues. In particular, at the amino group of the 2-aminothiazole scaffold, an aromatic ring, preferably adorned with bulky and lipophilic functional groups such as chlorine, is well tolerated; on the other side of the molecule, the phenyl ring attached at the C-4 position of the 2-aminothiazole, might be adorned either with lipophilic substituents of various sizes or with a more polar group (such as the methoxy moiety); however, this latter seems to be more suitable in order to combine the anti-TB activity and low cytotoxicity. This suggest that further modification at

the C-4 position of the 2-aminothiazole ring with more polar group could be worthy of further investigation.<sup>72</sup>

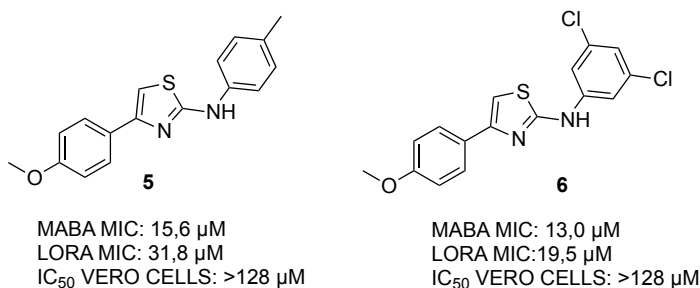


**Figure 3:** Hit compounds.

In addition, it can be speculated that the activity might be granted by the presence of two aromatic rings, suitably substituted, connected through a 5-term heterocycle. This allowed to obtain a preliminary illustration of the pharmacophore of these molecules, as reported in Figure 4.

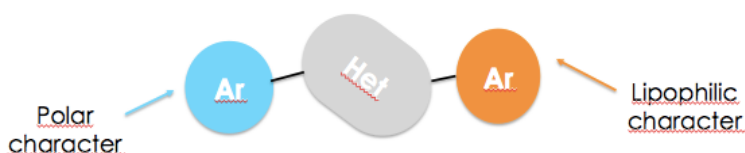


**Figure 4:** Predicted pharmacophore of 2-aminothiazole derivatives.

To prove this idea, an in house library of diarylimidazoles, that maintains the above reported structural pattern,<sup>74,75</sup> were tested in a whole-cell phenotypic assay against Mtb. The encouraging preliminary results inspired a wiser selection of further compounds to be tested, along with the synthesis of structurally related analogues. This iterative work led to the discovery of compound **7** (Figure 5), able to inhibit the growth of actively replicating Mtb at low  $\mu$ M concentration. This suggests that other heterocycles might be used in place of 2-aminothiazoles to modulate the activity of these compounds.

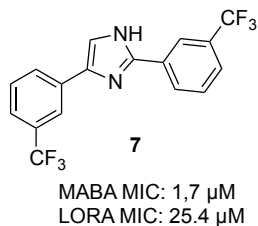


**Figure 5:** Compound 7.

Inspired by these considerations, in this PhD work I have focused my attention toward rational modifications of the 2-aminothiazole ring.

In particular, the following actions were taken:

### **2.2 Evolution of a series of 2-aminothiazoles**

### **2.3 Novel and efficient synthesis of 2-aminooxazoles**

## 2.2 Evolution of a series of 2-aminothiazoles

### 2.2.1 Rational design, results and discussion

Since the promising activity of compounds **5** and **6** above described, and taking advantage from the SAR hints reported, we have designed and synthesized novel series of anti-TB based on the 2-aminothiazole scaffold. At the position 2 of the aminothiazole ring, the p-tolyl and the 3,5-dichlorobenzene were kept since their contribution to the activity (see compounds **5** and **6**). With regard to the substituent at the C-4 position of the 2-aminothiazole, since the beneficial effect on the activity of a polar group such as the methoxy, we planned to increase the polarity at this part of the molecule through the introduction of different heterocycles.

Based on the structure of hit compounds **5** and **6**, several heterocycles, with different size, lipophilicity, hydrophilicity, and physico-chemical properties, and based on the synthetic accessibility, were selected and installed at the C-4 of the 2-aminothiazole core: pyridine, triazole, isoxazole, pyrazole and thiazole.

Pyridine was prepared as it is a bioisostere<sup>76</sup> of the benzene ring and it is the first 6-membered aromatic ring containing a heteroatom. In this case, the nitrogen is located at the 4-position, in order to have a more polar character at the same site as for compounds **5** and **6**.

The isoxazole moiety was chosen as it has already demonstrated to be a valuable scaffold for the anti-TB activity when properly substituted.<sup>77,78,79,80</sup> In particular, employing an efficient 1,3-dipolar cycloaddition protocol, it was possible to prepare the ethyl isoxazole-3-carboxylate,<sup>81</sup> that could be further functionalized.

We took advantage from the facile synthesis of isoxazole-3-carboxylate and

using the same protocol, but with different starting building blocks, other heterocycles such as the parasol and the triazole could be easily prepared. Finally, since the good activity of the 2-aminothiazole moiety, we prepared several bithiazole-2,2'-diamine derivatives.

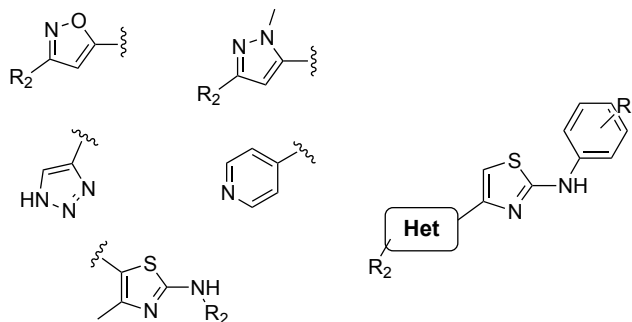


**Figure 6:** Rational design of 2-aminothiazole derivatives.

We planned to divide the study in 2 parts:

### 1) synthesis of heterocyclic compounds

### 2) further expansion of the most promising hits

#### 1) synthesis of heterocyclic compounds

**4-(pyridin-4-yl)thiazoles.** The substitution of the 4-methoxyphenyl group at the position C-4 of the 2-amithiazole with a pyridine-4-yl group led to loss of activity, regardless the functional group introduced at the 2-aminomoiety. Compounds **8**, **9** and **37** (Table 1) were synthesized and underwent to biological assays, resulting not active up to 64  $\mu\text{g}/\text{mL}$ .

**triazol-5-ylthiazol-2-amine.** A triazole derivative was prepared (compound **10**), taking advantage from the readily available click reaction with the common alkyne intermediate. Also in this case, the modification led to loss of activity (**36** MIC = >64  $\mu\text{g}/\text{mL}$ ).

**4-(isoxazol-5-yl)thiazol-2-amine.** Keeping intact the p-tolyl and the dichlorobenzene at the 2-amino position, a series of 4-(isoxazol-5-yl)thiazol-2-amine derivatives, bearing a 3-carboxylate ethyl ester moiety, were prepared. From one side, isoxazole-3-carboxylates have been already reported as anti-TB chemotype; then, the carboxylic appendage allowed for a further expansion of the series. The ethyl ester derivatives (**11** MIC: 0.5-1 µg/mL; **12** MIC: 4-8 µg/mL) showed reasonable activity, suitable for further investigation. However, it must be highlighted that, while this work was being prepared, GSK reported a series of anti-TB chemotypes suitable for further investigation and a derivative similar to those reported here was reported to show encouraging activity. Since the promising activity, further information on this series will be reported in a dedicated paragraph below.

**4-(pyrazol-5-yl)thiazol-2-amine.** Following the approach studied for the 4-(isoxazol-5-yl)thiazol-2-amine class, a series of 4-(pyrazol-5-yl)thiazol-2-amine derivatives were prepared. As above-mentioned, it was synthesized the ethyl pyrazole-3-carboxylate and the ethyl ester derivatives (**31** MIC: 16-32 µg/mL; **32** MIC: >64 µg/mL) presented somehow contrasting results. Nevertheless the SAR of these derivatives was further explored and further information on this series will be reported in a dedicated paragraph below.

**bithiazole-2,2'-diamine.** Since the good activity showed by the thiazole, we decided to introduce another thiazolyl moiety in the molecule, preparing a series of bithiazole-2,2'-diamine derivatives. It must be noticed that this scaffold is already known to exert various biological activities and we wanted to investigate whether this could apply also to the anti-TB.<sup>82-85</sup>

Although the biological results are not as encouraging as for the 4-(isoxazol-5-yl)thiazol-2-amine derivatives, bithiazole-2,2'-diamine showed interesting



activity, deserving further rounds of chemical manipulation in order to refine the SAR. In this preliminary study, we tested four compounds. **27** and **28** are symmetric compounds and we were very surprised to notice that, whereas the first one showed a good activity (**27** MIC: 4-8  $\mu\text{g/mL}$ ), the close analogue was found to be completely inactive (**28** MIC: > 64  $\mu\text{g/mL}$ ). Since this encouraging activity, we also evaluated **27** for its metabolic stability ( $t_{1/2}$ :  $23.0 \pm 0.6$  min  $CL'_{\text{int}}$ : 27.2 ml/min/kg). Also compounds **29** and **30**, in which the symmetry of the molecule is lost due to abolition of one aromatic portion, were synthesized and tested. Although being less active than the parent **27**, these compounds established bithiazole-2,2'-diamine scaffold as promising starting points for further investigation.

## 2) Further expansion of the most promising hits

In the first set of compounds synthesized three promising anti-TB chemotypes were identified: 4-(isoxazol-5-yl)thiazol-2-amine, pyrazol-5-yl)thiazol-2-amine and bithiazole-2,2'-diamine.

Of these series, the 4-(isoxazol-5-yl)thiazol-2-amine and the pyrazol-5-yl)thiazol-2-amine were selected for further expansion of the SAR. As reported before, the ethyl ester derivatives (**11** MIC: 0.5-1  $\mu\text{g/mL}$ ; **12** MIC: 4-8  $\mu\text{g/mL}$ ) showed reasonable activity. Despite the feasibility of the synthesis, the ester functionality is known to be quite labile in the biological systems, as it is easily hydrolysed, thus compounds **11** and **12** were promptly evaluated for their metabolic stability in HLM. We found that the ethyl ester moiety is really unstable (**11**  $t_{1/2}$ : < 1 min  $CL'_{\text{int}}$ : > 400 ml/min/kg ; **12**  $t_{1/2}$ :  $3.3 \pm 0.3$  min  $CL'_{\text{int}}$ : 188.8 ml/min/kg) and triple quadrupole analysis revealed that the parent acid is rapidly produced. Therefore, in order to

make these novel anti-TB chemotypes worthy of further investigation, we deemed that improving the stability of the compounds was the priority of this early project.

First, we prepared the corresponding acids in order to check whether the parent compounds could be used as pro-drugs. Unfortunately, the two acids were found to be devoid of any anti-TB activity (**13**, **14** MIC: >64  $\mu\text{g/mL}$ ), likely due to permeability issues. However, as expected, a clear improvement under the point of view of the metabolic stability was reached (**13**  $t_{1/2}$ :  $14.3 \pm 1.1$  min  $CL'_{int}$ : 43.7 ml/min/kg). Taking these findings under consideration, we reasoned that good activity coupled to reasonable stability could be obtained by preparing isosters of the ester moiety, but with a predicted enhanced stability to hydrolysis. The first round of modification was obviously the synthesis of various carboxyamides. Since the stability of amides depends on the substituents at the nitrogen atom, we decided to prepare carboxyamides that were different for hindrance and chemical properties. Mono-substituted Carboxyamides with small aliphatic group, aromatic and heteroaromatic rings or di-substituted with small aliphatic and bulky cycloaliphatic groups were synthesized and tested. A primary amide led a completely loss of the activity (**22** MIC: > 64  $\mu\text{g/mL}$ ) as in the case of the acid. The same unpleasant result was found in the case of the methyl amide derivative (**19** MIC: > 64  $\mu\text{g/mL}$ ), that is a close analogue of the ester **11** previously described. Diethyl substitution at the nitrogen atom led to compound **21** that showed some hint of activity (**21** MIC: 16-32  $\mu\text{g/mL}$ ), although still considerably lower than that of the ethyl ester compounds. Therefore, we can conclude that small aliphatic groups are not suitable to give the desired activity. Also bulkier aliphatic groups,

such as the 1-adamantyl **15** and the 1-piperidinyl **20** compounds were found to be inactive up to a concentration of 64 µg/mL. Therefore, it can be concluded that aliphatic groups, either small-sized or bulkier, are not suitable to confer the desired anti-TB activity. Compound bearing a carboxamide moiety substituted with an aromatic or heteroaromatic ring, such as the phenyl or the pyridine, were found to have an exceptionally strong activity toward Mtb strains, in the order of the submicromolar range (**17** MIC: 0.125-0.250 µg/mL; **18** MIC: 0.06-0.125 µg/mL). Since the remarkable activity, we confirmed these leads by testing them for the metabolic stability in HLM. We were pleased to notice a remarkable improvement in the stability of these derivatives, (**17**  $t_{1/2}$ : 35.1 ± 1.4 min  $CL'_{int}$ : 17.8 ml/min/kg; **18**  $t_{1/2}$ : 16.1 ± 0.2 min  $CL'_{int}$ : 38.8 ml/min/kg) being the half/life improved more than 10-fold compare to the ester. To further refine the biological profile of these leads, compounds **17** and **18** were also evaluated in human monocyte derived macrophage (HMDM) for their ex-vivo cytotoxicity in eukaryotic cells. Also in this case, compounds confirmed their goodness (**17** IC<sub>50</sub>: 184.7 µM; **18** IC<sub>50</sub>: 139.1 µM) showing a therapeutic index higher than 100 (**17** TI: 560; **18** TI: 926), and resulting apparently not toxic to human cells. Finally, compounds were also evaluated for their capability to inhibit efflux of EtBr from *M. smegmatis* mc<sup>2</sup>155 cells and against the pan-susceptible reference strain H37Rv, by real-time fluorometry, using TDZ and VER as controls (Table 2). We carried out this assay in order to investigate if our hit compounds can be substrates for efflux pumps, as we have already reported above that this is an important mechanism that bacteria use to generate resistance in Mtb. Both **17** and **18** did not present any efflux inhibitory activity compared to the reference

compounds verapamil and thioridazine, therefore it can be speculated that these derivatives are not substrate of efflux pumps and as such they likely will not be affected by efflux.

The investigation went ahead with the synthesis of the alcohol **23** derivative, that showed some hint of activity (**23** MIC: 16-32  $\mu\text{g}/\text{mL}$ ), whereas compound **26**, bearing a 2-thiazolyl moiety attached at the nitrogen atom, that is considered a bioisostere of the ester moiety, was prepared and tested, resulting unfortunately inactive. Compounds **24** and **25** were prepared because the 4-methoxyphenyl had proved to be a favourable moiety in the series that has inspired this work (see compounds **5** and **6**). The introduction of a 4-methoxyphenyl at position 3 of the isoxazole moiety led to divergent results, (**24** MIC: 4-8  $\mu\text{g}/\text{mL}$ ; **25** MIC: >64  $\mu\text{g}/\text{mL}$ ), and this data need further evaluation before being considered for SAR purpose.

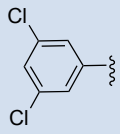
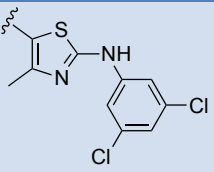
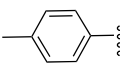
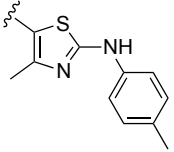
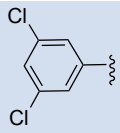
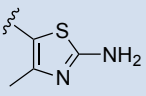
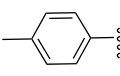
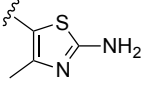
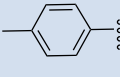
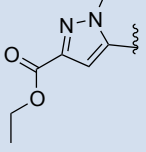
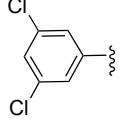
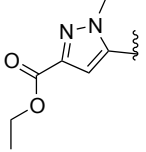
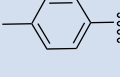
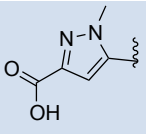
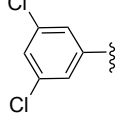
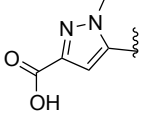
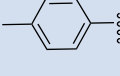
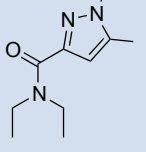
A similar approach was followed also for the 4-(pyrazol-5-yl)thiazol-2-amine derivatives. The ethyl ester derivatives led to somehow contrasting results, (**31** MIC: 16-32  $\mu\text{g}/\text{mL}$ ; **32** MIC: > 64  $\mu\text{g}/\text{mL}$ ). However, since also in this case the ethyl ester functionality would have been prone for hydrolysis in the biological systems, some of the amides already reported were prepared also in this scaffold.

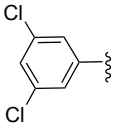
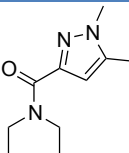
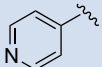
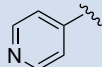
The synthesis and biological evaluation of the 2 corresponding acids (**33**, **34** MIC: >64  $\mu\text{g}/\text{mL}$ ) confirmed the loss of any anti-TB activity, likely due to some permeability issues. The modification of the ester with a small size tertiary amide led a completely loss of the activity (**35**, **36** MIC: >64  $\mu\text{g}/\text{mL}$ ). Although the small set of compounds synthesized, it seems apparent that the pyrazol-5-yl)thiazol-2-amine are, in general, less interesting than the

(isoxazol-5-yl)thiazol-2-amine as anti-TB chemotypes, and therefore we deemed worthless to further expand the series.

Comp	R <sub>1</sub>	R <sub>2</sub>	MIC <sup>a</sup>	t <sub>1/2</sub> <sup>b</sup>	CI' int <sup>c</sup>	IC <sub>50</sub>
8			>64	ND	ND	ND
9			>64	ND	ND	ND
10			>64	ND	ND	ND
11			0.5-1	<1	>400	ND
12			4-8	3.3 ± 0.3	188.8	ND
13			>64	14.3 ± 1.1	43.7	ND
14			>64	ND	ND	ND
15			>64	ND	ND	ND
16			>64	ND	ND	ND

17			0.125- 0.250	35.1 ± 1.4	17.8	184.7
18			0.06-0.125	16.1 ± 0.2	38.8	139.1
19			>64	ND	ND	ND
20			>64	ND	ND	ND
21			16-32	ND	ND	ND
22			>64	ND	ND	ND
23			16-32	ND	ND	ND
24			4-8	ND	ND	ND
25			>64	ND	ND	ND
26			>64	ND	ND	ND

27			4-8	23.0 ± 0.6	27.2	ND
28			>64	ND	ND	ND
29			8-16	ND	ND	ND
30			16-32	ND	ND	ND
31			16-32	ND	ND	ND
32			>64	ND	ND	ND
33			>64	ND	ND	ND
34			>64	ND	ND	ND
35			>64	ND	ND	ND

36			>64	ND	ND	ND
37			>64	ND	ND	ND

**Table 1:** Structure, anti-TB activity against Mtb H<sub>37</sub>Rv, metabolic stability in HLM and cytotoxicity of compounds **8-37**. <sup>a</sup>Minimum Inhibitory Concentration (µg/mL) <sup>b</sup>Half time (min) <sup>c</sup>Intrinsic clearance was calculated as:  $(0.693/in\ vitro\ t_{1/2}) * (ml\ incubation/mg\ microsomes) * (45\ mg\ microsomes/g\ liver) * (20\ g\ liver/kg\ Body\ Weight)$  (mL/min/Kg) <sup>d</sup> toxicity against human monocyte derived macrophage (µM). ND: not determined

RFF		
Comp	M. smegmatis	M. tuberculosis
	mc <sup>2</sup> 155	H37rv
17	-0.01	-0.39
18	-0.05	-0.35
TDZ	1.35	0.75
VER	2.48	1.5

**Table 2:** Relative final fluorescence (RFF) based on accumulation of EtBr at 0.25 µg/ml by *M. smegmatis* mc<sup>2</sup>155 and *M. tuberculosis* H37Rv in the absence of glucose and the compounds at half MIC.

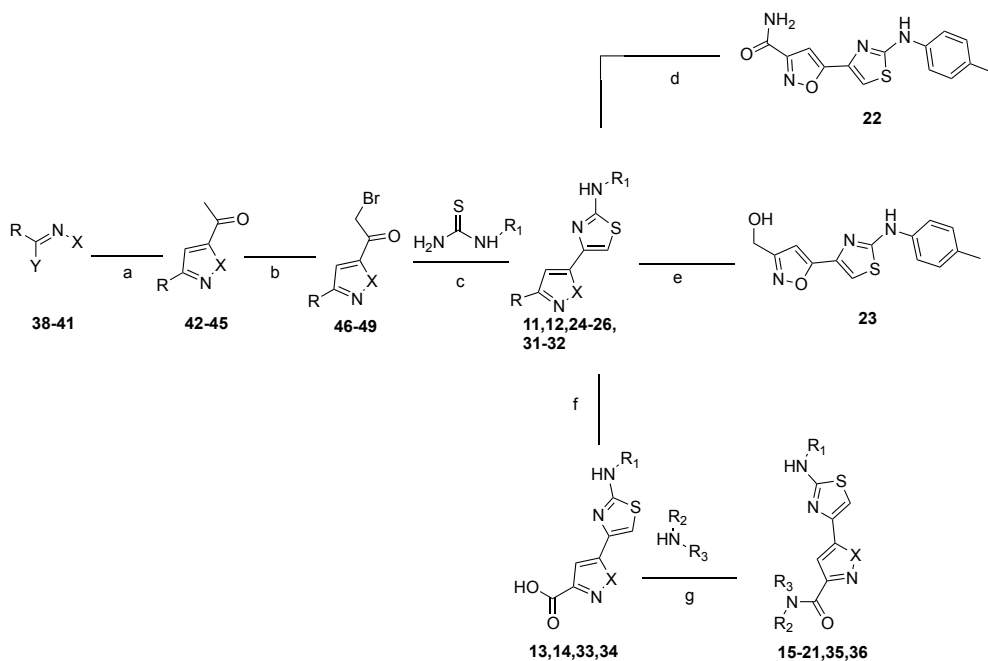


### 2.2.2 Chemistry

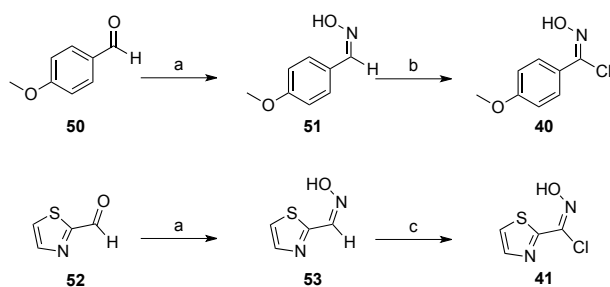
All the target compounds have a 2-aminothiazole ring, that was synthesized following the established Hantzsch protocol, refluxing the appropriate  $\alpha$ -bromoketone with the different thiourea in absolute ethanol. Thioureas, when not commercially available, were prepared refluxing the corresponding anilines and ammonium thiocyanate in 1 N HCl.

The synthesis of the different  $\alpha$ -bromoketone intermediates depends on the type of heterocycle. The isoxazole ring (Scheme 1) was prepared through a 1,3-dipolar cycloaddition between a nitrile oxide generated in situ by the proper chloro-oxime and 3-butyne-2-one.<sup>81,86,87</sup> When not commercially available, the chloro-oximes were prepared by condensation of different aldehyde and hydroxylamine hydrochloride, followed by the treatment of the resulting aldoxime with N-chlorosuccinimide,<sup>88</sup> to give intermediates **24-26** (Scheme 2). Bromination of the ketones was carried out with bromine and glacial acetic acid in chloroform at 50 °C, affording the  $\alpha$ -bromoketones in good yields, although sometimes with traces of  $\alpha$ -dibromoketones as collateral product.

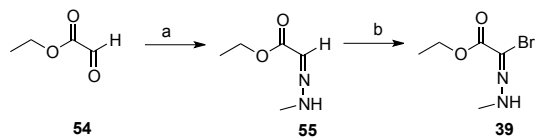
The synthesis of the pyrazole ring was performed according to the procedure of Oh *et al.*, still following a 1,3-dipolar cycloaddition reaction between a nitrile imine dipole, generated by base-promoted dehydrohalogenation of hydrazonoil halide, and 3-butyne-2-one.<sup>89</sup> Hydrazonoil halide was prepared by condensation of methylhydrazine and ethyl glyoxylate, followed by the bromination of the resulting hydrazine (Scheme 3). Then, the ketone was brominated at the  $\alpha$  position as reported earlier.



**Scheme 1:** General approach for the (isoxazol-5-yl)thiazol-2-amine and 4-(pyrazol-5-yl)thiazol-2-amine derivatives. Reagents and conditions: a) Triethylamine, benzene, 60°C, 1h; b) Br<sub>2</sub>, chloroform, AcOH, 50°C, 1h; c) EtOH, reflux, 2h; d) NH<sub>4</sub>OH, overnight; e) NaBH<sub>4</sub>, MeOH, rt, 30 min.; f) LiOH, THF/MeOH/H<sub>2</sub>O, rt, 2h; g) TBTU, EDC-HCl, TEA, DMF, rt, 2h.

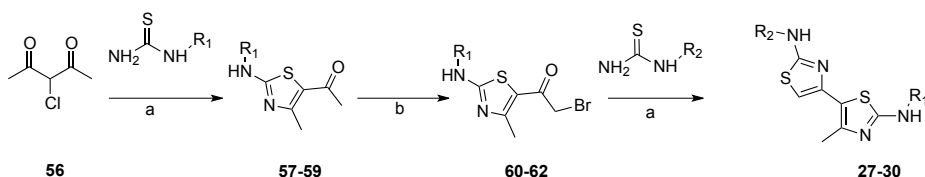


**Scheme 2:** Oxime synthesis. Reagents and conditions: a) NH<sub>2</sub>OH\* HCl, NaOH 10%, EtOH, H<sub>2</sub>O, r.t.; 30 min.; b) NCS, DMF, r.t., 1 hr; c) NCS, pyridine, DCM, 40°C, 3 hrs.



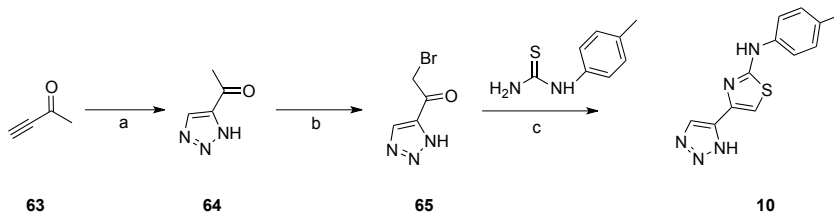
**Scheme 3:** Hydrazone synthesis. Reagents and conditions: a) MeNH-NH<sub>2</sub>, 40°C to 50°C, 1h; b) NBS, DCM, 0°C to rt

For the synthesis of 2-aminothiazole ring we refluxed 3-chloropentane-2,4-dione and the opportune thiourea in absolute ethanol.<sup>90</sup> The reaction afforded the ketones **57-59** in high yield, that were brominated according to a procedure slightly different from that already reported, using bromine and HBr solution in 1,4-dioxane at 50 °C.



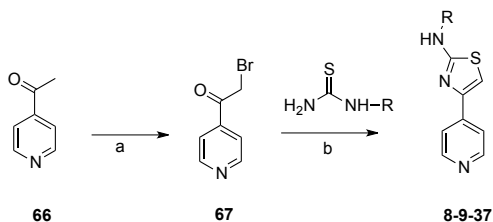
**Scheme 4:** Synthesis of bithiazole-2,2'-diamine derivatives. Reagents and conditions: a) EtOH, reflux; b) Br<sub>2</sub>, HBr solution, 1,4-dioxane, 50°C, 1h

The triazole ring was formed by click reaction stirring 3-butyn-2-one and sodium azide in DMF at 60 °C. Then, with the same conditions employed for thiazole ring, the ketone **64** was brominated to give intermediate **65**.



**Scheme 5:** Synthesis of compound **10**. Reagents and conditions: a) NaN<sub>3</sub>, DMF; b) Br<sub>2</sub>, chloroform, AcOH, 50°C, 1h; c) EtOH, reflux, 2h.

For the synthesis of compounds **8**, **9** and **37**, commercially available 4-acetyl pyridine was brominated with Br<sub>2</sub> in a mixture of 1,4-dioxane and diethyl ether at room temperature.



**Scheme 6:** Synthesis of compounds **8**, **9** and **37**. Reagents and conditions: *a*) Br<sub>2</sub>; 1,4-dioxane/diethyl ether, rt, 1h; *b*) EtOH, reflux, 2h.

Generally, the ethyl ester moiety was hydrolysed to carboxylic acid with LiOH in THF/MeOH/H<sub>2</sub>O at room temperature.<sup>91</sup> For the synthesis of amides, the carboxylic acid was firstly activated with TBTU and EDC hydrochloride, and then coupled with the appropriate amide and Et<sub>3</sub>N, to yield the corresponding amide.<sup>59</sup> Amide **22** was obtained in good yield stirring the ethyl ester and NH<sub>4</sub>OH overnight at room temperature.<sup>92</sup> Compound **23** was obtained from ethyl ester **11** after reduction with sodium borohydride.<sup>93</sup>

### 2.2.3 Conclusion

A total of 29 compounds were synthesized in this work and underwent to biologic assays in order to identify novel chemotypes for anti-TB therapy. Most of the compounds had MICs in the low  $\mu\text{g/mL}$  range, and, more importantly, two derivatives, namely **17** and **18**, showed remarkable activity in the sub  $\mu\text{g/mL}$  range. Further biological evaluations of these derivatives were made. First, their apparent cytotoxicity was measured *ex-vivo* against human monocyte derived macrophage, and the compounds resulted not toxic. Compounds **17** and **18** were investigated for their metabolic profile and both are higher stable than the corresponding ethyl ester **11**. Finally they were evaluated for their tendency to be substrate of efflux systems, resulting also in this case valuable candidates. In addition to all of these experimental data, also *in silico* drug-likeness evaluation (ClogP, TPSA, natoms, nON, nOHNH, nviolations and nrotb) confirmed that these compounds comply with the Lipinski rules of five and therefore they are mature hits ready for *in vivo* experiments. Along with the above reported hits, in this work another novel anti-TB chemotypes worth of further investigation, that is the bisthiazoles, was disclosed. Efforts to further expand the series and to identify the mechanism of action are currently on going in our laboratories.

## 2.3 Novel and efficient synthesis of 2-aminoxazoles

### 2.3.1 Rationale

As above reported, the substitution of the central 2-aminothiazole with another heterocycle core might be well tolerated. Therefore, we decided to investigate the effect on the anti-TB activity of another heterocycle in place of the 2-aminothiazole. A sound choice seemed to substitute the sulfur atom of the thiazole with the isoster oxygen, producing a series of 2-aminoxazoles. Hinsberg applied the concept of isosterism not only to the single atoms, but also to heterocycles, according to the “ring equivalents” theory: specific groups can be exchanged for one another in aromatic ring systems without drastic changes in physico-chemical properties relative to the parent structure.

From the moment that, according this theory, benzene, thiophene, pyridine and furan are ring equivalents, we deemed of interest to substitute the 2-aminothiazole with a 2-aminoxazole, so as to investigate the effect of this substitution in terms of activity, cytotoxicity, and metabolic profile.

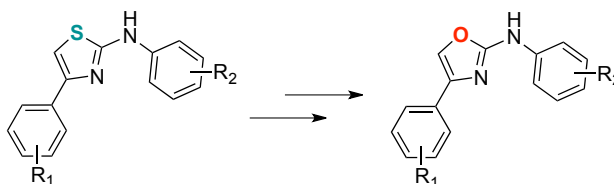


**Figure 7:** Substitution of the sulphur atom with oxygen.

For the synthesis of these new derivatives, we planned to exploit the same protocol as for the 2-aminothiazole, that is the Hantzsch reaction, with a condensation between the opportune  $\alpha$ -bromoketone and a substituted

urea in order to obtain, in one step, the final compound. Unfortunately, this reaction did not allow to isolate the desired 2-aminooxazoles and even more surprising was the fact that procedures to construct the 2-aminooxazole core were scarcely reported in the literature. Especially when the aromatic rings at position C-4 and attached to the nitrogen atom of the 2-aminooxazole present a pattern of substitution like that reported in our compounds (Figure 7), straightforward syntheses are seldom reported and difficult to reproduce.

A summary list of these procedures is reported below:

### **1. Synthesis of 2-aminooxazoles in absolute ethanol**

This is the procedure that we have used to synthesized the above-mentioned 2-aminothiazoles. We tried this procedure in which the starting materials (bromoketone and urea) were solubilized in ethanol and heated to reflux for different hours. Unfortunately with this approach we obtained only the complete decomposition of both the starting material without any traces of the target compound.<sup>94</sup>

### **2. Catalyst-free synthesis of 2-aminooxazoles in PEG-400**

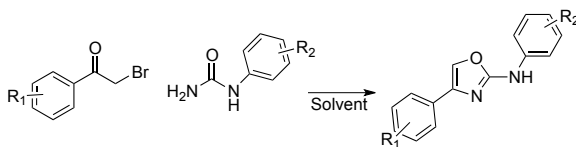
In a paper published, it was reported a Hantzsch-like procedure in which the  $\alpha$ -bromoketone and the substituted urea were reacted in PEG-400 at room temperature for different hours. The authors after 5 hours were able to obtain the final compounds in high yields. This approach appeared to be very versatile and different type of substituted ketones were employed.<sup>95</sup> Unfortunately, following this approach, we could not obtain the desired compounds after several attempts.

### 3. Catalyst-free synthesis of 2-aminoxazoles in glycerine

In another procedure, it was reported the same reaction at room temperature in glycerine.<sup>96</sup> Following this procedure, we could not obtain the target compounds because the reactions with these conditions did not worked.

### 4. Synthesis of 2-aminoxazoles in DMF

In a patent, it was reported the same reaction but with the use of DMF as the solvent, and the reaction mixture was heated at 90° C for 24 hours.<sup>97</sup> Also this approach did not lead the desired compound.



**Scheme 7:** General synthesis of 2-aminoxazoles following a Hantzsch-like approach.

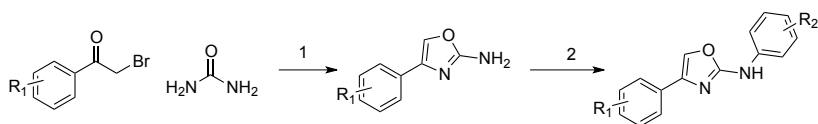
Since these findings, we reasoned that, besides the scope of the SAR investigation, developing a new and versatile synthetic strategy to efficiently obtain substituted 2-aminoxazoles (Figure 7) could have been of interest for the chemistry community.



### 2.3.2 Synthetic strategy

The new designed approach consists of 2 steps, each optimized to give the most rewarding result:

1. Condensation with unsubstituted urea
2. Buchwald-Hartwig cross coupling with the proper aryl halide.



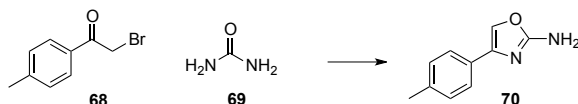
**Scheme 8:** New synthetic approach.

1. The first step is a condensation between a general  $\alpha$ -bromoketone and urea. This reaction leads to intermediates characterized by the 2-amino-oxazole ring substituted at C-4.
2. In the second step, a Buchwald-Hartwig reaction is used to obtain a new C-N bond starting from an amine and aryl halide. We performed this reaction between the 4-aryl-amino-oxazole and aryl halide to obtain the final compound substituted at position N-2.

This work can be divided into three iterative phases of optimization.

- a) Optimization of the condensation reaction (first step)
- b) Optimization of the Buchwald-Hartwig coupling (second step)
- c) Validation of the versatility of the methods

### a) Optimization of the condensation reaction



**Scheme 9:** Condensation reaction.

Although the many issues encountered in the Hantzsch reaction between a  $\alpha$ -bromoketone and a substituted urea, however, the reaction with unsubstituted urea is reported with many  $\alpha$ -bromoketones. In this initial phase, we used 2-bromo-1-(*p*-tolyl)ethanone **68** as reference compound.

The parameters that we wanted to check initially were:

- Solvent
- Stoichiometry
- Traditional heating vs  $\mu$ W irradiation

We performed the reaction with some of the solvents already reported in literature for this reaction: CH<sub>3</sub>CN, EtOH and PEG-400. Unfortunately, none of these solvents allowed to obtain the desired product. Successively, we tried the condensation with non-reported solvents such as DMF, NMP, DMSO and DME.

We were able to obtain the target compound **70** only with DMF and NMP. Yields and conditions are reported in table 3.

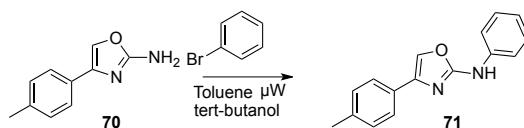
Subsequently, in order to improve the yields, we modified reaction time and temperature. We found that high amount of urea and high temperatures are necessary to obtain the product in acceptable yield (37%-45%). Moreover we further optimized the reaction in DMF with the microwave irradiation, heating the starting material for 3 or 15 minutes, obtaining compound 70 in 53% and 56% yields, respectively. A similar result

was obtained when NMP is used as the solvent, although DMF still performs better.

Solvents	Eq of reagents	Time	Temperature	Yield
DMF	1/2	8 hrs	80 °C	18%
DMF	1/10	2 hrs	80 °C	37%
DMF	1/10	30 min	120 °C	45%
<b>DMF</b>	<b>1/10</b>	<b>15 min</b>	<b>80 °C <math>\mu</math>W</b>	<b>56%</b>
<b>DMF</b>	<b>1/10</b>	<b>3 min</b>	<b>120 °C <math>\mu</math>W</b>	<b>53%</b>
NMP	1/10	15 min	80°C $\mu$ W	50%
NMP	1/10	3 min	120 °C $\mu$ W	45%
DME	1/10	o.n.	80°C	0%
DMSO	1/10	3 hrs	80 °C	0%
EtOH	1/2	o.n.	80 °C	0%
EtOH	1/10	o.n.	80 °C	0%
CH <sub>3</sub> CN	1/2	o.n.	80°C	0%
CH <sub>3</sub> CN	1/10	o.n.	80°C	0%
PEG 400	1/2	o.n.	20°C	0%

**Table 3:** Optimization of condensation reaction. o.n.: overnight

### b) Optimization of the Buchwald-Hartwig coupling



**Scheme 10:** Buchwald-Hartwig reaction.

The Buchwald-Hartwig reaction is a cross-coupling reaction of an aryl halide with an amine using palladium as the catalyst and a strong base. The reaction mechanism is reported below:

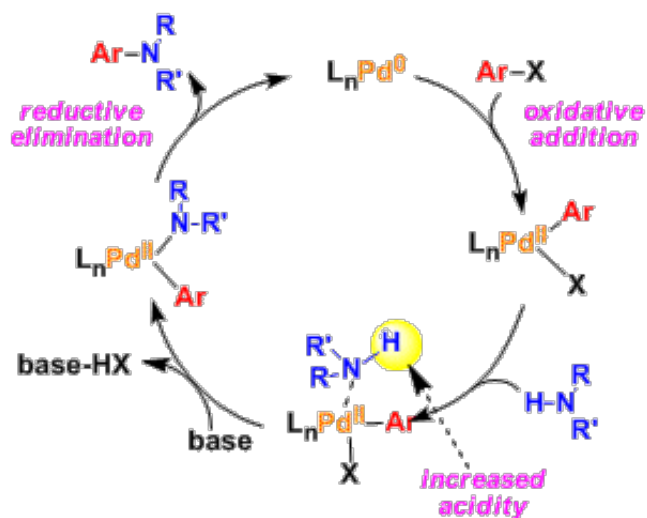


**Figure 8:** Buchwald-Hartwig reaction mechanism.

The reaction begins by oxidative addition of the aryl halide to the palladium, which is followed by coordination of the amine to the palladium. The strong base then abstracts a proton from the amine, forming an amide, which in turn attacks the palladium and kicks out the halide as a leaving group. Reductive elimination then produces the final aryl amine product and regenerates the catalyst.<sup>98,99</sup>

Contrary to the condensation optimization, for this kind of structures we were not able to find any reported procedure on the scientific databases, with the exception of one paper that reported this reaction on similar scaffold such as 2-aminothiazoles and benzoxazoles, using an extremely expensive catalyst.<sup>100</sup>

We performed the reaction with 3 different type of catalyst/ligand: X-Phos Pd G2, S-Phos Pd G2 and DavePhos/Pd(OAc)<sub>2</sub>; two of them belong to the second-generation Buchwald catalysts, and they have Pd and ligand already

linked together. For each catalyst we tried 4 different bases: NaOtBu, Cs<sub>2</sub>CO<sub>3</sub>, K<sub>2</sub>CO<sub>3</sub> and K<sub>3</sub>PO<sub>4</sub> (Table 4).

Ligand	Catalyst	Base	Conditions	Yield
<b>X-Phos Pd G2</b>		<b>NaOtBu</b>	<b>130 °C 10 min (μW)</b>	<b>50%</b>
X-Phos Pd G2		Cs <sub>2</sub> CO <sub>3</sub>	130 °C 10 min (μW)	42%
X-Phos Pd G2		K <sub>2</sub> CO <sub>3</sub>	130 °C 10 min (μW)	0%
X-Phos Pd G2		K <sub>3</sub> PO <sub>4</sub>	130 °C 10 min (μW)	37%
S-Phos Pd G2		NaOtBu	130 °C 10 min (μW)	49%
S-Phos Pd G2		Cs <sub>2</sub> CO <sub>3</sub>	130 °C 10 min (μW)	20%
S-Phos Pd G2		K <sub>2</sub> CO <sub>3</sub>	130 °C 10 min (μW)	0%
S-Phos Pd G2		K <sub>3</sub> PO <sub>4</sub>	130 °C 10 min (μW)	28%
Dave- Phos	Pd(OAc) <sub>2</sub>	NaOtBu	130 °C 10 min (μW)	8%
Dave- Phos	Pd(OAc) <sub>2</sub>	Cs <sub>2</sub> CO <sub>3</sub>	130 °C 10 min (μW)	8%
Dave- Phos	Pd(OAc) <sub>2</sub>	K <sub>2</sub> CO <sub>3</sub>	130 °C 10 min (μW)	11%
Dave- Phos	Pd(OAc) <sub>2</sub>	K <sub>3</sub> PO <sub>4</sub>	130 °C 10 min (μW)	11%

**Table 4:** Optimization Buchwald-Hartwig cross coupling.

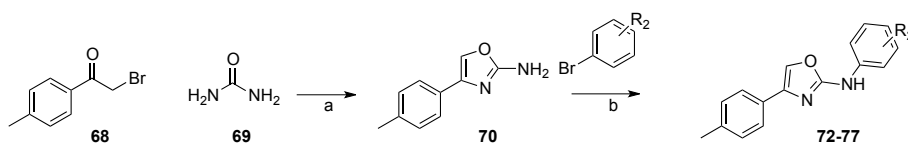
All the reaction were performed with the use of toluene as solvent and under microwave irradiation for 10 minutes at 130°C, because similar conditions were reported for this kind of reactions when performed under conventional heating.

In table 4 are summarized all the reaction performed and the procedure that gives the most encouraging data relied on the use of X-Phos Pd G2 as the catalyst and NaOtBu as the base, leading to the target compound with the 50% yield.

### c) Validation of the versatility of the methods

In the last part of this work, we applied the procedures that gave the best results in steps **a** and **b** to  $\alpha$ -bromoketones and aryl halide variously substituted. In particular, different electron-withdrawing or electron-donor substituents, at various position of the aromatic ring, were used as starting materials. To further corroborate the versatility of our synthetic approach, we synthesized also the corresponding 2-aminoxazoles of some of our most active 2-aminotiazoles, that are compounds **93-95** (Figure 9).

First, we investigated the effect on the reactivity of the substituents at the aryl halide, that was reacted with intermediate **70**.

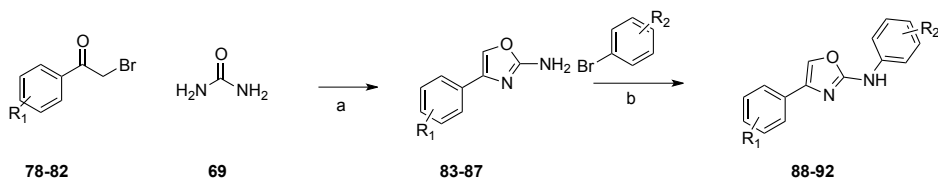


**Scheme 11:** Proof of the new protocol versatility  $R_2$  modification.

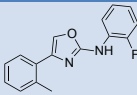
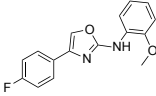
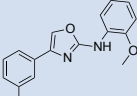
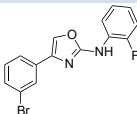
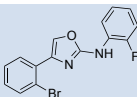
Comp	Structure	Yield
72		53%
73		48%
74		59%
75		71%
76		59%
77		37%

**Table 5:** Compounds **72-77**.

Successively, once individuated the substituent better tolerated in the Buchwald-Hartwig reaction (that is *o*-OCH<sub>3</sub> or *o*-F), we proved the versatility of step one.



**Scheme 12:** Proof of the new protocol versatility R<sub>1</sub> modification.

Comp	Structure	Yield a	Yield b
88		52%	40%
89		41%	70%
90		52%	37%
91		57%	35%
92		40%	15%

**Table 6:** Compounds **88-92**.

After the optimization of this novel and efficient synthesis of 2-aminoxazoles, we used this approach to synthesize the 2-aminoxazoles **93-95**, bearing those substituents that grant the best activity in the case of the 2-aminothiazole series.<sup>72</sup>

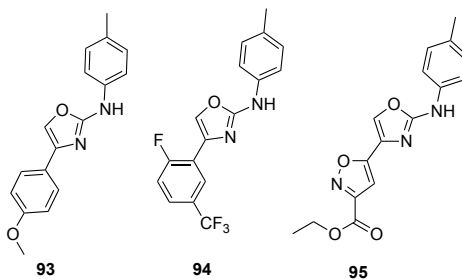
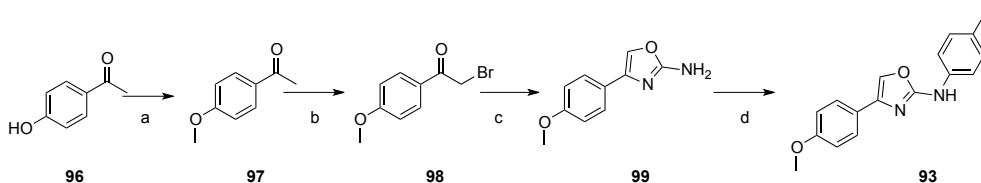


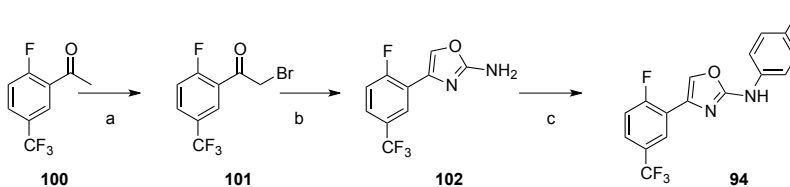
**Figure 9:** Compounds **93-95**.



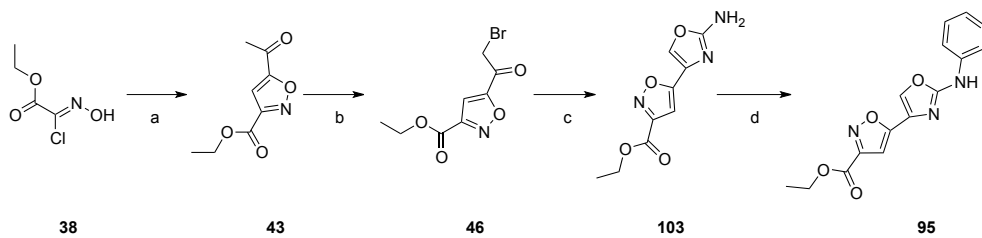
For the synthesis of the  $\alpha$ -bromoketones **98**, **101** and **46**, we followed a protocol already reported or described before. On these intermediates, the previously explained procedure was performed, leading to the preparation of the desired 2-aminoxazoles. It must be noticed that, to our knowledge, this is the only effective method for the synthesis of these substituted scaffolds.



**Scheme 13:** Compound **93**. Reagents and conditions: a)  $\text{CH}_3\text{I}$ ,  $\text{K}_2\text{CO}_3$ , acetone,  $60^\circ\text{C}$ , on; b)  $\text{Br}_2$ ,  $\text{CH}_3\text{COOH}$ ,  $\text{CHCl}_3$ ,  $50^\circ\text{C}$ , 2 h; c) urea, DMF,  $120^\circ\text{C}$ , 3 min.; d) 4-bromotoluene,  $\text{NaOtBu}$ , X-Phos Pd G2, *t*-BuOH, toluene;  $130^\circ\text{C}$ , 15 min.



**Scheme 14:** Compound **94**. Reagents and conditions: a)  $\text{Br}_2$ ,  $\text{CH}_3\text{COOH}$ ,  $\text{CHCl}_3$ ,  $50^\circ\text{C}$ , 2 h; b) urea, DMF,  $120^\circ\text{C}$ , 3 min.; c) 4-bromotoluene,  $\text{NaOtBu}$ , X-Phos Pd G2, *t*-BuOH, toluene;  $130^\circ\text{C}$ , 15 min.



**Scheme 15:** Compound **95**. Reagents and conditions: a) Triethylamine, benzene, 60°C, 1h; b) Br<sub>2</sub>, CH<sub>3</sub>COOH, CHCl<sub>3</sub>, 50°C, 2 h; c) urea, DMF, 120°C, 3 min.; d) 4-bromotoluene, NaOtBu, X-Phos Pd G2, t-BuOH, toluene; 130°C, 15 min.

### 2.3.3 Antitubercular activity

Although the synthesis of the majority of these compounds was made for the sake of chemical investigation, we were also interested in their biological evaluation. A total of 10 compounds were synthesized, among which 7 were synthesized during the protocol optimization and 3 were synthesized to evaluate the influence of the central heterocyclic ring on the anti-TB activity. All of the derivatives were evaluated for their anti-TB activity in MABA assay and cytotoxicity in Vero cells.

Comp	MIC ( $\mu\text{g/mL}$ ) <sup>a</sup>	IC50 ( $\mu\text{g/mL}$ ) <sup>b</sup>	LORA MIC ( $\mu\text{g/mL}$ )
72	> 100	47.85	ND
73	> 100	72.29	ND
74	> 100	59.01	ND
75	> 100	62.44	ND
76	> 100	>100	ND
89	> 100	39.54	ND
92	> 100	62.62	ND
93	> 100	96.47	ND
94	12.29	53.51	ND
95	2.3	66.12	23.31

**Table 7:** MABA MIC, cytotoxicity and LORA MIC of 2-aminothiazole derivatives. <sup>a</sup> MIC values determined by MABA assays <sup>b</sup> Cytotoxicity to Vero cells.

Unfortunately, all the derivatives synthesized during the protocol optimization are completely inactive. However, this was somehow expected, since the premises described. Compound **93**, parent of 2-aminothiazole **5** (Figure 3), lost the anti-TB activity. However, compounds **94** and **95** maintained the same inhibitory activities as the corresponding 2-

aminothiazoles derivatives (**94** MIC<sub>oxazole</sub>: 12.29 µg/mL vs MIC<sub>thiazole</sub>: 15.6 µM; **95** MIC<sub>oxazole</sub>: 2.3 µg/mL vs MIC<sub>thiazole</sub>: 0.5-1 µg/mL).

Further studies aimed at investigating the different pharmacological properties of these 2-aminooxazoles are on-going in our laboratory

#### **2.3.4 Conclusion**

In this part of the thesis, it is reported a method that we have developed for the synthesis of 2-aminooxazoles variously substituted.

The project was subdivided in 3 steps:

- a) Optimization of the condensation reaction
- b) Optimization of the Buchwald-Hartwig coupling
- c) Proof of the new protocol versatility

In points **a** and **b** we work on the optimization of the reactions allowing to obtain good yields, in the final part we demonstrated the versatility of the protocol, performing the reactions on a number of different substrates.

Since the low information obtained in literature about the 2-aminooxazole scaffold, we believe the scope of this investigation can go beyond the SAR investigation for novel anti-TB chemotypes.

All the synthesized compounds were evaluated for their anti-TB activity and two derivatives (**94** and **95**) lead to interesting results despite the slight improvement of the cytotoxicity if compared to the corresponding aminothiazole. Efforts to further expand the series are currently on going in our laboratories.

### **3. Development of efflux pump inhibitors that will increase the concentration of antibacterial agents into the Mtb**

#### **3.1 Introduction**

Efflux pumps (EP) contribute to the intrinsic resistance to antibacterial agents and to the development of the acquired one in many pathogens. Usually they confer low-to-intermediate levels of resistance, however, the constant pressure of subinhibitory concentrations of the antibiotic promotes the selection of spontaneous mutants.

Therefore:

- a)* EP are effectors of the innate drug-resistance mechanism
- b)* they are crucial in conferring a low-level of drug resistance
- c)* they contribute to lower the concentration of the drug inside the mycobacterial cell, allowing the emergence of a high-level of resistance
- d)* it has been demonstrated that efflux pump inhibitors (EPIs) are able to improve the activity of old drugs towards which the bacteria had become resistant.<sup>101</sup>

In spite of this knowledge, the extent to which an antimicrobial compound is a substrate of efflux is seldom evaluated, and this is not considered an important parameter in the optimization of novel anti-TB drugs. The recent discovery by Lee and colleagues of spectinamides as anti-TB candidates,<sup>54</sup> also by virtue of their scarce tendency to be extruded by EP, confirms the importance of taking into account efflux when the design of new drugs is planned.<sup>55</sup> In addition to these findings, although the mechanism of

adaptation of Mtb to the hostile environment is still a matter of discussion, Adams and colleagues have recently reported that bacterial efflux pumps mediate multi-drug tolerance and the bacterial survival in macrophages, leading to a long-lasting therapy.<sup>102,103</sup>

It is therefore possible to claim that inhibition of efflux would lead to a number of beneficial effects:

- a) increasing the activity of the anti-TB drugs subject to efflux
- b) keeping the concentration of the drug at the therapeutic dose, minimizing the possibility to select mutants
- c) drastically shorten the duration of treatment by reducing multi-drug tolerance.

This could be priceless in order to repurpose old drugs and preserve the efficacy of those novel compounds, such as bedaquiline, that are either next to be introduced in the anti-TB arena or that already are.

### **3.1.1 Efflux pumps inhibitors (EPIs)**

**Thioridazine** (TDZ) is an neuroleptic agent found to possess efflux inhibitory properties,<sup>104</sup> that has recently attracted the attention of many researchers since it hits drug resistant strains, likely by virtue of the EP inhibitory properties.<sup>105</sup> In a clinical trial in Argentina, TDZ was used for the treatment of patients with XDR-TB in combination with known anti-TB drugs, showing good results.<sup>106</sup> Moreover it has been demonstrated that TDZ works not only as inhibitor of Mtb bacterial efflux pumps, but it may also induce the acidification of the phagosome inside infected macrophages, potentiating the effect of the immune system and avoiding intracellular Mtb growth (Figure 1).<sup>105,107,108,109</sup>

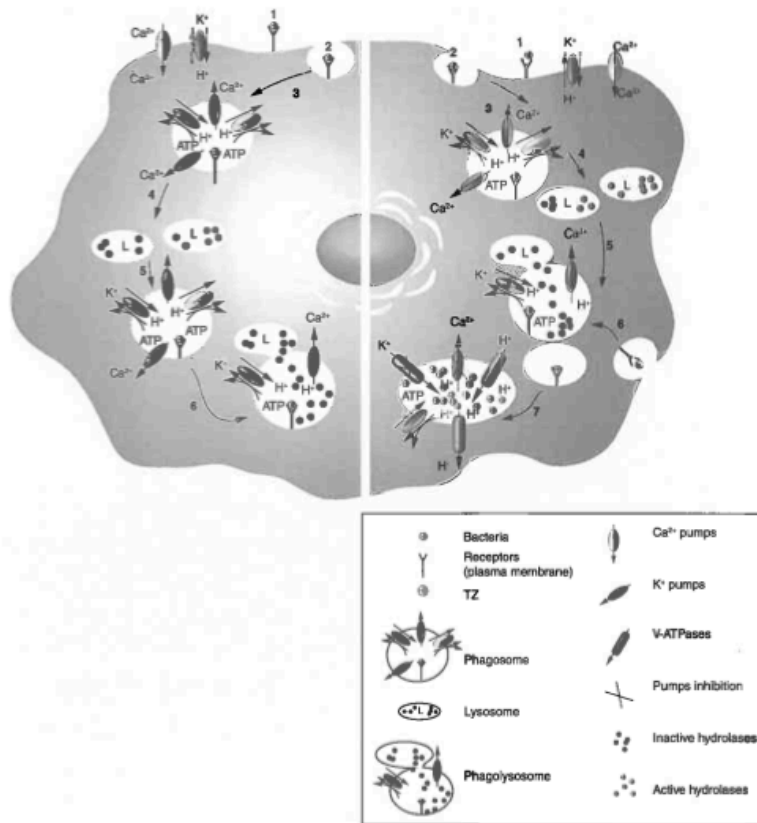


**Figure 1:** Theoretical model proposed for the enhancement of the macrophage-killing activity by EPIs. A) Infected macrophage B) Infected macrophage treated with EPIs.<sup>67</sup>

When the macrophage is infected by Mtb (Figure 1-A) a series of metabolically events take place, and the bacterium is first recognized (Figure 1-A1) then internalized into the phagosome (Figure 1-A2,3). The pumps present in the plasma membrane of the macrophages normally transport potassium (K<sup>+</sup>) into the macrophage, but since the invagination of the bacterial material, these pumps extrude K<sup>+</sup> from the macrophage lumen to the cytoplasm. When the phagosome fuses with the lysosome, to form

the phagolysosome, these pumps are responsible for the depletion of  $K^+$  and other cations, impairing the process of phagolysosome acidification that, on turn, lead to hydrolases malfunction and therefore bacterial survive. (Figure 1-A4,6)

On the other hand, when the infected macrophage is treated with EPIs, the cascade of events is similar to that described before, (Figure 1-B1,5) but in this case the potassium pumps of the phagolysosome are inhibited, so the concentration of  $K^+$  is increased inside the phagolysosome, and proton-ATPases are activated to compensate the hypertonicity of the organelle, pumping protons into the lumen. Therefore the pH level is suitable for the activation of hydrolases and killing of intramacrophageal Mtb. (Figure 1-B6,7)<sup>67</sup>

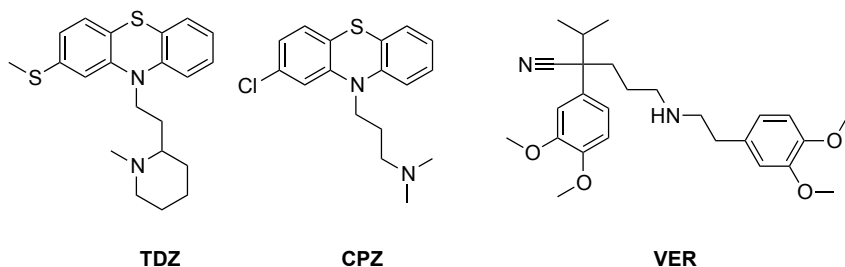


**Figure 2:** Efflux pumps inhibitors (EPIs).

Although one of the most studied, TDZ is not the only efflux inhibitor used as adjuvant for the treatment of TB. Also **Chlorpromazine** (CPZ), another neuroleptic with efflux inhibitory properties, was tested along with its metabolites against *M. smegmatis*, a non-pathogenic specie similar to Mtb, and exhibited synergistic activity when administered in combination with known anti-TB drugs.<sup>110,111</sup>



The antiarrhythmic **Verapamil** (VER) is another efflux pump inhibitor that has shown an antimicrobial-potentiating effect in the treatment of Mtb both *in vitro* and *in vivo*.<sup>112</sup> It has been demonstrated that inhibition of mycobacterial efflux pumps by VER reduces the bacterial drug tolerance induced in the intracellular compartment inside the macrophages and in zebrafish granuloma-like lesions.<sup>102</sup> Despite these encouraging premises, the use of TDZ and/or VER, at concentrations at which they would be effective in the treatment of TB, are limited by the numerous side effects and general toxicity.

Recently, were reported a series of novel structural EPIs designed via fusion of the VER substructure with various tricyclic as well as non-tricyclic chemosensitizer core substructure motifs (required for a molecule to sensitize a resistant strain to a drug) or their structural motifs derived from phenothiazines, dibenzazapine, cyproheptadiene, thioxanthene, dibenzosuberyl, and diphenylmethane. These new approach demonstrate that developing EPIs is a viable strategy and may have added advantage for the anti-TB therapy.<sup>113</sup>

As mentioned before, in this chapter two different approaches act to inhibit the efflux are reported:

### **3.2 Rational design and synthesis of Thioridazine analogues as enhancers of the antituberculosis therapy**

### **3.3 Development of new chemotypes as inhibitors of efflux**

## 3.2 Rational design and synthesis of Thioridazine analogues as enhancers of the antituberculosis therapy

### 3.2.1 Rational design

Inspired by these considerations, in this PhD work I report the design and synthesis of a number of TDZ derivatives, and their biological evaluation as efflux inhibitors and synergistic effect with known anti-TB drugs both *in vitro* and on infected human monocyte-derived macrophages.<sup>152</sup>

Since the lack of detailed information about the structure of the efflux systems, the new compounds were prepared following a Ligand-Based Drug Design approach. TDZ was used as template, given its well-known and deeply investigated anti-TB properties when administered in combination with first-line drugs. The aim of this work was therefore to chemically modify TDZ in order to obtain a compound with improved adjuvant properties while limiting the onset of side effects, especially at the CNS level.

First, we thought it was necessary to **escape from the phenothiazine core** because, according to the very well known SAR of antipsychotic drugs,<sup>114</sup> it is crucial in conferring the desired neuroleptic activity. Moreover, although with a few exceptions,<sup>115</sup> a series of TDZ analogues in which the phenothiazine core was kept intact has already been reported as inhibitors of efflux in other bacteria, but with scarce results.<sup>112,116</sup> In addition to this, efflux systems are known to be affine to charged quaternary ammonium salt such ethidium bromide (EtBr) and berberine, and to molecules bearing basic amino groups (TDZ, VER, reserpine), that likely occur to be protonated at the acidic pH of the sites infected by Mtb. Given these premises, chemical manipulation was carried out keeping intact the N-

methylpiperidine moiety, whereas modifying the nature of the heterocyclic attached to it and the length of the spacer.

Several heterocycles, embodying a variable number of rings, were attached by the nitrogen atom to an N-methyl-2-piperidinyl appendage through an ethylene linker (compounds **104-112**, chart 1).

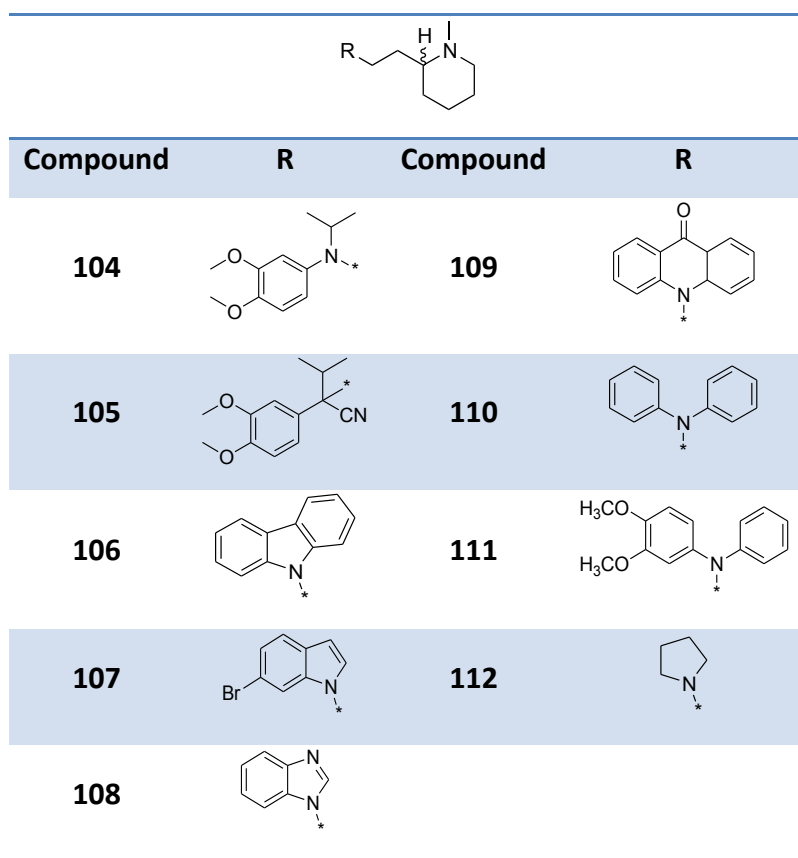


**Chart 1:** Structure of compound **104-112**.

The carbazole (**106**) and the acridone (**109**), that are tricyclic flat structures, were chosen for their close resemblance with the phenothiazine core. The indole (**107**), and the benzimidazole (**108**) are among the most privileged scaffolds used in medicinal chemistry, and could afford extended chemical

manipulation of the series. The diphenylamines (**110** and **111**) were synthesized to check whether the planar structure of the phenothiazine could be disrupted without loss of the inhibitory activity. The pyrrolidine (**112**) was prepared to check whether a small ring could still be a suitable substrate of efflux.

Once the preliminary assays had corroborated the design of compound **106**, other appendages were attached to the carbazole core in place of the N-methyl-2-piperidinyl one, order to understand the **importance of the appendage**. To start, a less polar and flatter substrate such as the 2-ethylpyridine (**113**) was attached to the carbazole nitrogen; then, the distance between the nitrogen of carbazole and that of the appendage was shortened by one methylene unit in compound **114**.

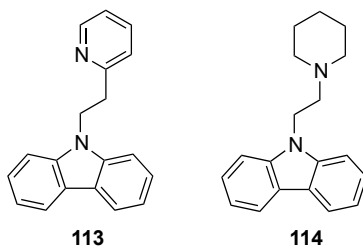
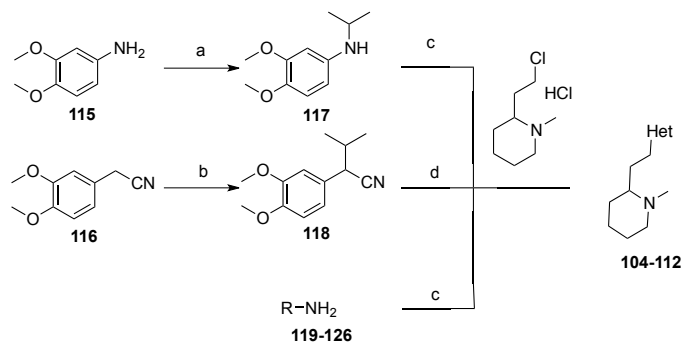


**Figure 3:** Structure of compounds **113** and **114**.

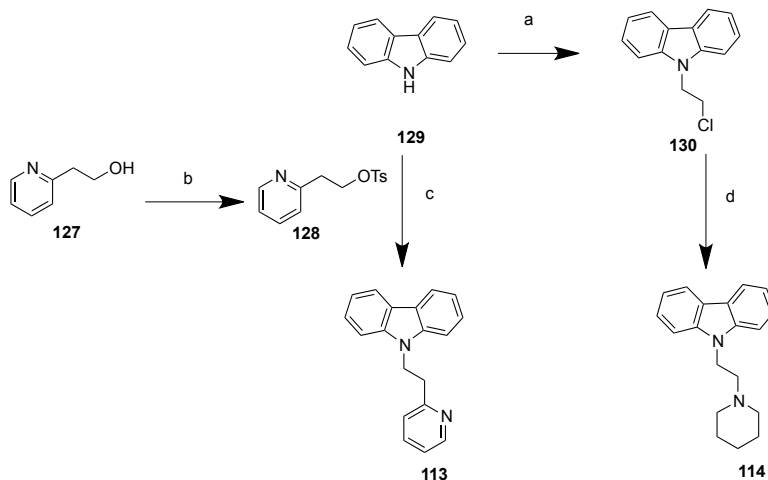
Finally, since the recent interest in the use of VER and its derivatives in the treatment of TB,<sup>117,118</sup> we have tried to **merge the two structures of TDZ and VER** in one hybrid molecule (Figure 4), and therefore compounds **104** and **105** (chart 1) were synthesized and tested.





**Scheme 1:** Preparation of the thioridazine analogues. Reagents and conditions: a) Isopropyl iodide, triethylamine, MeOH, reflux, 18h, 50%; b) Isopropyl bromide, NaH, DMF, rt, 18h, 47%; c) NaH, DMF, reflux, 18-72h, 9-70%; d) NaNH<sub>2</sub>, Toluene,  $\mu$ W, 110 °C, 30 min, 50%.

For the synthesis of compound **113**, first 2-(hydroxymethyl)-pyridine was treated with *p*-toluenesulfonyl chloride and triethylamine in dichloromethane to give the tosyl derivative **128**, and then the ameliorated leaving group is displaced by carbazole according to the conditions reported by Cheng (Scheme 2).<sup>121</sup> In the case of compound **114**, carbazole was first treated with dichloroethane to give N-(chloroethyl)carbazole **130**, that was reacted with piperidine in DMF at room temperature using K<sub>2</sub>CO<sub>3</sub> as the base to give **114** (Scheme 2).<sup>122</sup>



**Scheme 2:** Preparation of the carbazole derivatives. Reagents and conditions: a) Dichloroethane, KOH,  $K_2CO_3$ , TBAF, 60 °C, 18h, 40%; b) *p*-Toluensulfonyl chloride, triethylamine, DCM, rt; c) NaH, DMF, rt, 24h, 4%; d) piperidine,  $K_2CO_3$ , DMF, 60°C, 24h, 44%; 18h, 75%;

### 3.2.3 Results and discussion

A total of 13 compounds were synthesized in this study (**104-114**), that underwent biological assays. The main biological assays that we have performed are:

1. Efflux inhibitory activity
2. Evaluation of the synergistic effect of the selected TDZ analogues in combination with first- and second-line anti-TB drugs
3. Evaluation of the intracellular anti-TB activity of the selected TDZ analogues

## **1. Efflux inhibitory activity**

In order to set up a faster and cheaper model for screening the activity of the compounds, they were first evaluated for their antimycobacterial and efflux inhibitory activity against *M. smegmatis* mc<sup>2</sup>155 reference strain. For those compounds showing inhibitory activity higher than TDZ, cytotoxicity on human-monocyte derived macrophages was assessed. Compounds showing less cytotoxicity and higher efflux inhibitory activity than that of TDZ, were further evaluated on Mtb H37rv, as described herein. The procedures and the results obtained are reported below.

### **a) Antimycobacterial and efflux inhibitory activity against *M. smegmatis* mc<sup>2</sup>155**

The compounds were first tested for their capability to inhibit the growth of *M. smegmatis* strain mc<sup>2</sup>155 in a microdilution assay (Table 1). The compounds demonstrated extremely poor or absent antimycobacterial activity against *M. smegmatis*, especially if compared with TDZ, which was used as positive control. This was considered a good result, as high bactericidal/bacteriostatic activity could affect the following experiments of synergy with first- and second-line anti-TB agents. Due to the reduced solubility and the low antimycobacterial activity, it was not possible to determine the exact MIC values for some compounds (**104, 105, 108, 110, 112, 113, 114**). As such, when bacterial growth is still noticed at the maximum concentration tested, the MIC was indicated by ">MIC". For instance, >256 µg/mL means that the MIC of this compound is higher than 256 µg/mL, as it was technically impossible to determine it. After determining their MICs, the compounds were tested for their capability to



inhibit efflux of EtBr from *M. smegmatis* mc<sup>2</sup>155 cells by real-time fluorometry, using TDZ and VER as controls (Table 1). Relative final fluorescence (RFF) is based on accumulation of EtBr at 0.25 µg/mL and the results are presented as the average of three independent assays plus standard deviation ( $\pm$  SD). According to a widely used protocol for this kind of assay,<sup>123</sup> in order not to compromise the cellular viability, all of the compounds were tested at  $\frac{1}{2}$  of their MIC. For those compounds for which the exact MIC could not be determined (above reported), the last concentration value that could be technically determined was considered  $\frac{1}{2}$  of the MIC.

Comp	<i>M. smegmatis</i> mc <sup>2</sup> 155		IC <sub>50</sub> µg/mL(µM)
	MIC (µg/mL)	RFF ± SD	
104	>256	1.17 ± 0.46*	84.8 (264.7)
105	>256	0.72 ± 0.19*	ND
106	256	0.95 ± 0.15*	8.8 (30)
107	64	0.81 ± 0.27*	10.5 (32.51)
108	>256	15.34 ± 0.82***	170.8 (701.8)
109	64	0.94 ± 0.079**	0.762
110	>64	0.61 ± 0.16*	ND
111	256	0.76 ± 0.04**	ND
112	>256	0.39 ± 0.16*	ND
113	>64	-0.17 ± 0.16	ND
114	>256	0.08 ± 0.18	ND
TDZ	30	0.82 ± 0.1*	5.6 (13.78)
VER	800	2.21 ± 0.14**	50.5 (116.6)

**Table 1:** Screening of the antimycobacterial and efflux inhibitory activity of the compounds against *M. smegmatis* mc<sup>2</sup> 155 and their toxicity towards human monocyte derived macrophages. ND: not determined. The results were considered significant when \*P<0.05 and highly significant when \*\*P<0.01 and \*\*\*P<0.001.

**b) Cytotoxicity evaluation of compounds 104, 106, 107, 108 and 109**

Compounds **104, 106, 107, 108** and **109**, that resulted more active than TDZ in inhibiting the efflux of EtBr out of *M. smegmatis* cells, were evaluated against human-monocyte derived macrophages to assess their *in vitro* cytotoxicity (Table 1). We were pleased to notice that, with the exception of compound **109** (IC<sub>50</sub> = 0.762 µg/mL) all of the tested compounds were found to be less cytotoxic than TDZ in this assay. Compounds **106** and **107**,

(IC<sub>50</sub> = 8.8 µg/mL and 10.5 µg/mL, respectively) are two-fold less cytotoxic than TDZ (IC<sub>50</sub> = 5.6 µg/mL), whereas compounds **104** and **108** (IC<sub>50</sub> = 84.8 µg/mL and 170.8 µg/mL) were found to be safe towards human macrophages. Overall, these preliminary data clearly suggest that the replacement of the phenothiazine core with other ring systems allows maintaining the efflux inhibitory activity with the possibility to decrease the cytotoxicity.

**c) Evaluation of compounds 104, 106, 107 and 108 antimycobacterial and efflux inhibitory activity against Mtb H37Rv**

Compounds **104**, **106**, **107** and **108** were tested against the pan-susceptible reference strain H37Rv, following the same rationale used for *M. smegmatis*, i.e. the determination of antimycobacterial activity and the evaluation of their effect on EtBr efflux (Table 2). As observed for *M. smegmatis*, the selected derivatives showed no antimycobacterial activity against Mtb, therefore excluding the possibility of bias during the following assays. With regard to their activity as inhibitors of EtBr efflux, the compounds were tested with the same procedure used as in the case of *M. smegmatis*, the RFF is based on accumulation of EtBr at 0.5 µg/mL and the results are presented as the average of three independent assays plus standard deviation (± SD). Compound **106** showed similar activity to that of TDZ, whereas compounds **104**, **107** and **108** were found to be 2-4 fold more potent than TDZ, although less active than VER (Table 2). Although quite active, the benzimidazole derivative **108** failed to reproduce the extraordinary efflux inhibitory effect observed against *M. smegmatis*. This is not surprising and can be somehow explained on the basis of the faster

metabolism of *M. smegmatis* compared to that of Mtb, that accounts for the higher susceptibility to the efflux inhibitory effect. Our own experience shows that RFF values are always scaled down Mtb in comparison to those observed for the same compounds in *M. smegmatis*, although maintaining the inhibitory relation.<sup>124,125</sup> Regardless, we can claim that, in the conditions reported, all of the tested compounds have maintained their superior capability of inhibiting efflux compare to TDZ against Mtb.

Comp	<i>M. tuberculosis</i> H37Rv	
	MIC (µg/mL)	RFF ± SD
<b>104</b>	>256	0.84 ± 0.02*
<b>106</b>	128	0.33 ± 0.11
<b>107</b>	>256	1.22 ± 0.09*
<b>108</b>	>256	1.00 ± 0.19
<b>TDZ</b>	15	0.27 ± 0.02
<b>VER</b>	512	1.94 ± 0.005**

**Table 2:** Evaluation of the antimycobacterial and efflux inhibitory activity of the selected compounds against Mtb H37Rv. The results were considered significant when \*P<0.05 and highly significant when \*\*P<0.01.

## **2. Evaluation of synergistic effect of the selected TDZ analogues in combination with first- and second-line anti-TB drugs and determination of the fractional inhibitory concentration (FIC).**

Once that the inhibition of efflux was confirmed, the study went ahead evaluating compounds **104**, **106**, **107** and **108** for their effect in combination with the current first-line (INH and RIF) and second-line (AMK and OFX) drugs used for the treatment of TB. Their effect was also tested in

combination with EtBr, to correlate its efflux with the efflux of the anti-TB drugs.<sup>126</sup> The MICs of INH, RIF, AMK and OFX were calculated in the absence and in the presence of scalar sub-inhibitory concentrations of each compound against Mtb H37Rv, that is known to have intrinsic and readable efflux activity of these anti-TB drugs<sup>124,127</sup> (Table 3). For some compounds was also determined the modulation factor (MF), it reflects a reduction of the MIC values of a given antibiotic in the presence of an inhibitor and was considered significant when  $MF \geq 4$  ( $\geq$ four-fold reduction). MF was calculated with the following formula:  $MF = \frac{MIC_{\text{antibiotic}}}{MIC_{\text{combination}}}$ .

Comp	test conc <sup>a</sup>	MIC (µg/mL) against Mtb H37Rv (MF) <sup>b</sup>				
		INH	RIF	AMK	OFX	EtBr
	no comp	0.1	1	2	2	12.5
104	256	0.1	<0.015(>↓64)	2	1	12.5
	128	0.1	0.25(↓4)	2	2	12.5
	64	0.1	0.25(↓4)	2	2	12.5
	32	0.1	0.25(↓4)	2	2	12.5
	16	0.1	0.25(↓4)	2	2	12.5
	8	0.1	0.25(↓4)	2	2	12.5
	4	0.1	0.25(↓4)	2	2	12.5
106		<0.0007				
	64	8 (↓>128)	<0.015(>↓64)	<0.015(> ↓128)	<0.015(> ↓128)	<0.195 (>↓64)
	32	0.05	0.062 (↓16)	0.625 (↓4)	1	1.56 (↓4)
	16	0.1	0.5	1	1	6.25
	8	0.1	0.5	1	1	12.5
	4	0.1	1	1	1	12.5
	2	0.1	1	1	1	12.5
1	0.1	1	1	1	12.5	
107		<0.0007				
	256	8 (↓>128)	<0.015(>↓64)	<0.0156 (>↓128)	<0.0156( >↓128)	<0.195 (>↓64)
	128	<0.0015 (>↓64)	<0.015(>↓64)	<0.0156 (>↓128)	<0.0156( >↓128)	<0.195 (>↓64)
	64	0.05	<0.015(>↓64)	>0.0156 (>↓128)	<0.0156( >↓128)	1.56 (↓8)
	32	0.1	0.031(↓32)	1	1	6.25
	16	0.1	0.062(↓16)	1	1	12.5
	8	0.1	0.25(↓4)	1	1	12.5
4	0.1	0.5	1	1	12.5	
108		<0.0007				
	256	8 (↓>128)	<0.015(>↓64)	<0.015(> ↓128)	<0.015(> ↓128)	<0.195 (>↓64)
	128	0.1	0.5	1	1	12.5
	64	0.1	0.5	1	1	12.5
	32	0.1	0.5	1	1	12.5
	16	0.1	0.5	1	1	12.5
	8	0.1	0.5	1	1	12.5
4	0.1	0.5	1	1	12.5	
TDZ	7.5	<0.0007	<0.015(>↓64)	<0.015	<0.015(>	<0.195

	8 (↓>128)		(>↓128)	↓128)	(>↓64)	
	3.75	0.05	1	1	1	3.125 (↓4)
	1.88	0.1	1	1	1	6.25
	0.94	0.1	1	1	1	6.25
	0.47	0.1	1	1	1	6.25
	0.23	0.1	1	1	1	6.25
	0.12	0.1	1	1	1	6.25
	<0.0007					
	128	8 (↓>128)	<0.015(>↓64)	<0.015 (>↓128)	<0.015(> ↓128)	<0.195 (>↓64)
	64	0.05	0.25 (↓4)	1	1	3.125 (↓4)
VER	32	0.1	0.5	1	1	6.25
	16	0.1	0.5	1	1	6.25
	8	0.1	0.5	1	1	12.5
	4	0.1	1	1	1	12.5
	2	0.1	1	1	1	12.5

**Table 3:** Evaluation of the synergistic effect and determination of the modulation factor of the selected compounds with first- and second- line drugs against *M. tuberculosis* H37Rv. <sup>a</sup>Concentration at which the compound was tested (in µg/mL). <sup>b</sup> modulation factor.

Initially, compounds **104**, **106**, **107** and **108** were tested at ½ of their MIC, and then, according to the protocol widely used for this sort of investigations,<sup>123</sup> they were tested by two-dimensional broth microdilution checkerboard assay, to evaluate the extent of the synergism. Also in this case, as already explained in the case of the efflux inhibition assays, for those compounds for which the exact MIC could not be determined, ½ of the MIC was considered the concentration that was equal to the highest concentration where it was obtained growth. When tested at these concentrations, all of the newly synthesized compounds and the controls

demonstrated very high synergistic effect with both the antibiotics and EtBr. In this case, the MIC values of INH, RIF, AMK, OFX and EtBr could be reduced more than 64-fold (Table 3). Compound **107**, for which the inhibitory effect on efflux was already assessed, had in general a very high synergistic effect with the tested drugs and, in particular, with RIF. In fact, compound **107** was able to improve the activity of RIF by 4-fold at concentrations as low as 8 µg/mL (approx. 1/64 of its MIC), demonstrating a potent synergistic effect. Moreover, at a concentration of 64 µg/mL (approx. 1/8 of its MIC), compound **107** was also able to improve the activity of AMK and OFX by more than 128-fold, and EtBr by 8-fold (Table 3). Importantly, we have noticed that the synergistic activity demonstrated by the compounds in combination with EtBr correlates well with the results obtained with the inhibition of EtBr efflux by RFF.

One may argue that TDZ, considering the absolute concentrations at which the synergistic activity is measured, is slightly more active than compound **107**. However, seen under a more widespread perspective, compound **107** is less toxic, more active with regard the inhibition of efflux, and unlikely to possess CNS-related properties. This can be considered a good achievement, in particular considering that the aim of this paper was the selection of compounds devoid of antimycobacterial activity, with reduced toxicity to the human macrophage and with higher efflux inhibitory capability, so as to promote the antimycobacterial activity of the anti-TB drugs and be considered as a future adjuvant in the fighting against TB.

Surprisingly, despite the high activity in inhibiting the efflux, compound **108** was found to be not active in the combination assay. Compounds **104** and **106** were found to be slightly less active than **107** in the combination assay;



however, in the case of compound **104**, it must be noticed that it is able to improve the activity of RIF by 4-fold also at very low concentrations. It is intriguing to notice that compounds **104** and **106**, as compound **107**, demonstrated to have a significant synergistic effect in particular with RIF. The reason of this preferred synergism is worth of further investigation but, at this moment, it can only be speculated that **107**, as well as the other derivatives belonging to this series, although to a lesser extent, have high affinity for interfering with efflux systems that extrude RIF. However, it cannot be ruled out that the two derivatives interfere with other mechanism of resistance used by the cell in the presence of RIF. Finally, it is worth of consideration the fact that compounds **104**, **106** and **107** were more active in the combination assay than VER, another drug often investigated for its potential role as adjuvant in the TB treatment.

The synergistic activity between the compounds was also represented as the fractional inhibitory concentration (FIC), that is a value expressing the synergistic activity of the compounds in combination with the antibiotics and EtBr (Figure 5). FIC was determined for each anti-TB drug by dividing the MIC of each drug when used in combination, by the MIC of each drug used alone. Since a drug cannot interact with itself, the effect of a self-drug combination will always be additive, with an FIC index of 1. As such, when the FIC value is lower than 0.25, a synergistic effect is noticed between the modulator and the antimicrobial. When above 2, there is antagonism between the compounds tested, whereas within these two FIC values, indifference is noticed.

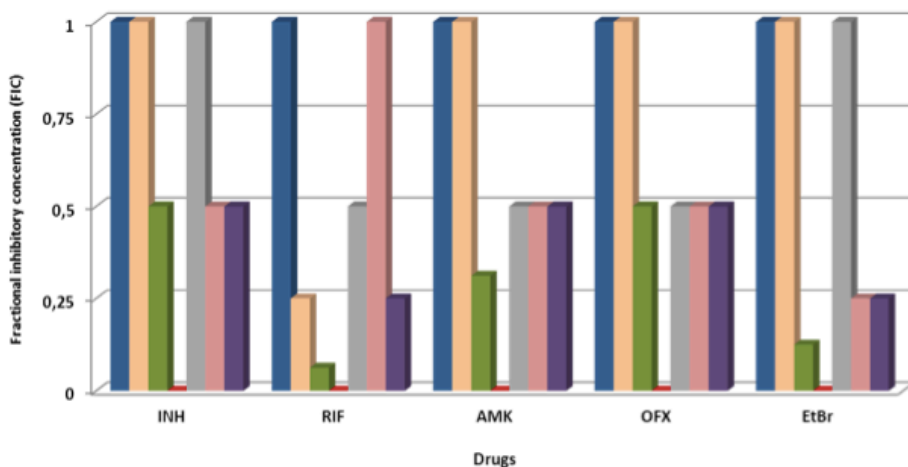


**Figure 5:** Fractional inhibitory concentration (FIC) determination for each combination against Mtb H37Rv. Blue (no EPIs), orange (**104**), green (**106**), red (**107**), grey (**108**), pink (TDZ) and purple (VER).

Isobolograms were constructed, by plotting changes in the MIC of antibiotics as a function of the tested compounds concentration (**104**, **107** and **108**, 128 µg/mL; **106**, 32 µg/mL; VER, 64 µg/mL, and TDZ, 3.75 µg/mL). As it can be seen, for the majority of the combinations of compound **107** with the antibiotics synergy was observed, with FIC values ranging from 1 to not possible to determine (ND) due to the very high synergistic effect, depending on the antibiotic combination.

### 3. Evaluation of the intracellular anti-TB activity of the selected TDZ analogues.

Finally, we evaluated the intracellular antimycobacterial activity of compounds **104**, **106**, **107** and **108** alone and in combination with INH or RIF against Mtb human monocyte-derived macrophages (Figure 6). This assay is a fair reproduction of what actual happens during the TB infection, and

therefore it can help in obtaining a clearer idea of the potential of our compounds. INH and RIF were used at  $\frac{1}{2}$  of its MIC (0.05 and 0.5  $\mu\text{g}/\text{mL}$ , respectively), therefore having no direct inhibitory effect on the bacteria at these concentrations. The compounds **104**, **106**, **107** and **108** were tested at nontoxic concentrations (16  $\mu\text{g}/\text{mL}$ , 0.078  $\mu\text{g}/\text{mL}$ ; 1.25  $\mu\text{g}/\text{mL}$ , and 40  $\mu\text{g}/\text{mL}$ , respectively) determined against human-monocyte derived macrophages. Above these concentrations, macrophage viability is reduced below 90%, nullifying the assay. At these concentrations, the compounds tested showed to be devoid of any antimycobacterial activity against intracellular Mtb. Consistent with the findings above reported, we were pleased to notice that the co-administration of the compounds with INH or RIF (at a non-antibiotic inhibitory concentration) led to a strong enhancement of the killing activity of the human macrophages against the H37Rv strain. This is comparable with the results previously obtained with TDZ and other efflux inhibitors that has been shown to have a dual bacterial-host boosting effect against Mtb.<sup>67</sup>

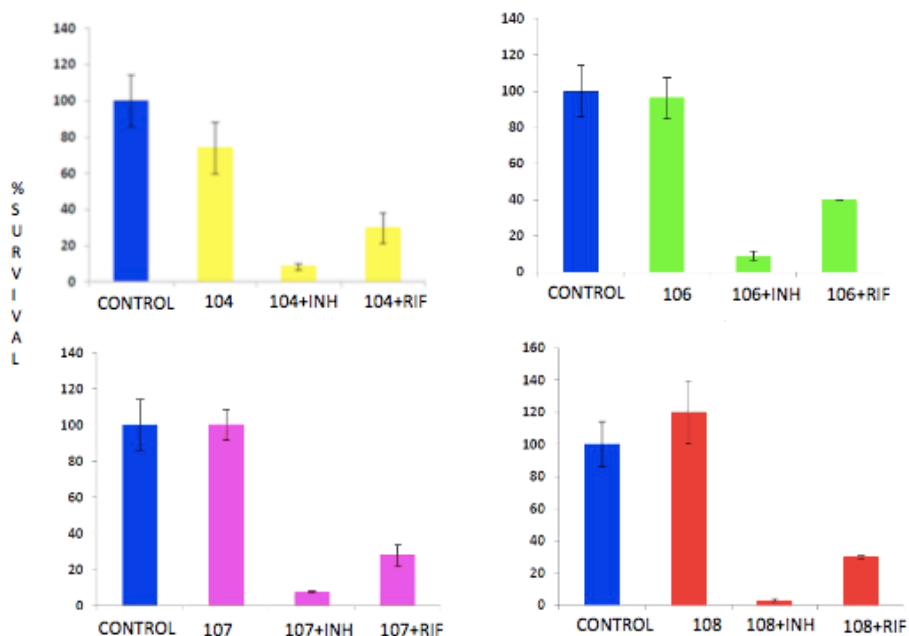


**Figure 6:** Determination of the intracellular activity of compounds **104**, **106**, **107** and **108** against *M. tuberculosis*-infected human macrophages.

### 3.2.4 Structure-Activity Relationships (SAR)

Despite the small set of compounds prepared for this study, a few SAR considerations can be made. In general, the majority of the compounds bearing the N-methyl-2-piperidinyl appendage had inhibitory effect on the efflux of EtBr. We were pleased to notice that compound **104**, designed as a hybrid molecule resembling both VER and TDZ, had a very good inhibitory activity of EtBr efflux. However, the same does not apply to the other hybrid compound **105**. It might be then speculated that the N-methyl-2-piperidinyl appendage must be attached, through an ethylene linker, to another nitrogen atom of the heterocyclic, yielding a more polar structure. When the N-methyl-2-piperidinyl appendage is attached through an ethylene linker either to tricyclic (compounds **106**, **109**), bicyclic

(compounds **107**, **108**) or more flexible ring structures (compounds **110**, **111**), a good inhibitory activity, sometimes higher than that of the parent compound TDZ, is noticed. However, small rings (compound **112**), has a detrimental impact on the efflux inhibitory properties. Surprisingly, the benzimidazole derivative **108** showed an exceptionally high activity, resulting by far more potent than VER. The distance between the nitrogen of the appendage and that of the heterocyclic seems to have pharmacological significance, since the activity of compound **113** is considerably low. Finally, the presence of a tertiary aliphatic amino moiety seems to be determinant, being compound **112** the least active of the series.

### **3.2.5 Conclusion**

The contribution of efflux systems to Mtb drug resistance and tolerance has been increasingly recognized, although only a few medicinal chemistry efforts have been made towards the synthesis of Mtb efflux inhibitors. Despite the amount of literature establishing TDZ as a valuable agent against TB, the numerous toxicity issues have always hampered its safe administration as an adjuvant of TB therapy. To our knowledge, this is the first medicinal chemistry campaign aimed at modifying TDZ with regard to its potential as adjuvant of TB therapy, with specific assays such as the determination of the efflux inhibition and the synergistic activity in combination with known anti-TB drugs both *in vitro* and *ex vivo*. Compared to TDZ, the representative derivatives tested were found to be less toxic toward human macrophages, ranging from two-fold (compound **106** and **107**) to more than 50-fold (compound **108**). Compound **104**, intended as a hybrid of TDZ and VER, showed a higher inhibitory activity than that of TDZ

itself and much less toxicity, therefore confirming the rationale of the design. More importantly, we have escaped from the phenothiazine scaffold, thus assuming a reduction of the onset of side effects at the CNS level. The newly synthesized compounds showed high synergistic activity when tested in combination with some of the most important first-line (INH, RIF) and second-line (AMK, OFX) drugs used for the treatment of TB. In particular compound **107** was able to improve the activity of RIF at concentration as low as approximately 1/64 of its MIC. Additionally, these compounds were able to improve the activity of INH and RIF against intracellular Mtb. Considering the data on inhibition of EtBr efflux, coupled to the low antimycobacterial activity, it might be claimed that the synergetic activity is due to their ability to hamper the intrinsic mycobacterial drug efflux.

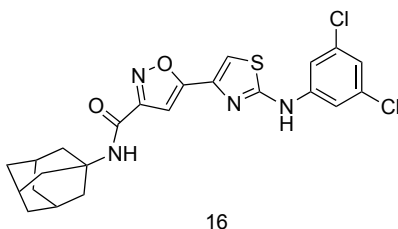
Finally, we confirmed *M. smegmatis* mc<sup>2</sup>155 as a suitable surrogate of Mtb for the preliminary assessment the efflux inhibitory activity, at a lower cost and time consuming rate. Altogether, these findings provide a solid base to further investigate compound **107** as a booster of the antimycobacterial chemotherapy when associated with first- and second-line drugs, by virtue of its capability to block the intrinsic efflux activity of mycobacteria. This might represent a lateral approach toward the cure of TB.

Studies expanding this versatile series and its mechanism of action and activity toward Mtb drug resistant strains, especially resistant to isoniazid and rifampicin (MDR-TB), are currently underway in our research groups.

### 3.3 Development of new chemotypes as inhibitors of efflux

As reported, the inhibition of efflux is a valuable and “lateral” approach to treat mycobacterial infections, so we were also interested in finding new EPIs *ex novo*. Therefore, we also screened selected compounds previously synthesized, that were avoid of anti-TB activity, and showing chemical features suitable for efflux inhibition.

Among the compounds tested, compound **16** was found to be particularly interesting.<sup>128</sup>



16

**Figure 7:** Structure of compound **16**.

After a preliminary evaluation as inhibitor of the efflux of ethidium bromide, compound **16** was used as a template for a wider scope study on the rapid screening of compounds with potential use against Mycobacteria. In this work, recently published,<sup>128</sup> using *M. smegmatis* as a model organism, a methodological strategy to identify compounds with antimycobacterial activity or with potential adjuvant properties, by either inhibition of efflux or other unrelated mechanisms, was developed. Such an approach may increase the rate of identification of promising molecules, to be further explored in pathogenic models for their potential use either as antimicrobials or as adjuvants, in combination with available therapeutic regimens for the treatment of mycobacterial infections.

The methodological flowchart presented proposes an approach in which the different biological effects of a given compound are evaluated in successive but nonexclusive steps, yielding maximum functional information for that molecule and its potential use. This approach allows optimizing several resources associated with the evaluation of a new molecule, such as time, laboratorial costs, and amount of the compound available for biological testing.

The design of this flowchart was based on establishing cut-off values for classifying compounds in different categories: antimycobacterial agents, adjuvants by inhibition of efflux activity, adjuvants by an unrelated mechanism, and compounds with no biological interest.

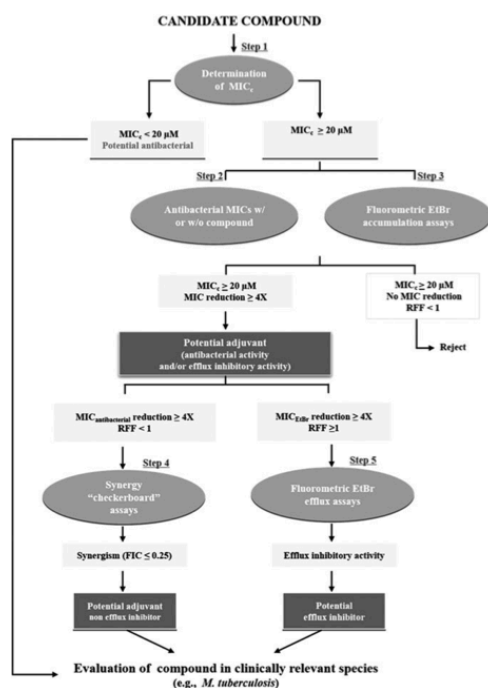


**Figure 8:** Algorithm designed for the rapid screening of new compounds with potential applications against mycobacteria.



The methodologies applied are simple, time-effective, and cost-effective, when compared with the direct evaluation of compounds on pathogenic species such as Mtb, which have higher requirements in terms of biosafety, quantity of compounds, and time consumption.<sup>129</sup>

## 4. Microwave-assisted synthesis of nucleotide phosphoroamidates

As part of my PhD program, I spent 3 months at the Cardiff University working on a project that is outside of the context of this thesis. The following chapter is about the optimization of a microwave-assisted synthesis of nucleotide phosphoroamidates.

### 4.1 Introduction

Nucleoside analogues (NAs) are a central class of molecules accounting for many of the antiviral and anticancer drugs currently on the market, indeed they play an essential role in the antiviral and anticancer treatment. NAs are similar to the natural nucleosides bearing modifications at the base and/or at the sugar moieties, which, in most of the cases, confer selectivity versus the targets.<sup>130</sup>

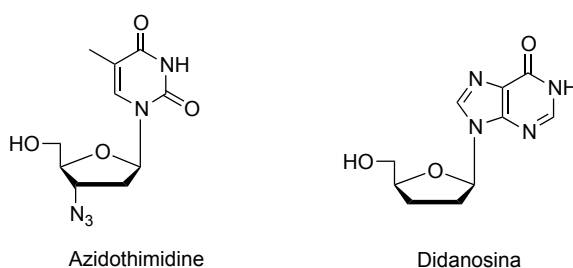


**Figure 1:** Nucleoside analogs (NAs).

NAs are prodrugs and need to be converted into their active species, which usually consists of the 5'- triphosphate form.<sup>131</sup> Their bioactivation pathway often involves three sequential phosphorylation steps, starting from the

parent nucleoside, which is converted to its mono-, di- and finally triphosphate form.

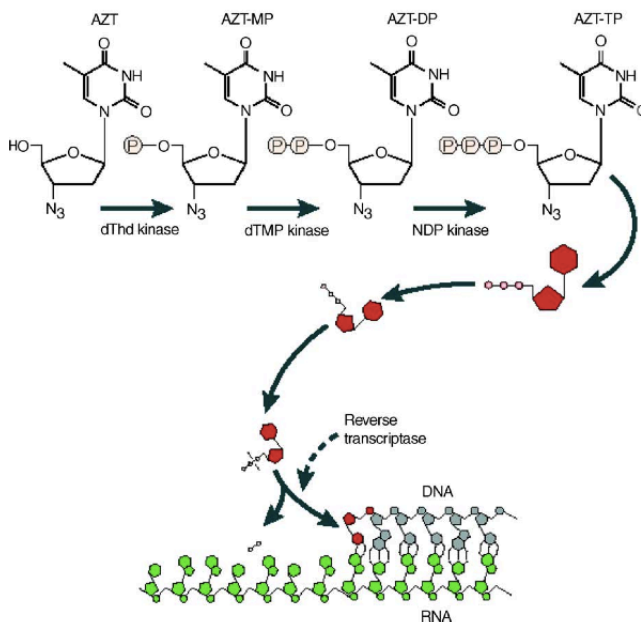


**Figure 2:** Mechanism of action of Azidothymidine (AZT).<sup>132</sup>

Some NAs, such as Abacavir or Famciclovir, require also additional bioactivation steps in order to display their biological activity.<sup>133,134</sup> The first step of phosphorylation is usually considered to be the rate-limiting step in the bioactivation of NAs, with few exceptions such as Zidovudine, for which the second phosphorylation may be the rate limiting step.<sup>135</sup> The nucleoside kinases activity, after a long-term treatment with NAs, may be decreased eventually leading to the advance of drug resistance. Moreover, many NAs are not phosphorylated effectively *in vivo*, being poor substrates for kinases, and thus their therapeutic potential is quite limited.<sup>136</sup>

In their triphosphate form, these molecules can act as competitive inhibitors of viral and cellular DNA or RNA polymerases or alternatively can

be incorporated into growing DNA or RNA strands, causing chain termination and thus affecting the proliferation of cancer cells or inhibiting the replication of the viral genome.<sup>132</sup>

Moreover, to overcome the first phosphorylation step, nucleotides with a phosphate moiety already attached to the nucleoside have been studied. However, due to the high polarity of the phosphate group, monophosphate nucleosides poorly penetrate through cell membranes and are also subjected to extracellular phosphatases, which rapidly convert the nucleotide back to its nucleoside.<sup>136</sup>

Several mono-phosphate prodrug strategies are currently under investigations to overcome these issues.<sup>137</sup>

## **4.2 ProTide Approach**

Nowadays, one of the most applied phosphate prodrug approaches is the ProTide technology. The development of this technology started by masking the 5'-O-monophosphate groups of therapeutic nucleosides with simple dialkyl, first, and haloalkyl, later, groups. However, these attempts did not lead to improved biological activity, most likely due to the inability of these masking groups to be hydrolysed *in vivo* to release the nucleoside monophosphate, which can be subsequently further phosphorylated to the active species.<sup>138</sup> Next, McGuigan and co-workers synthesized alkyloxy and haloalkyl phosphoramidate prodrugs, and these showed better activities than their parent nucleosides.<sup>139</sup> This was the first breakthrough in the development of ProTides and provided evidences that the masking of phosphate groups with biocleavable motifs may yield an effective prodrug system for the delivery of therapeutic nucleoside monophosphates.<sup>140</sup>

The ProTide approach consists of a nucleoside phosphate masked with a

phosphoroamidate prodrug, generally represented by an amino acid ester moiety linked with a P-N bond to a nucleoside aryl phosphate.<sup>136</sup>

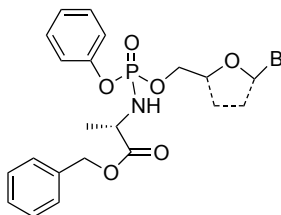


**Figure 3:** ProTides general structure.

The mode of action of these aryloxyphosphoroamidates, leading to the intracellular delivery of active nucleoside monophosphates, has been studied in detail over the years.<sup>141,142</sup> After crossing the cell membrane, the monophosphate deprotection is initiated by an esterase or cathepsin A, producing carboxylate A.<sup>143</sup> A spontaneous intramolecular cyclization to a five-membered ring occurs, releasing a molecule of phenol. Cyclic intermediate B undergoes chemical opening in the presence of water leading to phosphoroamidate diester C. Finally, cleavage of C by intracellular phosphoroamidase or histidine triad nucleotide-binding protein 1 (HINT-1) frees the nucleoside monophosphate.<sup>144</sup> (Figure 4)

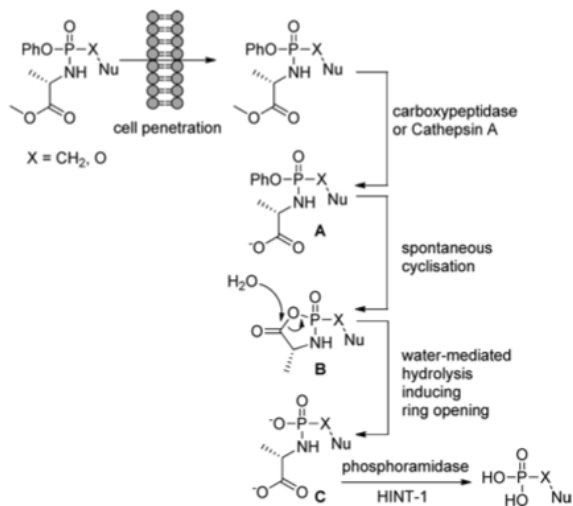


**Figure 4:** Mode of action of ProTides.<sup>144</sup>

Proof of concept for ProTide has now been clinically validated in the human immunodeficiency virus (HIV), hepatitis B (HBV), and hepatitis C virus (HCV), leading to several potent and selective prodrugs such as the FDA-approved sofosbuvir<sup>144</sup> (Figure 5).

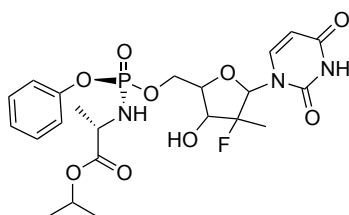


**Figure 5:** Sofosbuvir.

### 4.3 ProTide preparation

Aryloxyphosphoramidate nucleoside prodrugs are generally prepared by coupling of nucleosides with phosphorochloridate by either 5' deprotonation of the nucleoside with t-BuMgCl or by activation of the imidazolium intermediate with NMI<sup>145</sup> and subsequent substitution with chlorophosphoramidate or aryloxyphosphoramidate. These two approaches are substrate dependent, and it is very difficult to predict which one to use for the best outcome.

It should be noted that these synthetic approaches lead to around 1:1 mixtures of diastereoisomers at the phosphorus center, often inseparable by flash chromatography. These isomers have often different *in vitro* biological properties and this stimulated the researchers to developed a diastereoselective approach using enantiomerically pure aryloxyphosphoramidate reagents.<sup>144</sup>

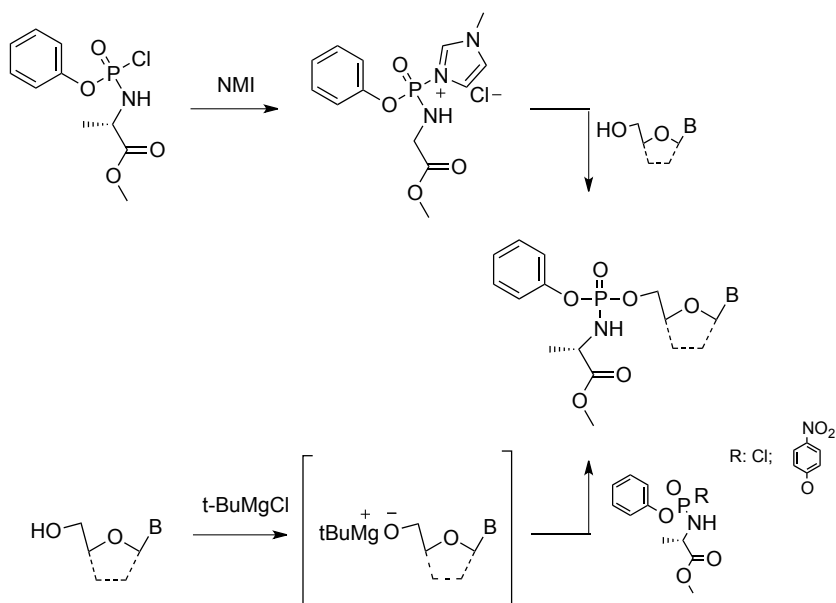


**Figure 6:** Mechanism to generate phosphoramidates nucleoside prodrugs.

During the past years, substitution of the phosphorochloridate has been

explored by modifying the nature of the aryloxy portion, the amino acid, and the amino acid ester.

The phosphochloridate reagents are generally prepared by reaction of phenyl dichlorophosphate with the appropriate amino acid ester in the presence of triethylamine and, for the synthesis of the compound with *p*-nitrophenol as the leaving group, the mixture was also reacted with *p*-nitrophenol. Phosphoroamidates are generally obtained as a mixture of diastereoisomers, they are often used crude but higher yields are observed when purified.<sup>144</sup>

However, the methodologies reported before (Figure 6) present some limitations:

- Long reaction time
- Low reaction yield

A small part of my PhD investigation has been focused on the improvement of the ProTide synthetic strategy.



#### 4.4 Aim of the work

Inspired by these considerations, the project in which I have been involved regards the optimization of a microwave-assisted synthesis of nucleotide phosphorimidates. The idea was to validate whether it was possible to develop a new microwave-assisted approach reducing the reaction time and improving the reaction yields.

During my period at the Cardiff University I have focused my attention on 3 nucleosides: guanosine, thymidine and adenosine.

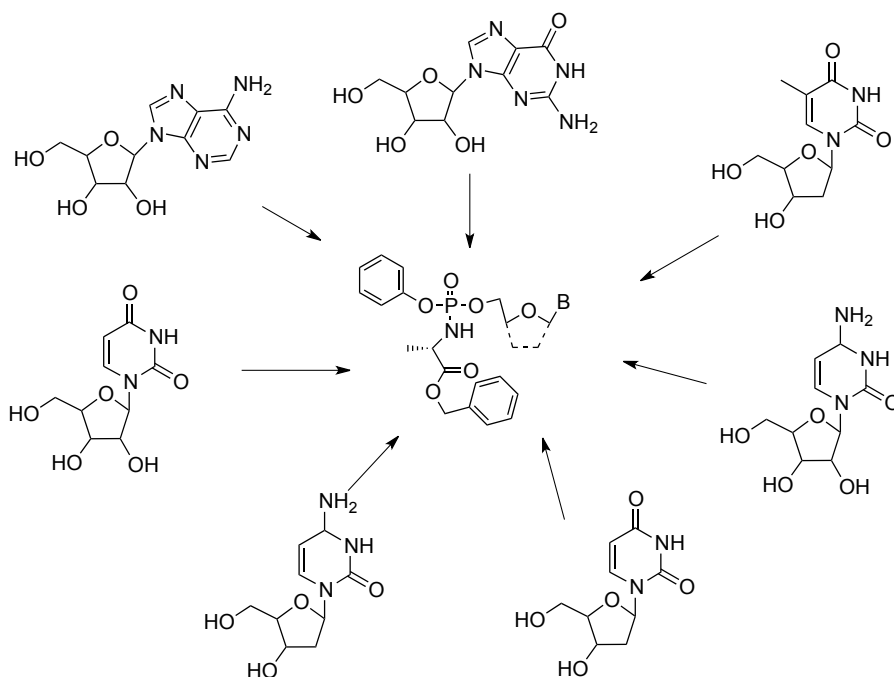


**Figure 7:** Aim of the work.

## 4.5 Results

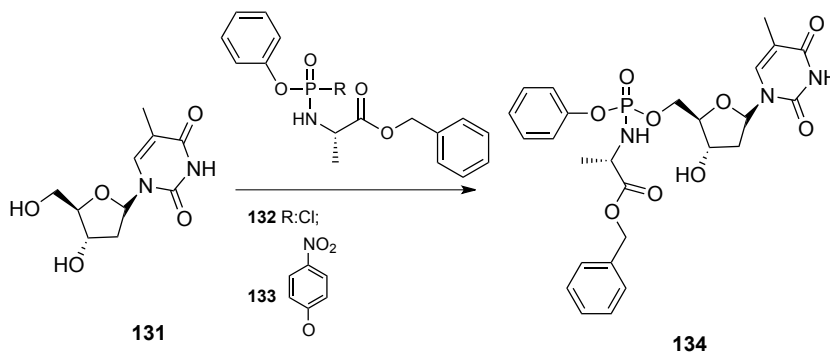
Starting with procedures retrieved in the literature<sup>136,146,147,148</sup>, the parameters that we have set were:

- NMI vs t-BuMgCl methodologies
- Solvent
- Stoichiometry
- Traditional heating vs  $\mu$ W irradiation

Each reaction was performed either with conventional heating and under microwave irradiation, to compare the different methodologies.

After the isolation of the ProTide and the eventual by-products, the percentage presence of each product (starting material, ProTide, and by-products) were calculated through the use of HPLC/UV (see table 1-4).

The first nucleoside that was investigated was thymidine:



### Scheme 1: Thymidine optimization.

For the thymidine optimization we started with the reported conditions of the t-BuMgCl methodology. Unfortunately, with this approach, the formation of the secondary product was predominant compare to the desired product (Figure 8).

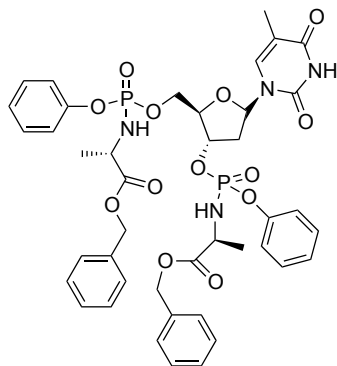


**Figure 8:** Thymidine by-product.

After the isolation of the di-substituted adduct, we modified the stoichiometry of the reactions (Table 1), but also in this case the ProTide yields resulted very low.

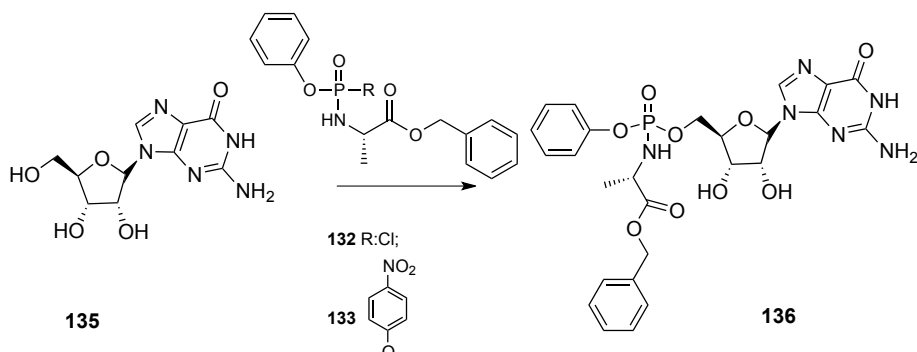
Successively, the focus was shifted on the selection of the solvent, and the reactions were performed in 1,4-dioxane and DMF but, unfortunately, we were not able to obtain the desired product in good yield.

Finally, the reactions were performed with the NMI methodology. With this procedure, we obtained the ProTide in high yields only under  $\mu\text{W}$  irradiation.

Reagents	Solvent	Eq	Starting material	Protide	By-product	Reaction type	Reaction time
t-BuMgCl R: p-NO <sub>2</sub>	THF/NMP	3/2	6.2%	25.2%	68.5%	μW 65°C	20 min
t-BuMgCl R: p-NO <sub>2</sub>	THF/NMP	3/2	8.6%	40.5%	51.0%	Conv 55 °C	1 h
t-BuMgCl R: p-NO <sub>2</sub>	THF/NMP	0.5 * 4	51.1	17.7-24.0%	2.6%	μW 65°C	1 h
t-BuMgCl R: p-NO <sub>2</sub>	THF/NMP	0.5 *4	15.8%	17.9-26.9 %	39.4%	Conv 55 °C	1.50 h
t-BuMgCl R: p-NO <sub>2</sub>	THF/NMP	1 * 3	5.5%	1.5%-3.2%	89.9%	Conv 55°C	1.25 h
t-BuMgCl R: p-NO <sub>2</sub>	THF/NMP	1.5/1. 5	26.0%	15.7-20.7%	37.6%	μW 65°C	40 min
t-BuMgCl R: p-NO <sub>2</sub>	THF/NMP	4/4	15.2%	4.6-10.1%	70.1%	Conv 55°C	4.30 h
t-BuMgCl R: p-NO <sub>2</sub>	1,4-dioxane	2/2	79.8%	8.5%	11.7%	μW 65°C	30 min
t-BuMgCl R: p-NO <sub>2</sub>	1,4-dioxane	2/2	23.4%	38.5%	38.1%	Conv 55°C	2.40 h
t-BuMgCl R: p-NO <sub>2</sub>	DMF	2/2	5.1%	15.4- 13.4%	66.1%	Conv 55°C	40 min
t-BuMgCl R: p-NO <sub>2</sub>	DMF	2/2	29.8%	45.1%	25.1%	μW 65°C	20 min
NMI R: Cl	<b>THF</b>	<b>6.3/3</b>	<b>1.4%</b>	<b>70.0%</b>	<b>28.8%</b>	<b>μW 65°C</b>	<b>5 min</b>
NMI R: Cl	THF	6.3/3	50.9%	28.7%	20.5%	Conv 55°C	4 h

**Table 1:** Thymidine optimization.

The second nucleoside that was investigated was guanosine:



### Scheme 2: Guanosine optimization.

For the guanosine optimization, we started with the standard conditions reported for the NMI methodology and, after the first reaction, we understood that for this nucleoside a long reaction time is needed. In order to reduce the reaction time, the temperature was increased up to 75°C and 85°C, although with no appreciable result. Finally, we performed the Grignard methodologies with phosphorochloridate, but also in this case the reaction did not lead to the desired compound.

Reagents	Solvent	Eq	Starting material	ProTide	Reaction type	Reaction time
NMI R: Cl	THF/Pyridine	6.3/3	51.4%	48.6%	Conv 55 C	24 h
NMI R: Cl	THF/Pyridine	6.3/3	87.2%	12.8%	$\mu$ W 65° C	35 min
NMI R: Cl	THF/Pyridine	6.3/3	100%		$\mu$ W 75° C	10 min
NMI R: Cl	THF/Pyridine	6.3/3	90.9%	9.1%	$\mu$ W 85° C	15 min
tBuMgCl R: Cl	THF	3/2	100%		Conv 55 C	4 h
tBuMgCl R: Cl	THF	3/2	100%		$\mu$ W 65 C	30 min

**Table 2:** Guanosine optimization (1).

Successively, the focus was shifted on the solvent. Reactions were performed in DMF and THF/NMP, to improve the solubility, but we did not obtain good results. Then, extending the reaction time, and raising the temperature up to 75°C and 85°C we could isolate the bis-adduct, although in very low yields.

Finally we modified the reaction stoichiometry, and we are very pleased to notice that, augmenting the amount of both the reagents (4/4), it was possible to obtain the desired product in 78.6% yield.

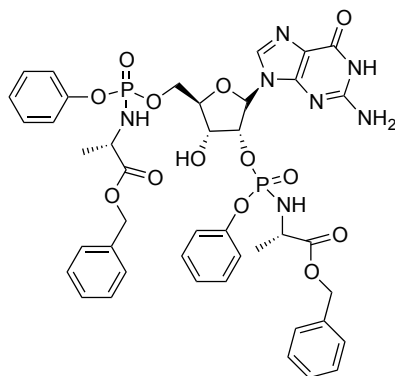
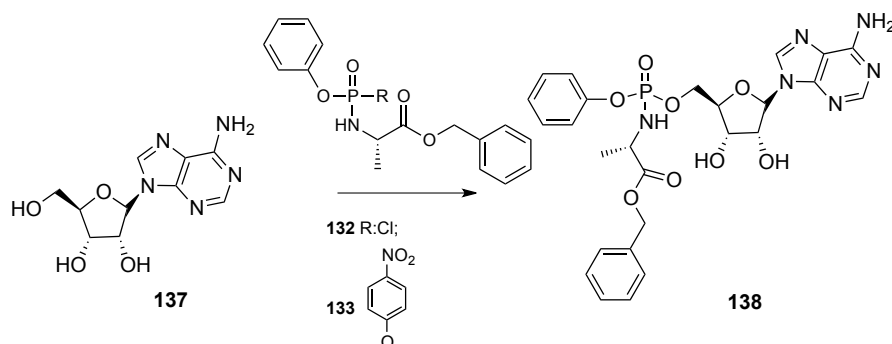


**Figure 9:** Guanosine by-product.

Reagents	Solvent	Eq	Starting material	ProTide	By-product	Reaction type	Reaction time
tBuMgCl R: p-NO <sub>2</sub>	DMF	3/2	32.5%	67.6%	0%	Conv 55° C	7.30 h
tBuMgCl R: p-NO <sub>2</sub>	DMF	3/2	75.4%	24.6%	0%	μW 65° C	35 min
tBuMgCl R: p-NO <sub>2</sub>	DMF	3/2	34.6%	29.1 %	36.3%	μW 65° C	1 h
tBuMgCl R: p-NO <sub>2</sub>	DMF	3/2	63.9%	36.1%	0%	μW 75° C	40 min
tBuMgCl R: p-NO <sub>2</sub>	DMF	3/2	76.4%	24.9%	0%	μW 85° C	5 min
tBuMgCl R: p-NO <sub>2</sub>	THF/NMP	3/2	83.0%	17.0%	0%	μW 65 C	20 min
tBuMgCl R: p-NO <sub>2</sub>	THF/NMP	4/2	100%	0%	0%	μW 65 C	30 min
tBuMgCl R: p-NO <sub>2</sub>	DMF	4/4	0	12.4	2.9%	Conv 55	4 h
<b>tBuMgCl R: p-NO<sub>2</sub></b>	<b>DMF</b>	<b>4/4</b>	<b>18.4%</b>	<b>78.6%</b>	<b>3.0%</b>	<b>μW 65</b>	<b>30 min</b>

**Table 3:** Guanosine optimization (2).

Adenosine was the last nucleoside taken under consideration. We performed the reactions following the standard conditions, but we were not able to obtain the target compound in good yields. The optimization for this nucleoside is still on going.



**Scheme 3:** Adenosine optimization.

Reagents	Solvent	Eq	Starting material	ProTide	Reaction type	Reaction time
NMI R= Cl	THF/Pyridine	6.3/3	74.8%	25.2%	$\mu$ W 65 C	35 min
NMI R= Cl	THF/Pyridine	6.3/3	44.7%	55.3%	Conv 55 C	3 h
t-BuMgCl R= p-NO <sub>2</sub>	THF/NMP	3/2	81.7%	18.3%	$\mu$ W 65°C	25 min
t-BuMgCl R= p-NO <sub>2</sub>	THF/NMP	3/2	73.0%	27.0%	Conv 55°C	2.30 h

**Table 4:** Adenosine optimization.



## 4.6 Conclusion

Antiviral and chemotherapeutic agents, based largely on nucleoside analogues, continue to make a major contribution to the current treatment of viral infections and different types of cancer.

In the 1990s, in the group of Prof McGuigan, several aryloxy 5'-phosphoramidate nucleoside prodrugs (ProTide) were shown to bypass the first problematic kinase-promoted phosphorylation step, and eventually furnish the active triphosphorilated species. After that the ProTide technology was successfully and extensively applied to a high number of nucleoside phosphates.

During my PhD, I have given my contribution to the wider scope of Protide preparation by developing a new microwave assisted methodology for the ProTide construction. In particular, I have focused my attention on the optimization of the previously described procedure for thymidine, guanosine and adenosine. For what concerns the synthesis of thymidine (1) and guanosine (2) ProTides some of the reaction conditions were optimized:

1. NMI/phosphorochloridate; 6.3/3 eq;  $\mu$ W; 65°C; 5minutes
2. t-BuMgCl/*p*-nitrophosphoramidate; 4/4 eq;  $\mu$ W; 65°C; 30 minutes

However, optimization of the adenosine is still on going.

## 5. Experimental section

### 5.1 Chemistry

General Information. All the reagents were purchased from Sigma-Aldrich, Alfa-Aesar, and Enamine at reagent purity and, unless otherwise noted, were used without any further purification. Dry solvents used in the reactions were obtained by distillation of technical grade materials over appropriate dehydrating agents. MCRs were performed using CEM microwave synthesizer Discover model. Reactions were monitored by thin layer chromatography on silica gel coated aluminum foils (silica gel on Al foils, SUPELCO Analytical, Sigma-Aldrich) at both 254 and 365 nm wavelengths. When indicated, intermediates and final products were purified through silica gel flash chromatography (silica gel, 0.040! 0.063 mm), using appropriate solvent mixtures. <sup>1</sup>H-NMR and <sup>13</sup>C-NMR spectra were recorded on a BRUKER AVANCE spectrometer at 300, 400, and 100 MHz, respectively, with TMS as internal standard. <sup>1</sup>H-NMR spectra are reported in this order: multiplicity and number of protons. Standard abbreviation indicating the multiplicity was used as follows: s = singlet, d = doublet, dd = doublet of doublets, t = triplet, q = quadruplet, m = multiplet and br = broad signal. HPLC/MS experiments were performed with HPLC instrumentation (Agilent 1100 series, equipped with a Waters Symmetry C18, 3.5 μm, 4.6 mm × 75 mm column) and MS instrumentation (Applied Biosystem/MDS SCIEX, with API 150EX ion source). HRMS experiments were performed with LTQ ORBITRAP XL THERMO.

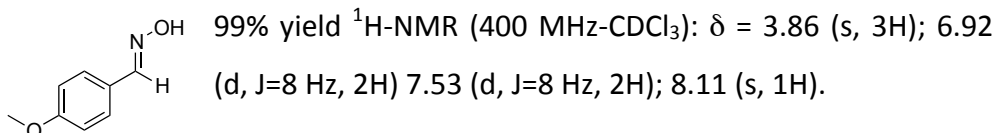
All compounds were tested as 95% purity samples or higher (by HPLC/MS).

### 5.1.1 Evolution of a series of 2-aminothiazoles

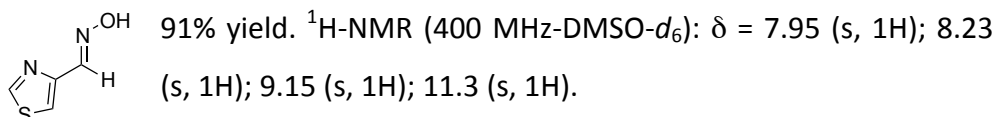
#### General procedure for the oxime synthesis

To a solution of hydroxylamine hydrochloride (1.2 eq) in water (0.7 mL/mmol) was added NaOH 10% (0.5 mL/mmol). Then a solution of the aldehyde (1 eq) in ethanol (3 mL/mmol) was added dropwise. Reaction mixture was stirred at room temperature for 30 minutes. Then the solvents were evaporated under pressure. The residue was solved in water and it was extracted with ethyl acetate. The organic layers were washed with brine and dried over Na<sub>2</sub>SO<sub>4</sub>. After filtration, the solvent was removed *in vacuo* and the crude material was used for the next step without further purification. Yields and analytical data are reported below:

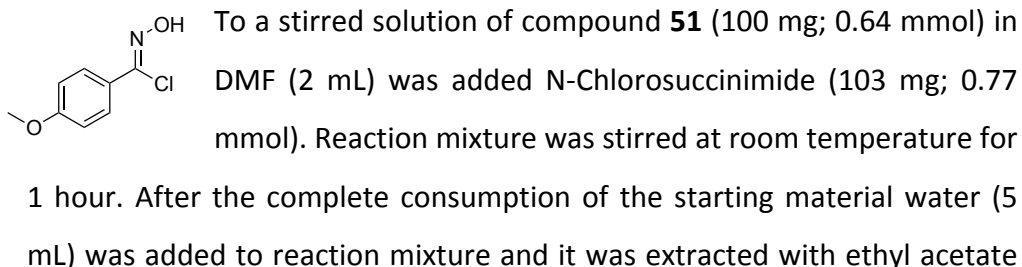
#### (E)-4-methoxybenzaldehyde oxime (51)



#### (E)-thiazole-4-carbaldehyde oxime (53)

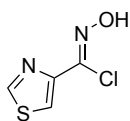


#### Synthesis of (Z)-N-hydroxy-4-methoxybenzimidoyl chloride (40)



(3\*10 mL). The combined organic layers were washed with brine, dried over Na<sub>2</sub>SO<sub>4</sub>, and evaporated under pressure. The crude material was used for the next step without further purification. Quantitative yield.

### Synthesis of (Z)-N-hydroxythiazole-4-carbimidoyl chloride (41)

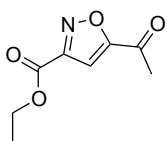


To a suspension of N-chlorosuccinimide (110 mg; 0.82 mmol) in a mixture of pyridine (6  $\mu$ L; 0.078 mmol) and dichloromethane (1.5 mL) was added **53** (100 mg; 0.78 mmol). Reaction mixture was stirred at 40 °C for 3 hours. After the complete consumption of the starting material NH<sub>4</sub>Cl (5 mL) was added to the mixture and it was extracted ethyl acetate (3\*10 mL). The organic layers were washed with brine and dried over Na<sub>2</sub>SO<sub>4</sub>. After filtration, the solvent was removed *in vacuo* and the crude material was used for the next step without further purification. Quantitative yield.

### General procedure for the isoxazole synthesis

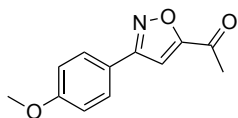
To a cooled to 0 °C solution of ethyl 2-chloro-2(hydroxyimino)acetate or **40** or **41** (1 eq) and 3-butyne-2-one (2 eq) in benzene (1.8 mL/mmol) was added triethylamine (1 eq) dropwise. Reaction mixture was stirred at 60 °C for 1 hour. After this time, HCl 1N was added to the mixture and it was extracted with ethyl acetate. The organic layers were washed with water, brine and dried over Na<sub>2</sub>SO<sub>4</sub>. After filtration, the solvent was removed *in vacuo* and the crude material was purified by silica gel flash chromatography column. Column eluent, yields and analytical data are reported below.

### ethyl 5-acetylisoxazole-3-carboxylate (42)



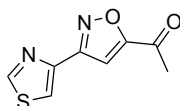
Column eluent: petroleum ether/ethyl acetate 9/1. 55% yield. <sup>1</sup>H-NMR (300 MHz-CDCl<sub>3</sub>):  $\delta$  = 1.34 (t, J=6 Hz, 3H); 2.65 (s, 3H); 4.43 (q, J=6 Hz, 2H); 7.26 (s, 1H).

### 1-(3-(4-methoxyphenyl)isoxazol-5-yl)ethanone (44)



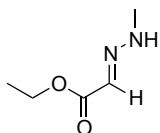
Column eluent: petroleum ether/ethyl acetate 9/1. 68% yield.  $^1\text{H-NMR}$  (400 MHz- $\text{CDCl}_3$ ):  $\delta$  = 2.68 (s, 3H); 3.89 (s, 3H), 7.01 (d,  $J=9$  Hz, 2H); 7.18 (s, 1H); 7.78 (d,  $J=9$  Hz, 2H).

### 1-(3-(thiazol-4-yl)isoxazol-5-yl)ethanone (45)



Column eluent: petroleum ether/ethyl acetate 9/1. 67% yield.  $^1\text{H-NMR}$  (400 MHz- $\text{CDCl}_3$ ):  $\delta$  = 2.68 (s, 3H); 7.41 (s, 1H); 8.07 (s, 1H); 8.95 (s, 1H).

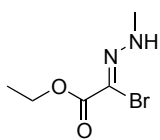
### (E)-ethyl 2-(2-methylhydrazono)acetate (55)



A solution of methylhydrazine (228  $\mu\text{L}$ ; 4.34 mmol) in methanol (0.33 mL/mmol) was heated to 40  $^\circ\text{C}$ , then ethyl glyoxilate 50% solution in toluene (400  $\mu\text{L}$ ; 4.03 mmol) and other methanol (0.013 mL/mmol) were added while maintaining the temperature below 50  $^\circ\text{C}$ . The mixture was heated to 50  $^\circ\text{C}$  for 3 hours and the TLC (colored with  $\text{KMnO}_4$ ) after this time showed the complete consumption of the starting material. Solvents and methylhydrazine were distilled off and the crude material was purified by silica gel flash chromatography with eluent petroleum ether/ethyl acetate from 75/25 to 50/50. 50% yield.

$^1\text{H-NMR}$  (400 MHz- $\text{DMSO}-d_6$ ):  $\delta$  = 1.18 (t,  $J=8$  Hz, 3H); 2.80 (s, 3H); 4.08 (q,  $J=8$  Hz, 2H); 6.53 (s, 1H); 8.81 (s, 1H).

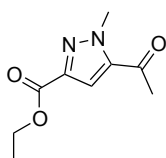
### Synthesis of (Z)-ethyl 2-bromo-2-(2-methylhydrazono)acetate (39)



A slurry of N-bromosuccinimide (68 mg; 0.38 mmol) in ethyl acetate (3 ml/mmol) was cooled to 0  $^\circ\text{C}$  and then a solution of **55** (50 mg; 0.38 mmol) in dichloromethane (3 ml/mmol).

Reaction mixture was stirred for 1 hour at 5 °C. Then the solvents were evaporated under pressure and the crude material was used for the next step without further purification.

### Synthesis of ethyl 1-methyl-5-propionyl-1H-pyrazole-3-carboxylate (43)

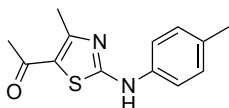


To a solution of **66** (70 mg; 0.33 mmol) and 3-butyne-2-one (52  $\mu$ L; 0.66 mmol) in benzene (1.8 mL/mmol) was added triethylamine (93  $\mu$ L; 0.66 mmol) dropwise. Reaction mixture was stirred at room temperature for 30 minutes. After this time, brine was added to the mixture (15 mL) and it was extracted with ethyl acetate (3\* 10 mL). The organic layers were washed with water (3\*10 mL), brine and dried over Na<sub>2</sub>SO<sub>4</sub>. After filtration, the solvent was removed *in vacuo* and the crude material was purified by silica gel chromatography column with eluent petroleum ether/ethyl acetate 8/2. 66% yield. <sup>1</sup>H-NMR (300 MHz-DMSO-*d*<sub>6</sub>):  $\delta$  = 1.28 (t, J=9 Hz; 3H); 2.54 (s, 3H); 4.10 (s, 3H); 4.26 (q, J=9 Hz; 2H); 7.60 (s, 1H).

### General synthesis for 2-aminothiazole ring

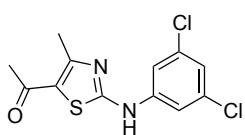
A solution of 3-chloropentane-2,4-dione (1 eq) and the opportune thiourea (1 eq) in ethanol (5 ml/mmol) was refluxed for different time. Then ice water was added to reaction mixture and a precipitate was formed. The white solid was collected *in vacuo* and it was used for the next step without further purification. Yields and analytical data are reported below:

### 1-(4-methyl-2-(*p*-tolylamino)thiazol-5-yl)ethanone (57)



70% yield <sup>1</sup>H-NMR (300 MHz-DMSO-*d*<sub>6</sub>):  $\delta$  = 2.26 (s, 3H); 2.47 (s, 3H); 2.53 (s, 3H); 7.15 (d, J=9 Hz, 2H); 7.44 (d, J=9 Hz, 2H); 10.64 (bs; 1H). HRMS (ESI) calculated for C<sub>13</sub>H<sub>14</sub>N<sub>2</sub>OS [M + H]<sup>+</sup> 247.0827 found 247.08958.

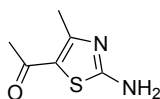
### 1-(2-((3,5-dichlorophenyl)amino)-4-methylthiazol-5-yl)ethanone (58)



73% yield.  $^1\text{H-NMR}$  (300 MHz-DMSO- $d_6$ ):  $\delta$  = 2.45 (s, 3H); 2.58 (s, 3H); 7.21 (d,  $J$  = 3 Hz, 1H); 7.71 (s, 2H); 11.02 (bs; 1H) HRMS (ESI) calculated for  $\text{C}_{12}\text{H}_{10}\text{Cl}_2\text{N}_2\text{OS}$

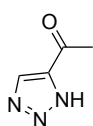
[M + H] $^+$  300.9891 found 300.99637.

### 1-(2-amino-4-methylthiazol-5-yl)ethanone (59)



40% yield  $^1\text{H-NMR}$  (400 MHz- $\text{CDCl}_3$ ):  $\delta$  = 2.45 (s, 3H); 2.56 (s, 3H); 9.63 (bs, 2H).

### Synthesis of 1-(1H-1,2,3-triazol-5-yl)ethanone (64)



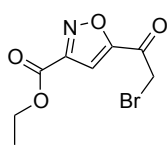
A suspension of sodium azide (143 mg; 2.20 mmol) in DMF (1 mL/mmol) was heated to 60 °C and then a solution of 3-butyn-2-one (114  $\mu\text{L}$ ; 1.46 mmol) in DMF (0.4 mL/mmol) was added over a period of 30 minutes. Reaction mixture was stirred at the same temperature for 1 hour. After this time water (10 mL) was added and it was extracted with dichloromethane (3\*10 mL). Then the aqueous layer was acidified with HCl 3N and extracted with ethyl acetate (3\*10 mL). The crude material was purified by silica gel flash chromatography eluting petroleum ether/ethyl acetate from 9/1 to 7/3. 30% yield.  $^1\text{H-NMR}$  (400 MHz-DMSO- $d_6$ ):  $\delta$  = 2.56 (s, 3H); 8.53 (s, 1H); 14.9 (bs, 1H).

### General procedure for the bromination of isoxazole and pyrazole ring

To a solution of the opportune ketone (1 eq) in chloroform (1.5 mL/mmol) was added acetic acid (0.1 mL/mmol) and reaction mixture was heated to 50 °C. Then a solution of bromine (1.05 eq) in chloroform (0.4 mL/mmol) was added dropwise. The mixture was stirred at the same temperature for 1 hour. After the complete consumption of the starting material, a

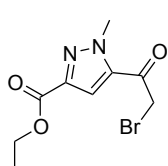
saturated aqueous solution of  $\text{NaHCO}_3$  was added and the aqueous layer was extracted with chloroform. The crude material was purified by silica gel flash chromatography. Column eluent, yields and analytical data are reported below.

#### ethyl 5-(2-bromoacetyl)isoxazole-3-carboxylate (46)



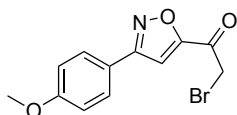
70% yield. Column eluent: petroleum ether/ethyl acetate 8/2.  $^1\text{H-NMR}$  (300 MHz- $\text{CDCl}_3$ ):  $\delta$  = 1.43 (t,  $J=6$  Hz, 3H); 4.45 (s, 2H); 4.47 (q,  $J=6$  Hz, 2H); 7.42 (s, 1H).

#### ethyl 5-(2-bromoacetyl)-1-methyl-1H-pyrazole-3-carboxylate (47)



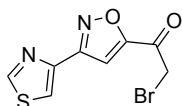
56% yield. Column eluent: petroleum ether/ethyl acetate 8/2.  $^1\text{H-NMR}$  (400 MHz- $\text{DMSO-}d_6$ ):  $\delta$  = 1.29 (t,  $J=8$  Hz, 3H); 4.13 (s, 3H); 4.30 (q,  $J=8$  Hz, 2H); 4.86 (s, 2H); 7.76 (s, 1H).

#### 2-bromo-1-(3-(4-methoxyphenyl)isoxazol-5-yl)ethanone (48)



91% yield. The crude material was used for the next step without further purification.  $^1\text{H-NMR}$  (400 MHz- $\text{DMSO-}d_6$ ):  $\delta$  = 3.42 (s, 3H); 4.86 (s, 2H); 7.11 (d,  $J=8$  Hz, 2H); 7.89 (d,  $J=8$  Hz, 2H); 8.05 (s, 1H).

#### 2-bromo-1-(3-(thiazol-4-yl)isoxazol-5-yl)ethanone (49)



35% yield. Column eluent: petroleum ether/ethyl acetate 9/1.  $^1\text{H-NMR}$  (300 MHz- $\text{DMSO-}d_6$ ):  $\delta$  = 4.91 (s, 2H); 7.95 (s, 1H); 8.51 (s, 1H); 9.34 (s, 1H).

#### General procedure for the bromination of 2-aminothiazole and triazole ring

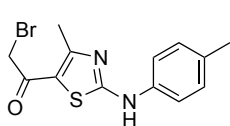
The appropriate ketone (1 eq) was solved in HBr solution 48% (4 mL/mmol), the solution was heated to 50 °C and then a solution of bromine (0.8 eq) in 1,4-dioxane (4 mL/mmol) was added dropwise. After the complete



consumption of the starting material, a saturated solution of aqueous NaHCO<sub>3</sub> was added to reaction mixture and it was extracted with ethyl acetate. The crude material was used for the next step without further purification.

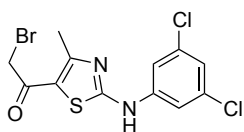
Yields and analytical data are reported below.

### 2-bromo-1-(4-methyl-2-(*p*-tolylamino)thiazol-5-yl)ethanone (60)



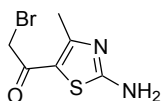
50% yield. <sup>1</sup>H-NMR (300 MHz-CDCl<sub>3</sub>): δ = 2.40 (s, 3H); 2.62 (s, 3H); 4.15 (s, 2H); 7.26 (s; 4H).

### 2-bromo-1-(2-((3,5-dichlorophenyl)amino)-4-methylthiazol-5-yl)ethanone (61)



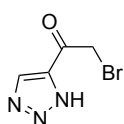
30% yield. <sup>1</sup>H-NMR (300 MHz-CDCl<sub>3</sub>): δ = 2.62 (s, 3H); 4.15 (s, 2H); 7.11-7.15 (m, 2H); 7.26 (s; 1H).

### 1-(2-amino-4-methylthiazol-5-yl)-2-bromoethanone (62)



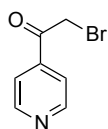
70% yield. <sup>1</sup>H-NMR (300 MHz-DMSO-*d*<sub>6</sub>): δ = 2.52 (s, 3H); 4.45 (s, 2H); 8.03 (s, 2H).

### 2-bromo-1-(1*H*-1,2,3-triazol-5-yl)ethanone (65)



15% yield. <sup>1</sup>H-NMR (300 MHz-DMSO-*d*<sub>6</sub>): δ = 4.30 (s, 2H); 8.53 (s, 1H); 14.9 (bs, 1H).

### Synthesis of 2-bromo-1-(pyridin-4-yl)ethanone (67)



To a solution of 4-acetylpyridine (456 μL; 4.10 mmol) in 1,4-dioxane/diethyl ether 1/1 (4.8 mL) cooled to 0° C was added a solution of bromine (294 μL; 5.76 mmol) in diethyl ether (2.8 mL) dropwise over 30 minutes. Reaction mixture was stirred overnight, then saturated solution of aqueous NaHCO<sub>3</sub> (20 mL) was added and it was

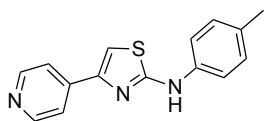
extracted with ethyl acetate (3\*10 mL). The organic layers were washed with water (3\*10 mL), brine and dried over Na<sub>2</sub>SO<sub>4</sub>. After filtration, the solvent was removed *in vacuo* and the crude material was purified by silica gel chromatography column with eluent petroleum ether/ethyl acetate 7/3. 50% yield. <sup>1</sup>H-NMR (300 MHz-CDCl<sub>3</sub>): δ = 3.10 (s, 2H); 8.53 (d, J=6 Hz, 2H); 8.62 (d, J=6 Hz, 2H).

### General procedure for Hantzsch synthesis

The properly substituted bromoacetophenone (1 equiv) and thioureas (1 equiv) were solubilized in dry ethanol (20 mL/mmol) and reacted at 70° C until consumption of the starting materials as indicated by TLC. After cooling, the solvent was evaporated and the crude material was purified by silica gel flash column chromatography or by precipitation.

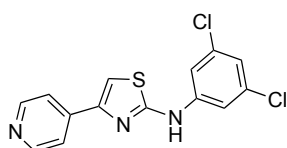
Yields, purification methods and other analytical data are reported below.

### 4-(pyridin-4-yl)-N-(p-tolyl)thiazol-2-amine (8)



65% yield. Column eluent: ethyl acetate/methanol from 95/5 to 85/15. <sup>1</sup>H-NMR (400 MHz-DMSO-*d*<sub>6</sub>): δ = 2.27 (s, 3H); 7.16 (d, J=8 Hz, 2H); 7.59 (d, J=8 Hz, 2H), 7.69 (s, 1H); 7.84 (dd, J<sub>1</sub>= 1.56 Hz J<sub>2</sub>= 4.52 Hz, 2H); 8.61 (dd, J<sub>1</sub>= 1.56 Hz J<sub>2</sub>=4.59 Hz, 2H); 10.86 (s, 1H). <sup>13</sup>C-NMR (100.6 MHz- DMSO-*d*<sub>6</sub>): δ = 20.87; 107.75; 117.60; 120.38; 129.87; 130.75; 139.11; 141.58; 149.07; 150.63; 164.15. MS (ESI) calculated for C<sub>15</sub>H<sub>13</sub>N<sub>3</sub>S [M + H]<sup>+</sup> 268.08, found 268.4. HRMS (ESI) calculated for C<sub>15</sub>H<sub>13</sub>N<sub>3</sub>S [M + H]<sup>+</sup> 268.0830 found 268.08984.

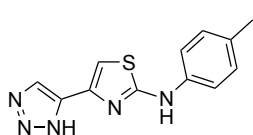
### N-(3,5-dichlorophenyl)-4-(pyridin-4-yl)thiazol-2-amine (9)



63% yield. Column eluent: ethyl acetate/methanol from 95/5 to 85/15. <sup>1</sup>H-NMR (300 MHz-DMSO-*d*<sub>6</sub>): δ = 7.17 (t, J=3 Hz, 1H); 7.82-7.84 (m, 4H), 7.86 (s,

1H); 7.84 (dd,  $J_1 = 1.56$  Hz  $J_2 = 4.52$  Hz, 2H); 8.64 (dd,  $J_1 = 1.56$  Hz  $J_2 = 4.52$  Hz, 2H); 10.27 (s, 1H).  $^{13}\text{C-NMR}$  (100.6 MHz- DMSO- $d_6$ ):  $\delta = 109.58$ ; 115.39; 120.25; 120.68; 134.73; 141.26; 143.48; 148.05; 150.76; 163.06. MS (ESI) calculated for  $\text{C}_{14}\text{H}_9\text{Cl}_2\text{N}_3\text{S}$  [M + H] $^+$  321.21, found 321.3. HRMS (ESI) calculated for  $\text{C}_{14}\text{H}_9\text{Cl}_2\text{N}_3\text{S}$  [M + H] $^+$  321.9894, found 321.99649.

### **N-(p-tolyl)-4-(1H-1,2,3-triazol-5-yl)thiazol-2-amine (10)**

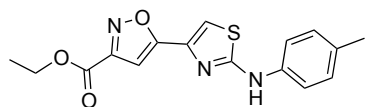


24% yield. Column eluent: dichloromethane/methanol 98/2.

$^1\text{H-NMR}$  (300 MHz-DMSO- $d_6$ ):  $\delta = 2.34$  (s, 3H); 7.33 (d,  $J = 6$  Hz, 2H); 7.40 (d,  $J = 6$  Hz, 2H); 7.48 (s, 1H); 10.2 (bs, 1H); 15.5 (bs, 1H).  $^{13}\text{C-NMR}$  (100.6 MHz- DMSO- $d_6$ ):  $\delta = 21.3$ ; 104.8; 120.3; 129.8; 130.4; 130.7; 137.5; 142.8; 159.1.

HRMS (ESI) calculated for  $\text{C}_{12}\text{H}_{11}\text{N}_5\text{S}$  [M + H] $^+$  258.0735 found 258.08079.

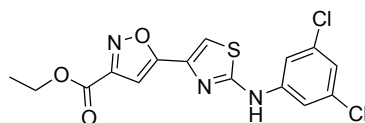
### **ethyl 5-(2-(p-tolylamino)thiazol-4-yl)isoxazole-3-carboxylate (11)**



70% yield. Column eluent petroleum ether/ethyl acetate from 9/1 to 7/3.  $^1\text{H-NMR}$

(400 MHz-DMSO- $d_6$ ):  $\delta = 1.34$  (t,  $J = 8$  Hz, 3H); 2.27 (s, 3H); 4.38 (q,  $J = 8$  Hz, 2H); 7.13 (s, 1H); 7.16 (d,  $J = 8$  Hz, 2H); 7.56 (d,  $J = 8$  Hz, 2H); 7.69 (s, 1H); 10.38 (s, 1H).  $^{13}\text{C-NMR}$  (100.6 MHz- DMSO- $d_6$ ):  $\delta = 14.43$ ; 20.86; 62.41; 101.27; 110.39; 117.87; 129.96; 131.22; 138.14; 138.74; 157.03; 159.75; 165.00; 167.40. HRMS (ESI) calculated for  $\text{C}_{16}\text{H}_{15}\text{N}_3\text{O}_3\text{S}$  [M + H] $^+$  330.0834 found 330.09030.

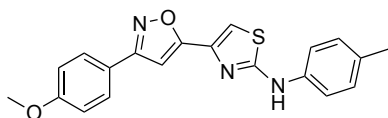
### **ethyl 5-(2-((3,5-dichlorophenyl)amino)thiazol-4-yl)isoxazole-3-carboxylate (12)**



40% yield. Column eluent petroleum ether/ethyl acetate from 9/1 to 8/2.  $^1\text{H-NMR}$

(400 MHz-DMSO- $d_6$ ):  $\delta$  = 1.34 (t, J=8 Hz, 3H); 4.38 (q, J=8 Hz, 2H); 7.12 (s, 1H); 7.20 (s, 1H); 7.76 (s, 1H); 7.77 (s, 1H); 7.88 (s, 1H); 10.90 (s, 1H).  $^{13}\text{C}$ -NMR (100.6 MHz- DMSO- $d_6$ ):  $\delta$  = 14.41; 62.45; 101.39; 112.27; 115.60; 121.11; 134.81; 138.05; 143.12; 157.04; 159.68; 163.88; 166.98. HRMS (ESI) calculated for  $\text{C}_{15}\text{H}_{11}\text{Cl}_2\text{N}_3\text{O}_3\text{S}$  [M + H] $^+$  383.9898 found 383.99709.

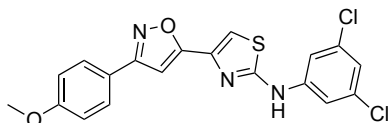
#### 4-(3-(4-methoxyphenyl)isoxazol-5-yl)-N-(p-tolyl)thiazol-2-amine (24)



99% yield. During the reaction a precipitate was formed which was collected *in vacuo*.

$^1\text{H}$ -NMR (300 MHz-DMSO- $d_6$ ):  $\delta$  = 2.28 (s, 3H); 3.83 (s, 3H); 7.07 (d, J=9 Hz, 2H); 7.15 (d, J=9 Hz, 2H); 7.26 (s, 1H); 7.52 (s, 1H); 7.58 (d, J=9 Hz, 2H); 7.89 (d, J=9 Hz, 2H); 10.33 (s, 1H).  $^{13}\text{C}$ -NMR (100.6 MHz- DMSO- $d_6$ ):  $\delta$  = 19.02; 55.80; 99.80; 108.89; 114.95; 117.87; 121.31; 121.31; 128.72; 129.93; 131.08; 138.88; 139.08; 161.26; 162.38; 164.80; 165.95. HRMS (ESI) calculated for  $\text{C}_{20}\text{H}_{17}\text{N}_3\text{O}_2\text{S}$  [M + H] $^+$  364.1041 found 364.11142.

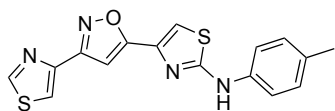
#### N-(3,5-dichlorophenyl)-4-(3-(4-methoxyphenyl)isoxazol-5-yl)thiazol-2-amine (25)



43% yield. During the reaction a precipitate was formed which was collected *in vacuo*.

$^1\text{H}$ -NMR (300 MHz-DMSO- $d_6$ ):  $\delta$  = 3.83 (s, 3H); 7.07-7.10 (m, 2H); 7.16 (t, J=6 Hz, 1H); 7.23 (s, 1H); 7.70 (s, 1H); 7.76 (d, J=3 Hz, 2H); 7.87-7.90 (m, 2H); 10.84 (s, 1H).  $^{13}\text{C}$ -NMR (100.6 MHz- DMSO- $d_6$ ):  $\delta$  = 55.78; 99.26; 110.89; 114.99; 115.57; 121.05; 121.20; 128.70; 134.85; 139.09; 143.25; 161.29; 162.42; 163.74; 165.54. HRMS (ESI) calculated for  $\text{C}_{19}\text{H}_{13}\text{Cl}_2\text{N}_3\text{O}_2\text{S}$  [M + H] $^+$  418.2964 found 418.01783.

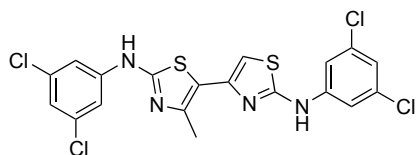
#### 4-(3-(thiazol-4-yl)isoxazol-5-yl)-N-(p-tolyl)thiazol-2-amine (26)



84% yield. Column eluent: petroleum ether/ethyl acetate from 8/2.  $^1\text{H-NMR}$  (300 MHz-DMSO- $d_6$ ):  $\delta$  = 2.27 (s, 3H); 7.16 (s, 1H);

7.19 (d,  $J=5$  Hz, 2H); 7.57 (s, 1H); 7.59 (d,  $J=5$  Hz, 2H); 8.45 (d,  $J=2$  Hz; 1H); 9.31 (d,  $J=2$  Hz, 1H); 10.35 (s, 1H).  $^{13}\text{C-NMR}$  (100.6 MHz- DMSO- $d_6$ ):  $\delta$  = 20.87; 100.11; 109.35; 117.87; 120.65; 129.95; 131.17; 138.80; 138.84; 145.18; 156.23; 158.81; 164.90; 166.10. HRMS (ESI) calculated for  $\text{C}_{16}\text{H}_{12}\text{N}_4\text{OS}_2$  [M + H] $^+$  341.0453 found 341.05253.

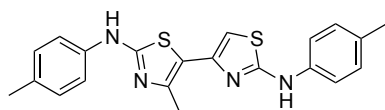
**$N^2, N^{2'}$ -bis(3,5-dichlorophenyl)-4'-methyl-[4,5'-bithiazole]-2,2'-diamine (27)**



54% yield. During the reaction a precipitate was formed which was collected *in vacuo*.  $^1\text{H-NMR}$  (300 MHz-DMSO- $d_6$ ):  $\delta$  = 2.51 (s, 3H); 6.99 (s, 1H); 7.11-7-15 (m, 2H); 7.72-7.76 (m, 4H); 10.72 (s, 1H); 10.75 (s, 1H). NMR (100.6 MHz- DMSO- $d_6$ ):  $\delta$  = 12.2;

104.8; 114.8; 117.3; 119.2; 129.2; 142.4; 145.2; 147.9; 159.5. MS (ESI) calculated for  $\text{C}_{19}\text{H}_{12}\text{Cl}_4\text{N}_4\text{S}_2$  [M + H] $^+$  500.92, found 500.2. HRMS (ESI) calculated for  $\text{C}_{19}\text{H}_{12}\text{Cl}_4\text{N}_4\text{S}_2$  [M + H] $^+$  500.9257 found 500.93303.

**4'-methyl- $N^2, N^{2'}$ -di-*p*-tolyl-[4,5'-bithiazole]-2,2'-diamine (28)**

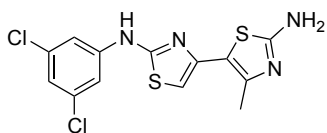


70% yield. During the reaction a precipitate was formed which was collected *in vacuo*.

$^1\text{H-NMR}$  (300 MHz-DMSO- $d_6$ ):  $\delta$  = 2.26 (s, 3H); 2.30 (s, 3H); 2.47 (s, 3H); 6.88 (s, 1H); 7.11 (d,  $J=8$  Hz, 2H); 7.45 (d,  $J=9$  Hz, 2H) 7.49 (d,  $J=9$  Hz, 2H); 10.26 (s, 1H); 10.75 (s, 1H). NMR (100.6 MHz- DMSO- $d_6$ ):  $\delta$  = 16.58; 20.82; 20.92; 102.25; 114.56; 115.67; 116.78; 117.55; 119.43; 129.85; 130.17; 130.77; 130.91; 139.01; 142.40; 163.48; 167.04. MS (ESI) calculated for  $\text{C}_{21}\text{H}_{20}\text{N}_4\text{S}_2$

[M + H]<sup>+</sup> 393.54, found 393.4. HRMS (ESI) calculated for C<sub>21</sub>H<sub>20</sub>N<sub>4</sub>S<sub>2</sub> [M + H]<sup>+</sup> 393.1129, found 393.11942

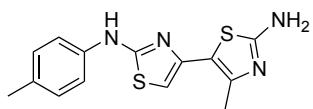
**N<sup>2</sup>-(3,5-dichlorophenyl)-4'-methyl-[4,5'-bithiazole]-2,2'-diamine (29)**



33% yield. Reaction mixture was cooled to 0 °C and a precipitate was formed which was collected *in vacuo*. <sup>1</sup>H-NMR (300 MHz-DMSO-*d*<sub>6</sub>):

δ = 2.34 (s, 3H); 6.71 (s, 1H); 7.02 (s, 2H); 7.12 (s, 1H); 7.77 (s, 2H); 10.72 (s, 1H). <sup>13</sup>C-NMR (100.6 MHz- DMSO-*d*<sub>6</sub>): δ = 17.49; 101.66; 114.25; 115.24; 120.36; 134.65; 143.60; 143.97; 145.06; 161.80; 166.26. HRMS (ESI) calculated for C<sub>13</sub>H<sub>10</sub>Cl<sub>2</sub>N<sub>4</sub>S<sub>2</sub> [M + H]<sup>+</sup> 356.9724, found 356.97922.

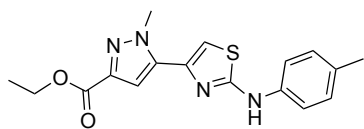
**4'-methyl-N<sup>2</sup>-(*p*-tolyl)-[4,5'-bithiazole]-2,2'-diamine (30)**



20% yield. Column eluent: ethyl acetate/methanol from 95/5 to 85/15. <sup>1</sup>H-NMR (300 MHz-DMSO-*d*<sub>6</sub>):

δ = 2.24 (s, 3H); 2.31 (s, 3H); 6.54 (s, 1H); 6.93 (s, 2H); 7.09 (d, J=7 Hz, 2H); 7.50 (d, J=7 Hz, 2H); 10.12 (s, 1H). <sup>13</sup>C-NMR (100.6 MHz- DMSO-*d*<sub>6</sub>): δ = 17.46; 20.81; 99.91; 114.78; 117.39; 129.77; 130.56; 139.23; 143.98; 144.58; 162.96; 166.19. HRMS (ESI) calculated for C<sub>14</sub>H<sub>14</sub>N<sub>4</sub>S<sub>2</sub> [M + H]<sup>+</sup> 303.0660, found 303.07248.

**ethyl 1-methyl-5-(2-(*p*-tolylamino)thiazol-4-yl)-1*H*-pyrazole-3-carboxylate (31)**

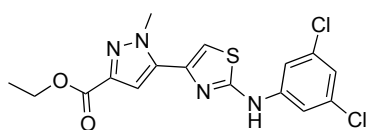


81% yield. During the reaction a precipitate was formed which was collected *in vacuo*. <sup>1</sup>H-

NMR (300 MHz-DMSO-*d*<sub>6</sub>): δ = 1.28 (t, J=6 Hz, 3H); 2.25 (s, 3H); 4.18 (s, 3H); 4.24 (q, J=6 Hz, 2H); 7.09 (s, 1H); 7.13 (d, J=8 Hz, 2H); 7.37 (s, 1H); 7.51 (d, J=8 Hz, 2H); 10.28 (s, 1H). <sup>13</sup>C-NMR (100.6 MHz- DMSO-*d*<sub>6</sub>): δ = 14.7; 20.81; 60.65; 107.65; 108.43; 117.71; 129.91; 130.97; 138.91; 139.41; 139.94;

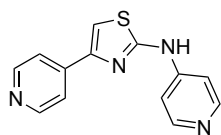
141.67; 161.01; 164.29. HRMS (ESI) calculated for  $C_{17}H_{18}N_4O_2S$   $[M + H]^+$  343.1150, found 343.12170.

**ethyl 5-(2-((3,5-dichlorophenyl)amino)thiazol-4-yl)-1-methyl-1H-pyrazole-3-carboxylate (32)**



95% yield. During the reaction a precipitate was formed which was collected *in vacuo*.  $^1H$ -NMR (300 MHz-DMSO- $d_6$ ):  $\delta$  = 1.27 (t, J=6 Hz, 3H); 4.20 (s, 3H); 4.25 (q, J=6 Hz, 2H); 7.13-7.16 (m, 2H); 7.55 (s, 1H); 7.73 (d, J=3 Hz, 2H); 10.82 (s, 1H).  $^{13}C$ -NMR (100.6 MHz- DMSO- $d_6$ ):  $\delta$  = 14.6; 60.7; 108.62; 109.35; 115.51; 120.80; 134.78; 139.05; 140.04; 141.76; 143.27; 161.94; 163.11. HRMS (ESI) calculated for  $C_{16}H_{14}Cl_2N_4O_2S$   $[M + H]^+$  397.0215, found 397.02363.

**N,4-di(pyridin-4-yl)thiazol-2-amine (37)**



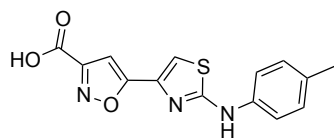
70% yield. Column eluent: petroleum ether/ethyl acetate from 9/1 to 7/3.  $^1H$ -NMR (400 MHz-DMSO- $d_6$ ):  $\delta$  = 7.87-7.90 (m, 2H); 7.92 (dd,  $J_1$ = 1.48 Hz  $J_2$ = 4.56 Hz, 2H); 8.00 (s, 1H); 8.51 (d, J=8 Hz, 2H); 8.65 (dd,  $J_1$ = 1.48 Hz  $J_2$ =4.56 Hz, 2H); 11.5 (bs, 1H).  $^{13}C$ -NMR (100.6 MHz- DMSO- $d_6$ ):  $\delta$  = 111.37; 112.15; 120.52; 141.09; 146.66; 148.48; 150.16; 150.70; 162.17. MS (ESI) calculated for  $C_{13}H_{10}N_4S$   $[M + H]^+$  255.06, found 255.2; HRMS (ESI) calculated for  $C_{13}H_{10}N_4S$   $[M + H]^+$  255.0626, found 255.06989.

**General procedure for the hydrolysis**

The appropriate ester (1 eq) and LiOH  $H_2O$  (4 eq) were dissolved in solution of THF/MeOH/ $H_2O$  (3/1/1, 1 mL/mmol) and stirred at room temperature for different time. The reaction mixture is then evaporated *in vacuo*, and the crude is washed with  $H_2O$ , acidified with HCl 2 N and extracted with ethyl

acetate. After evaporation of the solvent, the product is used for the next reaction step without further purification.

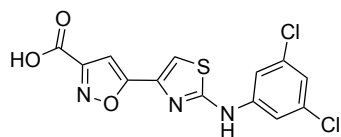
**5-(2-(*p*-tolylamino)thiazol-4-yl)isoxazole-3-carboxylic acid (13)**



96% yield.  $^1\text{H-NMR}$  (400 MHz- $\text{CDCl}_3$ ):  $\delta$  = 2.27 (s, 3H); 7.05 (s, 1H); 7.16 (d,  $J=6$  Hz, 2H); 7.55 (d,  $J=6$  Hz, 2H); 7.65 (s, 1H); 10.37 (s, 1H); 14.09 (bs, 1H).

$^{13}\text{C-NMR}$  (100.6 MHz-  $\text{DMSO-}d_6$ ):  $\delta$  = 20.86; 101.40; 110.04; 117.88; 129.95; 131.21; 138.29; 138.76; 157.92; 161.19; 164.98; 167.18. HRMS (ESI) calculated for  $\text{C}_{14}\text{H}_{11}\text{N}_3\text{O}_3\text{S}$  [ $\text{M} + \text{H}$ ] $^+$  302.0521, found 302.05902.

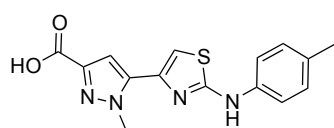
**5-(2-((3,5-dichlorophenyl)amino)thiazol-4-yl)isoxazole-3-carboxylic acid (14)**



77% yield.  $^1\text{H-NMR}$  (400 MHz- $\text{DMSO-}d_6$ ):  $\delta$  = 7.03 (s, 1H); 7.20 (s, 1H); 7.76 (s, 1H); 7.77 (s, 1H); 7.84 (s, 1H); 10.89 (s, 1H); 14.10 (bs, 1H).

$^{13}\text{C-NMR}$  (100.6 MHz-  $\text{DMSO-}d_6$ ):  $\delta$  = 101.50; 111.95; 115.61; 121.10; 134.82; 138.21; 143.15; 158.07; 161.13; 163.86; 166.78. HRMS (ESI) calculated for  $\text{C}_{13}\text{H}_7\text{Cl}_2\text{N}_3\text{O}_3\text{S}$  [ $\text{M} + \text{H}$ ] $^+$  355.9585 found 355.96579.

**1-methyl-5-(2-(*p*-tolylamino)thiazol-4-yl)-1H-pyrazole-3-carboxylic acid (33)**

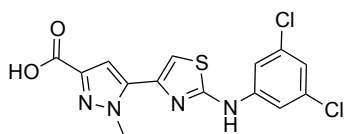


78% yield.  $^1\text{H-NMR}$  (300 MHz-  $\text{DMSO-}d_6$ ):  $\delta$  = 2.27 (s, 3H); 4.15 (s, 3H); 6.98 (s, 1H); 7.13 (d,  $J=8$  Hz, 2H); 7.31 (s, 1H); 7.51 (d,  $J=8$  Hz, 2H); 10.29 (s, 1H); 14.09 (bs, 1H).

$^{13}\text{C-NMR}$  (100.6 MHz-  $\text{DMSO-}d_6$ ):  $\delta$  = 20.82; 65.39; 107.32; 108.44; 117.64; 129.92; 130.91; 138.94; 139.27; 139.67; 140.26; 140.38; 164.19. HRMS (ESI) calculated for  $\text{C}_{15}\text{H}_{14}\text{N}_4\text{O}_2\text{S}$  [ $\text{M} + \text{H}$ ] $^+$  315.0837, found 315.09073.



### 5-(2-((3,5-dichlorophenyl)amino)thiazol-4-yl)-1-methyl-1H-pyrazole-3-



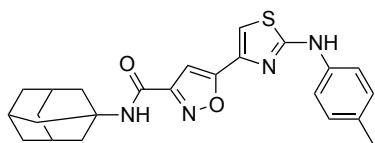
#### carboxylic acid (34)

98% yield.  $^1\text{H-NMR}$  (300 MHz-DMSO- $d_6$ ):  $\delta$  = 4.18 (s, 3H); 7.05 (s, 1H); 7.14 (t,  $J=2$  Hz, 1H); 7.50 (s, 1H); 7.80 (d,  $J=2$  Hz, 2H); 11.23 (s, 1H); 13.10 (bs, 1H).  $^{13}\text{C-NMR}$  (100.6 MHz- DMSO- $d_6$ ):  $\delta$  = 45.22; 108.52; 109.19; 115.45; 120.51; 134.65; 139.00; 140.01; 143.12; 143.55; 163.10; 163.53. HRMS (ESI) calculated for  $\text{C}_{14}\text{H}_{10}\text{Cl}_2\text{N}_4\text{O}_2\text{S}$  [ $\text{M} + \text{H}$ ] $^+$  368.6902 found 368.99743.

#### General procedure for secondary and tertiary amide formation

To a solution of the appropriate carboxylic acid (1 eq) in dry DMF (4 mL/mmol) were added *O*-(Benzotriazol-1-yl)-*N,N,N',N'*-tetramethyluronium tetrafluoroborate (TBTU) (1 eq) and *N*-(3-Dimethylaminopropyl)-*N'*-ethylcarbodiimide hydrochloride (EDC HCl) (1 eq). Reaction mixture was stirred at room temperature under  $\text{N}_2$  for 15 minutes, then triethylamine (1.5 eq) and the opportune amine (1 eq). The mixture was stirred at the same temperature until the complete consumption of the starting material.  $\text{H}_2\text{O}$  was added and it was extracted with ethyl acetate. The organic layers were washed with brine and dried over  $\text{Na}_2\text{SO}_4$ . After filtration, the solvent was removed *in vacuo* and the crude material was purified by silica gel chromatography column. Column eluent, yields and analytical data are reported below.

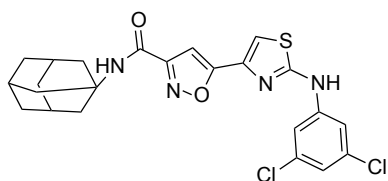
### *N*-((3*s*,5*s*,7*s*)-adamantan-1-yl)-5-(2-(*p*-tolylamino)thiazol-4-yl)isoxazole-3-carboxamide (15)



25% yield. Column eluent: petroleum ether/ethyl acetate from 9/1 to 8/2.  $^1\text{H-NMR}$  (400 MHz-DMSO- $d_6$ ):  $\delta$  = 1.67 (s, 6H); 2.08 (s,

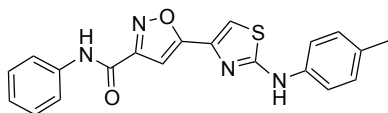
9H); 2.28 (s, 3H); 7.01 (s, 1H); 7.16 (d, J= 8 Hz, 2H); 7.55 (d, J=8 Hz, 2H); 7.61 (s, 1H); 7.91 (s, 1H); 11.37 (s, 1H).  $\delta$  = 20.82; 36.37; 36.58; 38.76; 39.67; 40.67; 41.18; 41.58; 52.58; 100.99; 112.55; 115.70; 121.10; 134.93; 139.37; 143.18; 159.05; 160.55; 167.05. HRMS (ESI) calculated for C<sub>24</sub>H<sub>26</sub>N<sub>4</sub>O<sub>2</sub>S [M + H]<sup>+</sup> 435.1776 found 435.18451.

***N*-((3*s*,5*s*,7*s*)-adamantan-1-yl)-5-(2-((3,5-dichlorophenyl)amino)thiazol-4-yl)isoxazole-3-carboxamide (16)**



45% yield. Column eluent: petroleum ether/ethyl acetate from 9/1 to 8/2. <sup>1</sup>H-NMR (400 MHz-DMSO-*d*<sub>6</sub>):  $\delta$  = 1.67 (s, 6H); 2.08 (s, 9H); 6.98 (s, 1H); 7.76 (d, J=4 Hz, 2H); 7.79 (s, 1H); 7.94 (s, 1H); 10.89 (s, 1H). <sup>13</sup>C-NMR (100.6 MHz- DMSO-*d*<sub>6</sub>):  $\delta$  = 36.38; 36.53; 38.71; 39.37; 40.62; 41.11; 41.48; 52.54; 100.55; 111.65; 115.60; 121.10; 134.83; 138.37; 143.18; 158.05; 160.45; 166.05. HRMS (ESI) calculated for C<sub>23</sub>H<sub>22</sub>Cl<sub>2</sub>N<sub>4</sub>O<sub>2</sub>S [M + H]<sup>+</sup> 489.0841 found 489.07029.

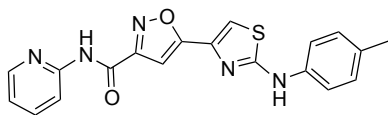
***N*-phenyl-5-(2-(*p*-tolylamino)thiazol-4-yl)isoxazole-3-carboxamide (17)**



85% yield. Column eluent: petroleum ether/ethyl acetate 7/3. <sup>1</sup>H-NMR (300 MHz-DMSO-*d*<sub>6</sub>):  $\delta$  = 2.27 (s, 3H); 7.16-7.19 (m, 4H); 7.37-7.41 (m, 2H); 7.56 (d, J=9 Hz, 2H); 7.79 (d, J=9 Hz, 2H); 7.67 (s, 1H); 10.39 (s, 1H); 10.74 (s, 1H). <sup>13</sup>C-NMR (100.6 MHz- DMSO-*d*<sub>6</sub>):  $\delta$  = 20.87; 100.75; 110.06; 117.92; 121.09; 124.93; 129.22; 129.97; 131.27; 138.34; 138.50; 138.77; 157.88; 160.07; 165.03; 166.89. HRMS (ESI) calculated for C<sub>20</sub>H<sub>16</sub>N<sub>4</sub>O<sub>2</sub>S [M + H]<sup>+</sup> 377.0994 found 377.10677.

***N*-(pyridin-2-yl)-5-(2-(*p*-tolylamino)thiazol-4-yl)isoxazole-3-carboxamide**

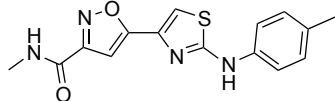
**(18)**



85% yield. Column eluent: petroleum ether/ethyl acetate 8/2. <sup>1</sup>H-NMR (300 MHz-DMSO-*d*<sub>6</sub>): δ = 2.27 (s, 3H); 7.16-7.31 (m, 4H); 7.57 (d, J=9 Hz, 2H); 7.66 (s, 1H); 7.89-7.92 (m, 1H); 8.12 (d, J=9 Hz, 2H);

8.42 (s, 1H); 10.39 (s, 1H); 10.82 (s, 1H). <sup>13</sup>C-NMR (100.6 MHz- DMSO-*d*<sub>6</sub>): δ = 20.87; 100.68; 110.07; 115.34; 117.87; 121.12; 129.96; 131.22; 138.34; 138.79; 138.94; 148.74; 151.33; 158.09; 159.57; 164.97; 166.98. HRMS (ESI) calculated for C<sub>19</sub>H<sub>15</sub>N<sub>5</sub>O<sub>2</sub>S [M + H]<sup>+</sup> 378.0946 found 378.08651.

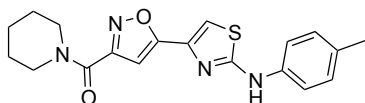
***N*-methyl-5-(2-(*p*-tolylamino)thiazol-4-yl)isoxazole-3-carboxamide (19)**



40% yield. Column eluent: dichloromethane/methanol 95/5. <sup>1</sup>H-NMR (300 MHz-DMSO-*d*<sub>6</sub>): δ = 2.26 (s, 3H); 2.78(d, J=5 Hz, 3H); 7.03 (s, 1H); 7.15 (d, J=6 Hz, 2H); 7.55 (d, J=6 Hz, 2H); 7.62 (s, 1H); 8.76

(d, J=5 Hz, 1H); 10.38 (s, 1H). <sup>13</sup>C-NMR (100.6 MHz- DMSO-*d*<sub>6</sub>): δ = 20.86; 53.34; 101.30; 110.42; 117.89; 129.96; 131.23; 138.12; 138.74; 156.84; 160.22; 165.02; 167.44. HRMS (ESI) calculated for C<sub>15</sub>H<sub>14</sub>N<sub>4</sub>O<sub>2</sub>S [M + H]<sup>+</sup> 315.0837 found 315.09102.

**piperidin-1-yl(5-(2-(*p*-tolylamino)thiazol-4-yl)isoxazol-3-yl)methanone (20)**

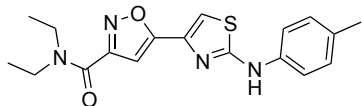


31% yield. Column eluent: petroleum ether/ethyl acetate 7/3. <sup>1</sup>H-NMR (300 MHz-DMSO-*d*<sub>6</sub>): δ = 1.55-1.64 (m, 6H); 2.27 (s, 3H); 3.51 (s, 2H); 3.63 (s, 2H); 6.95

(s, 1H); 7.14 (d, J=9 Hz, 2H); 7.55 (d, J=9 Hz, 2H); 7.60 (s, 1H); 10.36 (s, 1H). <sup>13</sup>C-NMR (100.6 MHz- DMSO-*d*<sub>6</sub>): δ = 20.84; 24.33; 25.69; 26.66; 43.00; 47.95; 101.15; 109.79; 117.86; 129.93; 131.19; 138.41; 138.79; 159.25;

159.46; 164.91; 165.85. HRMS (ESI) calculated for  $C_{19}H_{20}N_4O_2S$   $[M + H]^+$  369.1307 found 369.13697.

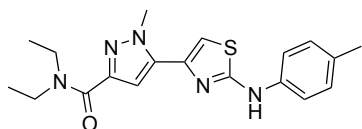
***N,N*-diethyl-5-(2-(*p*-tolylamino)thiazol-4-yl)isoxazole-3-carboxamide (21)**



36% yield. Column eluent: petroleum ether/ethyl acetate 7/3.  $^1H$ -NMR (400 MHz-DMSO- $d_6$ ):  $\delta$  = 1.14-1.19 (m, 6H); 2.27 (s, 3H);

3.41-3.51 (m, 4H); 6.99 (s, 1H); 7.15 (d,  $J=8$  Hz, 2H); 7.57 (d,  $J=8$  Hz, 2H); 7.62 (s, 1H); 10.38 (s, 1H).  $^{13}C$ -NMR (100.6 MHz-DMSO- $d_6$ ):  $\delta$  = 13.13; 14.98; 20.86; 38.90; 43.30; 101.20; 109.82; 117.86; 129.93; 131.16; 138.40; 138.80; 159.76; 160.32; 164.90; 165.75. HRMS (ESI) calculated for  $C_{18}H_{20}N_4O_2S$   $[M + H]^+$  357.1307 found 357.13742.

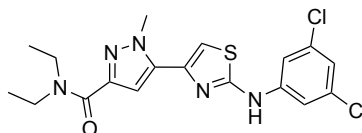
***N,N*-diethyl-1-methyl-5-(2-(*p*-tolylamino)thiazol-4-yl)-1*H*-pyrazole-3-carboxamide (35)**



66% yield. Column eluent: dichloromethane/methanol 98/2.  $^1H$ -NMR

(400 MHz-DMSO- $d_6$ ):  $\delta$  = 1.13-1.23 (m, 6H); 2.26 (s, 3H); 3.41-3.43 (m, 2H); 3.68-3.68 (m, 2H); 4.14 (s, 3H); 6.86 (s, 1H); 7.14 (d,  $J=8$  Hz, 2H); 7.29 (s, 1H); 7.53 (d,  $J=8$  Hz, 2H); 10.80 (s, 1H).  $^{13}C$ -NMR (100.6 MHz-DMSO- $d_6$ ):  $\delta$  = 13.29; 15.09; 20.82; 42.93; 107.13; 107.89; 117.66; 129.91; 130.90; 138.42; 138.99; 140.44; 146.29; 162.90; 164.20. HRMS (ESI) calculated for  $C_{19}H_{23}N_5OS$   $[M + H]^+$  370.1623 found 370.16904.

**5-(2-((3,5-dichlorophenyl)amino)thiazol-4-yl)-*N,N*-diethyl-1-methyl-1*H*-pyrazole-3-carboxamide (36)**

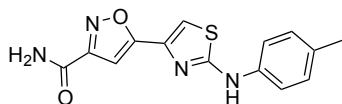


71% yield. Column eluent: dichloromethane/methanol 95/5.  $^1H$ -NMR

(400 MHz-DMSO- $d_6$ ):  $\delta$  = 1.14-1.19 (m, 6H); 3.41-3.43 (m, 2H); 3.67-3.69 (m,

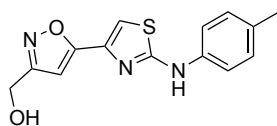
2H); 4.16 (s, 3H); 6.91 (s, 1H); 7.15 (s, 1H); 7.48 (s, 1H); 7.76 (s, 2H); 10.80 (s, 1H).  $^{13}\text{C-NMR}$  (100.6 MHz-  $\text{DMSO-}d_6$ ):  $\delta = 13.28; 15.08; 42.96; 108.03; 108.90; 115.50; 120.76; 134.79; 138.04; 140.41; 143.34; 146.34; 162.80; 163.04$ . HRMS (ESI) calculated for  $\text{C}_{14}\text{H}_{10}\text{Cl}_2\text{N}_4\text{O}_2\text{S}$   $[\text{M} + \text{H}]^+$  424.0687 found 424.07583.

### Synthesis of 5-(2-(*p*-tolylamino)thiazol-4-yl)isoxazole-3-carboxamide (**22**)



A suspension of compound **37** (50 mg; 0.15 mmol) in  $\text{NH}_4\text{OH}$  (2 ml) was stirred overnight at room temperature. Then water (8 mL) was added to the mixture and it was extracted with ethyl acetate (3\*10 mL). The organic layers were washed with brine and dried over  $\text{Na}_2\text{SO}_4$ . After filtration, the solvent was removed in vacuo and the crude material was purified by silica gel flash chromatography column eluting with petroleum ether/ethyl acetate 7/3 and then ethyl acetate. 82% Yield.  $^1\text{H-NMR}$  (400 MHz- $\text{DMSO-}d_6$ ):  $\delta = 2.27$  (s, 3H); 7.02 (s, 1H); 7.16 (d,  $J=8$  Hz, 2H); 7.55 (d,  $J=8$  Hz, 2H); 7.62 (s, 1H); 7.90 (s, 1H); 8.20 (s, 1H); 10.30 (s, 1H).  $^{13}\text{C-NMR}$  (100.6 MHz-  $\text{DMSO-}d_6$ ):  $\delta = 20.86; 100.49; 109.72; 117.88; 129.95; 131.22; 138.43; 138.78; 159.83; 160.49; 164.95; 166.73$ . HRMS (ESI) calculated for  $\text{C}_{14}\text{H}_{12}\text{N}_4\text{O}_2\text{S}$   $[\text{M} + \text{H}]^+$  301.0681 found 301.07501.

### Synthesis of (5-(2-(*p*-tolylamino)thiazol-4-yl)isoxazol-3-yl)methanol (**23**)

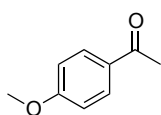


To a cooled to 0 °C solution of compound (ethyl ester) (20 mg; 0.06 mmol) in dry methanol (1 mL) was added Sodium borohydride (14 mg; 0.36 mmol). Reaction mixture was stirred at room temperature for 30 minutes. After the complete consumption of the starting material, the mixture was cooled to 0 °C and an aqueous saturated solution of ammonium chloride (5 mL) was

added. The aqueous layer was extracted with ethyl acetate (3\*8 mL). The organic layers were washed with brine and dried over Na<sub>2</sub>SO<sub>4</sub>. After filtration, the solvent was removed in vacuo. The crude material was purified by silica gel flash chromatography column eluting with dichloromethane/methanol from 98/2 to 95/5. 93% Yield. <sup>1</sup>H-NMR (400 MHz-CDCl<sub>3</sub>): δ = 2.38 (s, 3H); 4.84 (s, 2H); 6.66 (s, 1H); 7.14 (s, 1H); 7.23-7.27 (m, 2H); 7.29-7.31(m, 2H). <sup>13</sup>C-NMR (100.6 MHz- DMSO-*d*<sub>6</sub>): δ = 20.86; 55.45; 100.49; 108.58; 117.78; 129.92; 131.12; 138.87; 139.10; 164.78; 165.30; 165.49. HRMS (ESI) calculated for C<sub>14</sub>H<sub>13</sub>N<sub>3</sub>O<sub>2</sub>S [M + H]<sup>+</sup> 288,0728 found 288.07965.

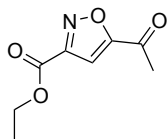
## 5.1.2 Novel and efficient synthesis of 2-aminoxazoles

### 1-(4-methoxyphenyl)ethanone (97)



To a solution of 1-(4-hydroxyphenyl)ethanone (2000 mg; 14.7 mmol) in acetone (6 mL) was added potassium carbonate (6000 mg; 44.0 mmol) and iodomethane (1800  $\mu$ L; 29.0 mmol). Reaction mixture was heated to 60°C overnight and checked by TLC with eluent petroleum ether/ethyl acetate 8/2. The mixture was quenched with H<sub>2</sub>O, was extracted with ethyl acetate and was purified by flash chromatography column petroleum ether/ethyl acetate from 9/1 to 8/2. 98% yield. <sup>1</sup>H-NMR (300 MHz-CDCl<sub>3</sub>):  $\delta$  = 2.48 (s, 3H); 3.83 (s, 3H); 7.10 (d, J= 6 Hz, 1H); 7.83 (d, J= 6 Hz, 1H).

### ethyl 5-acetylisoxazole-3-carboxylate (43)

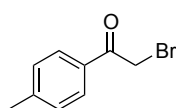


To a cooled to 0 °C solution of ethyl 2-chloro-2(hydroxyimino)acetate (1627 mg; 10.7 mmol) and 3-butyne-2-one (1680  $\mu$ L; 21.47 mmol) in benzene (19 mL) was added triethylamine (1498  $\mu$ L; 10.7 mmol) dropwise. Reaction mixture was stirred at 60 °C for 1 hour. After this time, HCl 1N was added to the mixture and it was extracted with ethyl acetate. The organic layers were washed with water, brine and dried over Na<sub>2</sub>SO<sub>4</sub>. After filtration, the solvent was removed *in vacuo* and the crude material was purified by silica gel chromatography column with eluent petroleum ether/ethyl acetate 9/1. 55% yield. <sup>1</sup>H-NMR (300 MHz-CDCl<sub>3</sub>):  $\delta$  = 1.34 (t, J=6 Hz, 3H); 2.65 (s, 3H); 4.43 (q, J=6 Hz, 2H); 7.26 (s, 1H).

### General procedure for the bromination

To a solution of the opportune ketone (1 eq) in chloroform (1.5 mL/mmol) was added acetic acid (0.1 mL/mmol) and reaction mixture was heated to 50 °C. Then a solution of bromine (1.05 eq) in chloroform (0.4 mL/mmol) was added dropwise. The mixture was stirred at the same temperature for 2 hours. After the complete consumption of the starting material, a saturated aqueous solution of NaHCO<sub>3</sub> was added and the aqueous layer was extracted with chloroform. The crude material was purified by silica gel flash chromatography. The analytical data obtained matched those reported in literature. Column eluent and yields are reported below.

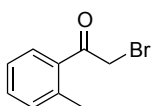
#### 2-bromo-1-(p-tolyl)ethanone (68)



Column eluent: petroleum ether/ethyl acetate 95/5.

88% yield

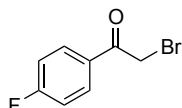
#### 2-bromo-1-(o-tolyl)ethanone (78)



Column eluent: petroleum ether/ethyl acetate 95/5

68 % yield

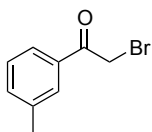
#### 2-bromo-1-(4-fluorophenyl)ethanone (79)



Column eluent: petroleum ether/ethyl acetate 97/3

77 % yield

#### 2-bromo-1-(m-tolyl)ethanone (80)

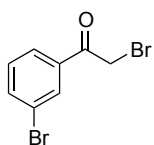


Column eluent: petroleum ether/ethyl acetate 98/2

86% yield

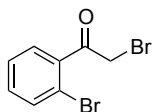


### 2-bromo-1-(3-bromophenyl)ethanone (81)



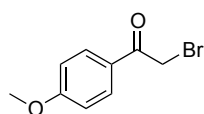
Column eluent: petroleum ether/ethyl acetate 98/2  
95% yield.

### 2-bromo-1-(2-bromophenyl)ethanone (82)



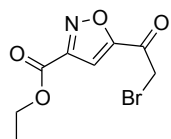
column eluent: petroleum ether/ethyl acetate 95/5  
60% yield

### 2-bromo-1-(4-methoxyphenyl)ethanone (98)



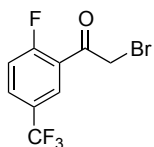
Column eluent: petroleum ether/ethyl acetate 9/1.  
85% yield.

### ethyl 5-(2-bromoacetyl)isoxazole-3-carboxylate (46)



The intermediate was used for the next step without further purification. Quantitative yield.

### 2-bromo-1-(2-fluoro-5-(trifluoromethyl)phenyl)ethanone (101)



Column eluent: petroleum ether/ethyl acetate 97/3.  
97% yield.

### **General procedure for the condensation reaction**

- Conventional heating

To a solution of  $\alpha$ -bromoketones (1 eq) in dry DMF (3 mL/mmol) was added urea (10 eq). Reaction mixture was heated to 120°C and was stirred at the same temperature until the complete consumption of the starting material. The reaction was quenched with H<sub>2</sub>O, extracted with ethyl acetate and purified by flash column chromatography.

- Microwave irradiation

To a solution of  $\alpha$ -bromoketones (1 eq) in dry DMF (3 mL/mmol) was added urea (10 eq).

Reaction mixture was irradiated in a microwave:

Temperature: 120°C

Time: 3 minutes

Pressure: 250 psi

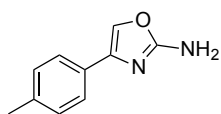
Power: 300 W

Power max: off

The reaction was monitored by TLC. After the complete consumption of the starting material, the mixture was quenched with H<sub>2</sub>O, extracted with ethyl acetate and purified by flash column chromatography.

Column eluent, yield and analytical data are reported below.

#### 4-(p-tolyl)oxazol-2-amine (70)

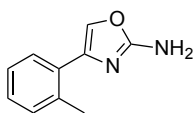


Column eluent: petroleum ether/ethyl acetate 8/2

66% yield

$^1\text{H-NMR}$  (300 MHz;  $\text{DMSO-d}_6$ ):  $\delta = 2.29$  ppm (s; 3H); 6.67 ppm (s; 2H); 7.15 ppm (d;  $J = 6$  Hz; 2H); 7.54 ppm (d;  $J = 6$  Hz; 2H); 7.80 ppm (s; 1H).

#### 4-(o-tolyl)oxazol-2-amine (83)

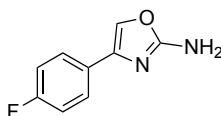


Column eluent: petroleum ether/ethyl acetate 8/2

52% yield

$^1\text{H-NMR}$  (300 MHz;  $\text{DMSO-d}_6$ ):  $\delta =$

#### 4-(4-fluorophenyl)oxazol-2-amine (84)

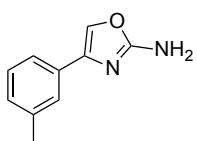


Column eluent: petroleum ether/ethyl acetate 7/3

53% yield

$^1\text{H-NMR}$  (400 MHz;  $\text{DMSO-d}_6$ ):  $\delta = 6.75$  ppm (s, 2H); 7.20 ppm (d;  $J = 8$  Hz; 2H); 7.66 ppm (d;  $J = 8$  Hz); 7.86 ppm (s; 1H).

#### 4-(m-tolyl)oxazol-2-amine (85)

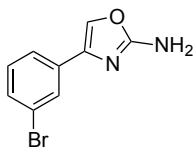


column eluent: petroleum ether/ethyl acetate 8/2

52% yield

$^1\text{H-NMR}$  (300 MHz;  $\text{DMSO-d}_6$ ):  $\delta =$

#### 4-(3-bromophenyl)oxazol-2-amine (86)

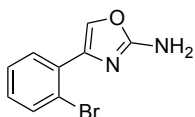


column eluent: petroleum ether/ethyl acetate 8/2

57% yield

$^1\text{H-NMR}$  (300 MHz;  $\text{DMSO-d}_6$ ):  $\delta =$

#### 4-(2-bromophenyl)oxazol-2-amine (87)

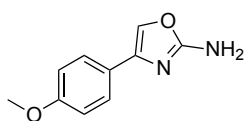


Column eluent: petroleum ether/ethyl acetate 8/2

40% yield

$^1\text{H-NMR}$  (300 MHz;  $\text{DMSO-d}_6$ ):  $\delta$  = 6.81 ppm (s; 2H); 7.24 ppm (td;  $J_1$  = 1.77 Hz,  $J_2$  = 7.62 Hz; 1H); 7.46-7.40 ppm (m, 1H); 7.69 ppm (dd; ;  $J_1$  = 1.77 Hz,  $J_2$  = 7.62 Hz; 1H); 7.93 ppm (dd;  $J_1$  = 3 Hz,  $J_2$  = 8 Hz; 1H); 8.04 ppm (s, 1H).

#### 4-(4-methoxyphenyl)oxazol-2-amine (99)

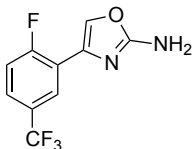


Column eluent: petroleum ether/ethyl acetate 7/3

38% yield

$^1\text{H-NMR}$  (300 MHz;  $\text{DMSO-d}_6$ ):  $\delta$  = 2.26 ppm (s, 3H); 6.97 ppm (s, 2H); 7.58 ppm (d,  $J$  = 8 Hz, 2H); 7.70 ppm (d,  $J$  = 8 Hz, 2H); 8.00 ppm (s, 1H).

#### 4-(2-fluoro-5-(trifluoromethyl)phenyl)oxazol-2-amine (102)

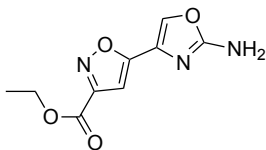


Column eluent: petroleum ether/ethyl acetate 7/3

25% yield

$^1\text{H-NMR}$  (300 MHz;  $\text{DMSO-d}_6$ ):  $\delta$  = 6.97 ppm (s, 2H); 7.56 ppm (t,  $J$  = 10 Hz, 1H); 7.71 ppm (d,  $J$  = 3 Hz, 1H); 7.86 (d,  $J$  = 3 Hz, 1H); 8.00 ppm (s, 1H).

#### ethyl 5-(2-aminoxazol-4-yl)isoxazole-3-carboxylate (103)



Column eluent: petroleum ether/ethyl acetate 5/5

49% yield

$^1\text{H-NMR}$  (400 MHz;  $\text{DMSO-d}_6$ ):  $\delta$  = 1.35 ppm (t,  $J$  = 8 Hz, 3H); 4.41 ppm (q,  $J$  = 8 Hz, 2H); 6.90 ppm (s, 1H); 7.07 ppm (s, 2H); 8.16 ppm (s, 1H).

## General procedure for the Buchwald-Hartwig cross coupling

- **Conventional heating**

A solution of 2-aminooxazole (1 eq), aryl halide (0.5 eq), NaOtBu (1 eq) in t-Butanol (0.5 mL/mmol) and dry toluene (2.5 mL/mmol) was stirred under argon flux for 15 minutes. After this time, X-Phos Pd G2 (0.1 eq) was added and the reaction mixture was heated and stirred at 130 °C for 1 hour. After the complete consumption of the starting material, the mixture was quenched with H<sub>2</sub>O, was extracted with ethyl acetate and purified by flash column chromatography.

- **Microwave irradiation**

In a 10 mL test tube for microwave, a solution of 2-aminooxazole (1 eq), aryl halide (0.5 eq), NaOtBu (1 eq) in t-Butanol (0.5 mL/mmol) and dry toluene (2.5 mL/mmol) was stirred under argon flux for 15 minutes. After this time, X-Phos Pd G2 (0.1 eq) was added and the reaction mixture was irradiated in a microwave:

Temperature: 130°C

Time: 15 minutes

Pressure: 250 psi

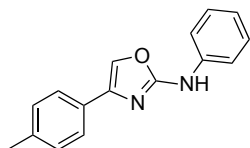
Power: 300 W

Power max: off

The reaction was monitored by TLC. After the complete consumption of the starting material, the mixture was quenched with H<sub>2</sub>O, extracted with ethyl acetate and purified by flash column chromatography.

Column eluent, yield and analytical data are reported below.

### **N-phenyl-4-(*p*-tolyl)oxazol-2-amine (71)**



Column eluent: petroleum ether/ethyl acetate 96/4

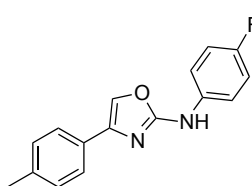
51% yield

$^1\text{H-NMR}$  (300 MHz;  $\text{DMSO-d}_6$ ):  $\delta = 2.33$  ppm (s, 3H);

6.95 ppm (m, 1H); 7.25 ppm (d,  $J = 6$  Hz, 2H); 7.33 ppm

(t,  $J = 6$  Hz, 2H); 7.72-7.66 (m, 4H); 8.10 ppm (s, 1H); 10.16 ppm (bs, 1H).

### **N-(4-fluorophenyl)-4-(*p*-tolyl)oxazol-2-amine (72)**



Column eluent: petroleum ether/ethyl acetate 96/4

53% yield

$^1\text{H-NMR}$  (400 MHz;  $\text{DMSO-d}_6$ ):  $\delta = 2.33$  ppm (s, 3H);

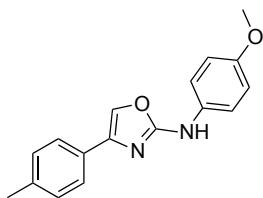
7.17-7.25 ppm (m, 4H); 7.67 ppm (d,  $J = 8$  Hz, 2H);

7.72-7.74 (m, 2H); 8.10 ppm (s, 1H); 10.2 ppm (bs, 1H).

$^{13}\text{C-NMR}$  (100.6 MHz;  $\text{DMSO-d}_6$ ):  $\delta = 21.34$ ; 115.82; 116.04; 118.30; 118.37;

125.31; 127.89; 129.65; 136.47; 137.32; 139.34; 157.17.

### **N-(4-methoxyphenyl)-4-(*p*-tolyl)oxazol-2-amine (73)**



Column eluent: petroleum ether/ethyl acetate 97/3

34% yield

$^1\text{H-NMR}$  (400 MHz;  $\text{DMSO-d}_6$ ):  $\delta = 2.33$  ppm (s, 3H);

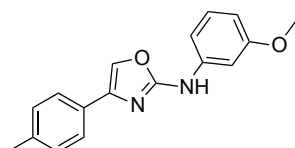
3.73 ppm (s, 3H); 6.92 ppm (d,  $J = 8$  Hz; 2H); 7.24 (d,  $J$

= 8 Hz, 2H); 7.64 ppm (m; 4H); 8.05 ppm (s, 1H); 9.93 ppm (bs, 1H).

$^{13}\text{C-NMR}$  (100.6 MHz;  $\text{DMSO-d}_6$ ):  $\delta = 21.34$ ; 55.67; 114.67; 118.38; 125.38;

127.59; 129.26; 129.63; 133.41; 137.21; 139.37; 154.36; 157.18.

### **N-(3-methoxyphenyl)-4-(*p*-tolyl)oxazol-2-amine (74)**



Column eluent: petroleum ether/ethyl acetate

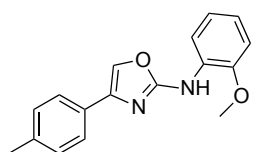
97/3

59% yield

<sup>1</sup>H-NMR (400 MHz; DMSO-d<sub>6</sub>): δ = 2.33 ppm (s, 3H); 3.77 ppm (s, 3H); 6.54-6.56 ppm (m, 1H); 7.21-7.25 ppm (m, 4H); 7.45 ppm (s, 1H); 7.65 ppm (d, J = 8 Hz, 2H); 8.10 ppm (s, 1H); 10.17 ppm (bs, 1H).

<sup>13</sup>C-NMR (100.6 Mhz; DMSO-d<sub>6</sub>): δ = 21.34; 55.36; 103.00; 106.19; 109.55; 125.28; 127.89; 129.12; 129.69; 130.19; 137.31; 139.40; 141.14; 157.03; 160.34.

### ***N*-(2-methoxyphenyl)-4-(*p*-tolyl)oxazol-2-amine (75)**



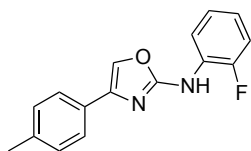
Column eluent: petroleum ether/ethyl acetate 97/3

71% yield

<sup>1</sup>H-NMR (400 MHz; DMSO-d<sub>6</sub>): δ = 2.33 ppm (s, 3H); 3.85 ppm (s, 3H); 6.97-7.05 ppm (m, 3H); 7.24 ppm (d, J = 8 Hz, 2H); 7.64 ppm (d, J = 8 Hz, 2H); 8.10 ppm (s, 1H); 8.26-8.27 ppm (m, 1H); 9.08 ppm (bs, 1H).

<sup>13</sup>C-NMR (100.6 Mhz; DMSO-d<sub>6</sub>): δ = 21.34; 55.36; 103.00; 106.19; 109.55; 125.28; 127.89; 129.12; 129.69; 130.19; 137.31; 139.40; 141.14; 157.03; 160.34.

### ***N*-(2-fluorophenyl)-4-(*p*-tolyl)oxazol-2-amine (76)**



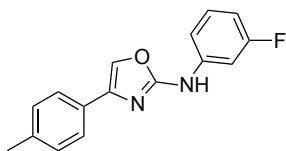
Column eluent: petroleum ether/ethyl acetate 97/3

59% yield

<sup>1</sup>H-NMR (400 MHz; DMSO-d<sub>6</sub>): δ = 2.33 ppm (s, 3H); 7.01-7.06 ppm (m, 1H); 7.23-7.28 ppm (m, 4H); 7.66 ppm (d, J = 8 Hz, 2H); 8.13 ppm (s, 1H); 8.32-8.44 ppm (t, J = 8 Hz, 1H); 9.94 ppm (bs, 1H).

<sup>13</sup>C-NMR (100.6 Mhz; DMSO-d<sub>6</sub>): δ = 21.34; 115.65; 115.85; 120.31; 122.94; 123.01; 125.33; 127.80; 128.46; 129.01; 129.67; 137.37; 139.42; 157.18.

### ***N*-(3-fluorophenyl)-4-(*p*-tolyl)oxazol-2-amine (77)**

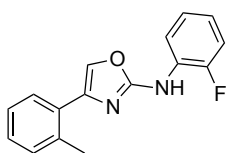


Column eluent: petroleum ether/ethyl acetate 97/3

37% yield

$^1\text{H-NMR}$  (300 MHz;  $\text{DMSO-d}_6$ ):  $\delta$  = 2.33 ppm (s, 3H); 6.75-6.80 ppm (m, 1H); 7.24-7.26 (d,  $J$  = 6 Hz, 2H); 7.35-7.42 ppm (m, 2H); 7.65-7.71 (m, 3H); 8.14 ppm (s, 1H); 10.45 ppm (bs, 1H).  $^{13}\text{C-NMR}$  (100.6 Mhz;  $\text{DMSO-d}_6$ ):  $\delta$  = 22.34; 114.35; 115.65; 121.31; 121.94; 123.01; 126.42; 127.50; 128.33; 129.09; 129.55; 137.77; 139.24; 157.19.

### ***N*-(2-fluorophenyl)-4-(*o*-tolyl)oxazol-2-amine (88)**

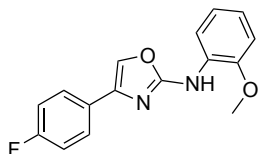


Column eluent: petroleum ether/ethyl acetate 97/3

40% yield.  $^1\text{H-NMR}$  (300 MHz;  $\text{DMSO-d}_6$ ):  $\delta$  = 2.53 ppm (s, 3H); 6.75-6.84 ppm (m, 4H); 7.29-7.33 (m, 3H); 7.35-

7.38 ppm (m, 1H); 8.06 ppm (s, 1H); 10.43 ppm (bs, 1H).  $^{13}\text{C-NMR}$  (100.6 Mhz;  $\text{DMSO-d}_6$ ):  $\delta$  = 21.32; 115.33; 115.65; 120.31; 121.55; 122.99; 123.15; 124.35; 125.33; 127.88; 128.99; 129.11; 129.67; 137.88; 139.42; 157.18.

### **4-(4-fluorophenyl)-*N*-(2-methoxyphenyl)oxazol-2-amine (89)**



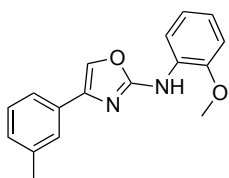
Column eluent: petroleum ether/ethyl acetate 98/2

70% yield

$^1\text{H-NMR}$  (400 MHz;  $\text{DMSO-d}_6$ ):  $\delta$  = 3.89 ppm (s, 3H); 6.58-7.02 ppm (m, 3H); 7.27 (t,  $J$  = 4 Hz, 2H); 7.82-7.85 ppm (m, 2H); 8.15 ppm (s, 1H); 8.28 ppm (t,  $J$  = 4 Hz, 1H); 9.17 ppm (bs, 1H).  $^{13}\text{C-NMR}$  (100.6 Mhz;  $\text{DMSO-d}_6$ ):  $\delta$  = 56.21; 111.51; 115.93; 116.14; 118.24; 121.08; 122.67; 125.95; 127.30; 128.39; 138.53; 148.65; 157.63; 163.22.



### ***N*-(2-methoxyphenyl)-4-(*m*-tolyl)oxazol-2-amine (90)**

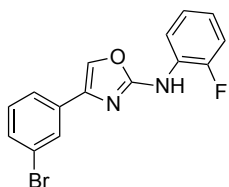


Column eluent: petroleum ether/ethyl acetate 98/2.

37% yield.  $^1\text{H-NMR}$  (400 MHz;  $\text{DMSO-d}_6$ ):  $\delta$  = 2.33 ppm (s, 3H); 3.85 ppm (s, 3H); 6.97-7.05 ppm (m, 4H); 7.45-7.50 (m, 3H); 7.78 ppm (s, 1H); 8.13 ppm (s, 1H); 8.26-

8.27 ppm (m, 1H); 9.08 ppm (bs, 1H).  $^{13}\text{C-NMR}$  (100.6 Mhz;  $\text{DMSO-d}_6$ ):  $\delta$  = 21.34; 55.36; 103.00; 106.19; 109.55; 125.28; 127.89; 129.12; 129.69; 130.19; 137.31; 139.40; 141.14; 157.03; 160.34.

### **4-(3-bromophenyl)-*N*-(2-fluorophenyl)oxazol-2-amine (91)**

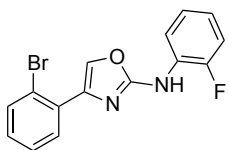


Column eluent: petroleum ether/ethyl acetate 97/3

35% yield.  $^1\text{H-NMR}$  (400 MHz;  $\text{DMSO-d}_6$ ):  $\delta$  =6.61-6.63 (m, 2H); 6.97-6.69 (m, 2H); 7.40-7.46 (m, 2H); 7.56-7.60 (m, 2H); 8.02 (s, 1H); 11.20 (bs, 1H).  $^{13}\text{C-NMR}$  (100.6

Mhz;  $\text{DMSO-d}_6$ ):  $\delta$  =116.30; 122.33; 123.40; 123.88; 125.33; 126.10; 126.58; 128.10; 128.40; 131.02; 135.05; 139.40; 140.44; 154.30; 160.69.

### **4-(2-bromophenyl)-*N*-(2-fluorophenyl)oxazol-2-amine (92)**



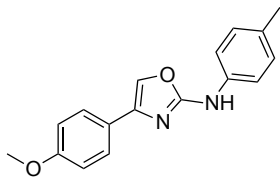
Column eluent: petroleum ether/ethyl acetate 9/1

15% yield

$^1\text{H-NMR}$  (400 MHz;  $\text{DMSO-d}_6$ ):  $\delta$  = 5.76 ppm (s, 1H);

7.12-7.18 (m, 2H); 7.35-7.38 ppm (m, 2H); 7.46 ppm (d,  $J$  = 8 Hz, 2H); 8.12 ppm (d,  $J$  = 8 Hz, 2H); 11.24 ppm (bs, 1H).  $^{13}\text{C-NMR}$  (100.6 Mhz;  $\text{DMSO-d}_6$ ):  $\delta$  = 111.51; 115.93; 116.14; 118.24; 121.08; 122.67; 125.95; 127.30; 127.38; 128.39; 128.72; 138.53; 148.65; 157.63; 163.22.

#### 4-(4-methoxyphenyl)-*N*-(*p*-tolyl)oxazol-2-amine (93)



Column eluent: dichloromethane/methanol 91/1

10% yield

$^1\text{H-NMR}$  (400 MHz;  $\text{DMSO-d}_6$ ):  $\delta = 3.26$  ppm (s, 3H);

3.79 ppm (s, 3H); 6.98 ppm (d,  $J = 8$  Hz, 2H); 7.12-

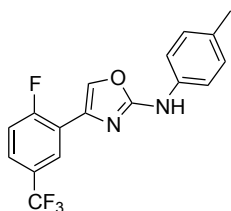
7.18 ppm (m, 1H); 7.58 ppm (d,  $J = 8$  Hz, 2H); 7.70 ppm (d,  $J = 8$  Hz, 2H);

8.00 ppm (s, 1H); 9.98 ppm (bs, 1H).  $^{13}\text{C-NMR}$  (100.6 MHz;  $\text{DMSO-d}_6$ ):  $\delta =$

111.51; 115.93; 116.14; 118.24; 121.08; 122.67; 125.95; 127.30; 127.38;

128.39; 128.72; 138.53; 148.65; 157.63; 163.22.

#### 4-(2-fluoro-5-(trifluoromethyl)phenyl)-*N*-(*p*-tolyl)oxazol-2-amine (94)



Column eluent: petroleum ether/ethyl acetate 98/2

31% yield

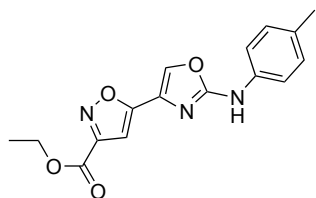
$^1\text{H-NMR}$  (300 MHz;  $\text{DMSO-d}_6$ ):  $\delta = 2.26$  ppm (s, 3H); 7.18

ppm (d,  $J = 9$  Hz, 2H); 7.53-7.62 ppm (m, 3H); 7.76-7.79

ppm (m, 1H); 8.11 ppm (d,  $J = 4$  Hz, 1H); 8.22 ppm (d,  $J = 4$  Hz, 1H); 10.24

ppm (bs, 1H).

#### ethyl 5-(2-(*p*-tolylamino)oxazol-4-yl)isoxazole-3-carboxylate (95)



Column eluent: petroleum ether/ethyl acetate

9/1

16% yield

$^1\text{H-NMR}$  (400 MHz;  $\text{DMSO-d}_6$ ):  $\delta = 1.35$  ppm (t,  $J =$

8 Hz, 3H); 2.27 ppm (s, 3H); 4.41 ppm (q,  $J = 8$  Hz, 2H); 7.10 ppm (s, 1H);

7.15-7.17 ppm (d,  $J = 2$  Hz, 2H); 7.53-7.55 (d,  $J = 8$  Hz, 2H); 8.42 ppm (s, 1H),

10.33 (bs, 1H).  $^{13}\text{C-NMR}$  (100.6 MHz;  $\text{DMSO-d}_6$ ):  $\delta = 14.42$ ; 20.82; 62.45;

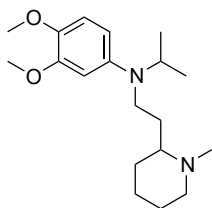
101.52; 117.39; 129.86; 131.05; 132.72; 136.99; 156.56; 136.99; 156.56;

158.31; 159.31; 159.35; 165.12.

### 5.1.3 Rational design and synthesis of Thioridazine analogues as enhancers of the antituberculosis therapy

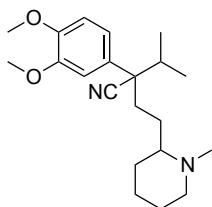
#### N-Isopropyl-3,4-dimethoxy-N-(2-(1-methylpiperidin-2-yl)-ethyl)aniline

(104)



To a solution of **117** (60 mg; 0.38 mmol) in dry toluene (2 mL) was added sodium amide (120 mg; 3.07 mmol) and 2-(2-chloroethyl)piperidine hydrochloride (244 mg; 1.23 mmol). The reaction mixture was stirred and heated in a microwave oven at 140 °C for 30 min. After quenching with brine (25 mL), the mixture was extracted with ethyl acetate (3 × 10 mL), and the combined organic layers were dried over anhydrous Na<sub>2</sub>SO<sub>4</sub> and evaporated under reduced pressure. The crude material was then purified through flash chromatography, eluting with dichloromethane/methanol 9/1. Yield: 16%.  
<sup>1</sup>H-NMR (400 MHz-CDCl<sub>3</sub>): δ 1.10-1.15 (m, 6 H); 1.20-1.87 (m, 8H), 2.30-2.35 (bs, 5H); 2.95-3.10 (m, 2H), 3.15-3.25 (m, 1H); 3.65-3.75 (m, 1H); 3.84 (s, 3H); 3.87, (s, 3H); 6.41 (d, J = 9 Hz, 1H); 6.49 (s, 1H); 6.79 (d, J = 9 Hz, 1H).  
<sup>13</sup>C NMR (100.6 MHz- CDCl<sub>3</sub>): δ 19.4, 20.2, 23.3, 28.3, 41.3, 53.8, 55.9, 56.3, 105.6, 111.9, 142.6, 143.7, 149.5. HRMS (ESI) calculated for C<sub>19</sub>H<sub>32</sub>N<sub>2</sub>O<sub>2</sub> [M + H]<sup>+</sup> 321.2464, found 321.25365.

#### 2-(3,4-Dimethoxyphenyl)-2-isopropyl-4-(1-methylpiperidin-2-yl)butanenitrile (105)



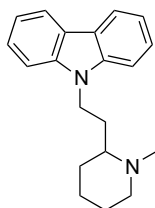
To a solution of **118** (70 mg; 0.31 mmol) in dry Toluene (2 mL) were added sodium amide (124 mg; 3.19 mmol) and 2-(2-chloroethyl)piperidine hydrochloride (252 mg; 1.25 mmol). The reaction mixture was stirred and heated in a

microwave oven at 140 °C for 30 min. After quenching with brine (25 mL), the mixture was extracted with ethyl acetate (3 × 10 mL), and the combined organic layers were dried over anhydrous Na<sub>2</sub>SO<sub>4</sub>. The crude material was then purified through flash column chromatography, eluting with dichloromethane/methanol 9/1. Yield: 50%. <sup>1</sup>H-NMR (300 MHz- CDCl<sub>3</sub>): δ 0.8 (dd, J<sub>1</sub> = 4 Hz, J<sub>2</sub> = 7 Hz, 3 H); 1.23-1.80 (m; 11H), 1.85-2.40 (m; 8H); 2.80-2.95 (m; 1H), 3.88 (s, 3H); 3.90 (s, 3H); 6.80-7.00 (m, 3H). <sup>13</sup>C-NMR (100.6 MHz-CDCl<sub>3</sub>): δ 18.7, 19.0, 24.0, 28.2, 29.9, 32.1, 32.5, 37.9, 53.4, 55.9, 56.0, 63.0, 109.1, 109.4, 111.0, 118.8, 121.1, 130.5, 148.3, 149.0. HRMS (ESI) calculated for C<sub>21</sub>H<sub>32</sub>N<sub>2</sub>O<sub>2</sub> [M + H]<sup>+</sup> 345.2464, found 345.25365.

### **General Procedure for the Synthesis of Compounds 106-112**

To a suspension of sodium hydride (60% suspension in mineral oil, 3 equiv) in DMF (5 mL/mmol) was added the suitable heterocyclic compound (1 equiv) at 0 °C. Reaction mixture was stirred for 15 min at the same temperature, and then 2-(2-chloroethyl)- piperidine hydrochloride (1.3 equiv) was added portionwise. The mixture was allowed to react at room temperature until consumption of the starting material. In some cases (5, 6, 13) reflux heating was necessary. After quenching with water, the mixture was extracted with ethyl acetate (3 × 10 mL), and the organic layers were washed with water and brine, dried over anhydrous Na<sub>2</sub>SO<sub>4</sub>, and concentrated under reduced pressure. The crude material was purified through flash chromatography. Reaction times and conditions, yields, purification methods, and other analytical data are reported below:

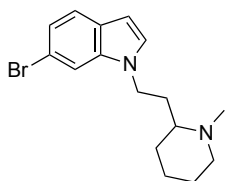
### 9-(2-(1-Methylpiperidin-2-yl)ethyl)-9H-carbazole (106)



Reaction mixture was stirred at room temperature for 48 hours. Purified by flash column chromatography (dichloromethane/methanol 9/1). Yield 53%. White powder.

$^1\text{H-NMR}$  (400 MHz- $\text{CDCl}_3$ ):  $\delta$  1.36-1.40 (m, 1H); 1.65-1.68 (m, 3H); 1.82-1.85 (m, 2H); 2.07-2.30 (m, 4H); 2.37 (s, 3H); 2.92-2.97 (m, 1H); 4.36-4.48 (m, 2H); 7.24-7.52 (m, 6H); 8.12 (d,  $J = 8$  Hz, 2H).  $^{13}\text{C-NMR}$  (100.6 MHz- $\text{CDCl}_3$ ):  $\delta$  24.2, 25.3, 30.5, 31.4, 39.2, 42.7, 56.9, 61.7, 108.5, 118.8, 120.4, 123.0, 125.7, 140.2. HRMS (ESI) calculated for  $\text{C}_{20}\text{H}_{24}\text{N}_2$  [ $\text{M} + \text{H}$ ] $^+$  293.1939, found 293.20123.

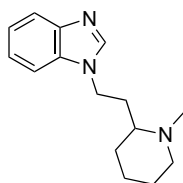
### 6-Bromo-1-(2-(1-methylpiperidin-2-yl)ethyl)-1H-indole (107)



Reaction mixture was stirred at room temperature for 48 hours. Purified by flash column chromatography (dichloromethane/methanol 95/5). Yield 61%. Yellow semisolid.  $^1\text{H-NMR}$  (300 MHz- $\text{CDCl}_3$ ):  $\delta$  1.26- 2.19 (m, 10H); 2.31 (s, 3H); 2.88-2.96 (m, 1H); 4.09- 4.27 (m, 2H); 6.44 (d,  $J = 3$ Hz, 1H); 7.12 (d,  $J = 3$ Hz, 1H), 7.20-7.32 (m, 2H); 7.76 (d,  $J = 3$ Hz, 1H).

$^{13}\text{C-NMR}$  (100.6 MHz- $\text{CDCl}_3$ ):  $\delta$  24.2, 25.3, 30.4, 33.2, 25.4, 30.4, 33.2, 41.7, 42.6, 56.8, 61.4, 100.8, 110.7, 123.4, 128.7, 130.3. HRMS (ESI) calculated for  $\text{C}_{16}\text{H}_{21}\text{BrN}_2$  [ $\text{M} + \text{H}$ ] $^+$  321.0888, found 321.09595.

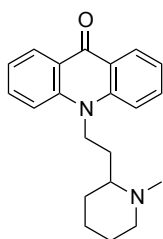
### 1-(2-(1-Methylpiperidin-2-yl)ethyl)-1H-benzo[d]imidazole (108)



Reaction mixture was stirred at room temperature for 48 hours. Purified by flash column chromatography (petroleum ether/ethyl acetate 9/1). Yield 72%. Yellow oil.  $^1\text{H-NMR}$  (300 MHz- $\text{CDCl}_3$ ):  $\delta$  1.27-1.77 (m, 6H); 2.02-

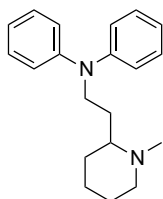
2.20 (m, 4H); 2.30 (s, 3H); 2.86-2.94 (m, 1H); 4.15- 4.36 (m, 2H); 7.20-7.34 (m, 2H); 7.39-7.44 (m, 1H); 7.80- 7.85 (m, 1H), 7.93 (s, 1H).  $^{13}\text{C-NMR}$ (100.6 MHz- $\text{CDCl}_3$ ):  $\delta$  24.2, 25.1, 30.2, 32.9, 41.3, 42.5, 56.7, 61.1, 64.4, 88.8, 109.6, 120.4, 122.1, 122.9, 142.8. HRMS (ESI) calculated for  $\text{C}_{15}\text{H}_{21}\text{N}_3$  [ $\text{M} + \text{H}$ ] $^+$  244,1735, found 244.18082.

### 10-(2-(1-Methylpiperidin-2-yl)ethyl)acridin-9-(10H)-one (109)



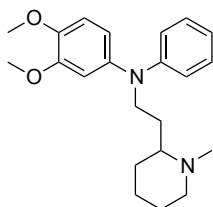
Reaction mixture was stirred at room temperature for 48 hours. Purified by flash column chromatography (dichloromethane/methanol 95/5). Yield 48%. Yellow powder.  $^1\text{H-NMR}$  (300 MHz- $\text{d}_6$ -DMSO):  $\delta$  1.20-2.15 (m, 10H); 2.29 (s, 3H); 4.08-4.12 (m, 1H); 4.44-4.60 (m, 2H); 7.36 (t,  $J = 9.0$  Hz, 2H); 7.76- 7.91 (m, 4H); 8.37 (dd,  $J_1 = 3$  Hz,  $J_2 = 9$  Hz, 2H).  $^{13}\text{C-NMR}$  (100.6 MHz- $\text{CDCl}_3$ ):  $\delta$  24.2, 25.1, 29.8, 30.2, 42.7, 42.9, 56.7, 61.7, 114.3, 121.2, 122.6, 128.1, 133.9, 141.7, 177.9. HRMS (ESI) calculated for  $\text{C}_{21}\text{H}_{24}\text{N}_2\text{O}$  [ $\text{M} + \text{H}$ ] $^+$  321,1889, found 321.19614.

### N-(2-(1-Methylpiperidin-2-yl)ethyl)-N-phenylaniline (110)



Reaction mixture was stirred at reflux temperature for 48 hours. Purified by flash column chromatography (dichloromethane/methanol 97/3). Yield 29%. Brown oil.  $^1\text{H-NMR}$ (400 MHz- $\text{CDCl}_3$ ):  $\delta$  1.32-1.34 (m, 1H); 1.50-1.55 (m, 1H); 1.60-1.95 (m, 5H); 2.04-2.06 (m, 1H); 2.23-2.30 (m, 5H); 2.95 (d,  $J = 12.0$  Hz, 1H); 3.73-3.89 (m, 2H); 6.95-7.00 (m, 6H); 7.25-7.30 (m, 4H).  $^{13}\text{C-NMR}$  (100.6 MHz- $\text{CDCl}_3$ ):  $\delta$  23.6, 24.7, 29.5, 29.9, 63.1 42.1, 48.5, 56.6, 62.2, 120.9, 121.3, 129.3, 147.8. HRMS (ESI) calculated for  $\text{C}_{20}\text{H}_{26}\text{N}_2$  [ $\text{M} + \text{H}$ ] $^+$  295,2096, found 295.21688.

### 3,4-Dimethoxy-N-(2-(1-methylpiperidin-2-yl)ethyl)-N-phenylaniline (111)

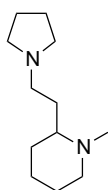


Reaction mixture was stirred at reflux temperature for 48 hours. Purified by flash column chromatography (dichloromethane/methanol 98/2). Yield 28%. Brown powder.  $^1\text{H-NMR}$  (300 MHz- $\text{CDCl}_3$ ):  $\delta$  1.50- 2.40 (m, 7 H);

2.61 (s, 3H); 3.48-3.66 (m, 2H); 3.66-3.68 (m, 1H); 3.83 (s, 3H); 3.91 (s, 3H); 4.12- 4.15 (m, 1H); 4.90-5.10 (m, 2H); 6.67-6.89 (m, 3H); 7.20-7.28 (m, 5H).

$^{13}\text{C-NMR}$  (100.6 MHz-  $\text{CDCl}_3$ ):  $\delta$  16.3, 18.9, 20.9, 23.8, 29.7, 48.5, 50.2, 56.0, 56.1, 58.1, 109.6, 111.9, 116.40, 117.5, 119.1, 129.2, 140.4, 146.3, 148.5, 149.9. HRMS (ESI) calculated for  $\text{C}_{22}\text{H}_{30}\text{N}_2\text{O}_2$   $[\text{M} + \text{H}]^+$  355,2307, found 355.23800.

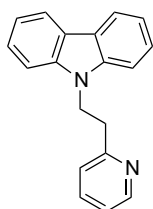
### 1-Methyl-2-(2-(pyrrolidin-1-yl)ethyl)piperidine (112)



Reaction mixture was stirred at room temperature for 48 hours. Purified by flash column chromatography (dichloromethane/methanol 95/5). Yield 33%. Yellow oil.  $^1\text{H-NMR}$  (300 MHz- $\text{CDCl}_3$ ):  $\delta$  1.22-1.54 (m, 3H); 1.68-2.30 (m, 8H); 2.30-

2.49 (m, 3H); 2.60-2.90 (m, 5H); 3.00-3.10 (m, 1H); 3.40-3.80 (m, 4H).  $^{13}\text{C-NMR}$  (100.6 MHz-  $\text{CDCl}_3$ ):  $\delta$  14.2, 16.3, 18.8, 20.8, 23.8, 29.9, 36.8, 40.4, 42.4, 49.3, 50.6, 55.3. HRMS (ESI) calculated for  $\text{C}_{12}\text{H}_{24}\text{N}_2$   $[\text{M} + \text{H}]^+$  197,1939, found 197.18702.

### 9-(2-(Pyridin-3-yl)ethyl)-9H-carbazole (113)

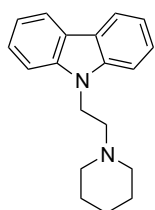


Compound 10 was prepared with a similar procedure, but using compound **128** in place of 2(2-chloroethyl)piperidine hydrochloride. Reaction mixture was stirred at room temperature for 18 hours. Purified by flash column

chromatography (petroleum ether/ethyl acetate 60/40). Yield 18%. Light

brown powder.  $^1\text{H-NMR}$  (400 MHz- $\text{CDCl}_3$ ):  $\delta$  3.33 (t,  $J = 7.2$  Hz, 2H); 4.77 (t,  $J = 7.2$  Hz, 2H); 6.84 (d,  $J = 8$  Hz, 1H); 7.11-7.46 (m, 8H); 8.11 (d,  $J = 7$  Hz, 2H); 8.65 (d,  $J = 2.4$  Hz, 1 H).  $^{13}\text{C-NMR}$  (100.6 MHz- $\text{CDCl}_3$ ):  $\delta$  37.2, 42.9, 108.6, 118.8, 120.20, 121.7, 122.8, 123.7, 125.6, 136.5, 140.2, 149.4, 158.6. HRMS (ESI) calculated for  $\text{C}_{19}\text{H}_{16}\text{N}_2$  [ $\text{M} + \text{H}$ ] $^+$  273.1313, found 273.13863.

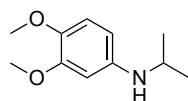
### 9-(2-(Piperidin-1-yl)ethyl)-9H-carbazole (114)



To a solution of piperidine (33  $\mu\text{L}$ ; 0.33 mmol) in DMF (15 mL/mmol) was added potassium carbonate (138 mg, 1 mmol). This mixture was stirred at room temperature for 20 min, and then the intermediate **130** (10 mg, 0.43 mmol) was added.

Reaction mixture was stirred to 60  $^\circ\text{C}$  overnight. After cooling, brine (25 mL) was added and the mixture was extracted with ethyl acetate (3  $\times$  10 mL). The combined organic layers were washed with water and brine, dried over anhydrous  $\text{Na}_2\text{SO}_4$ , and concentrated under reduced pressure. The crude material was purified through flash chromatography, eluting with petroleum ether/ethyl acetate 95/5, yielding the title compound as a white solid. Yield: 19%.  $^1\text{H-NMR}$  (400 MHz,  $\text{CDCl}_3$ ):  $\delta$  1.24-1.60 (m, 6H); 3.07 (bs, 2H); 3.39 (bs, 2H); 4.49 (t,  $J = 8$  Hz, 2H); 4.62 (t,  $J = 8$  Hz, 2H); 7.23-7.28 (m, 2H); 7.46-7.79 (m, 4H), 8.12 (d,  $J = 8$  Hz, 2H).  $^{13}\text{C-NMR}$  (100.6 MHz- $\text{CDCl}_3$ ):  $\delta$  24.2, 25.4, 42.1, 44.7, 62.8, 108.7, 119.1, 120.3, 123.0, 125.7, 140.5, 155.0. HRMS (ESI) calculated for  $\text{C}_{19}\text{H}_{22}\text{N}_2$  [ $\text{M} + \text{H}$ ] $^+$  279.1783, found 279.39258.

### N-isopropyl-3,4-dimethoxyaniline (117)



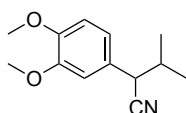
A solution of 3,4-dimethoxyaniline (500 mg; 3.26 mmol), isopropyl iodide (325  $\mu\text{l}$ ; 3.26 mmol) and triethylamine (453  $\mu\text{l}$ ; 3.26 mmol) in methanol (5 ml) was stirred at reflux

overnight. After quenching with water (25 mL), the mixture was extracted



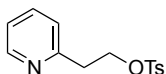
with ethyl acetate (3 × 10 mL), the combined organic layers were dried on anhydrous Na<sub>2</sub>SO<sub>4</sub> and evaporated under reduced pressure. The crude material was purified through flash chromatography eluting with petroleum ether/ethyl acetate 7/3. Yield 50%. Analytical data were consistent with those already published.

### 2-(3,4-Dimethoxyphenyl)-3-methylbutanenitrile (118)



To a suspension of sodium hydride 60% (225 mg; 5.60 mmol) in dry DMF (5 ml) was added 3,4-dimethoxyphenyl acetonitrile (500 mg; 2.80 mmol). After 5 h, 2-bromopropane (210 μl; 2.25 mmol) was added to reaction mixture that was stirred overnight. After quenching with HCl 1N (25 mL), the mixture was extracted with diethyl ether (3 × 10 mL), the combined organic layers were dried on anhydrous Na<sub>2</sub>SO<sub>4</sub> and evaporated under reduced pressure. The crude material was purified through flash chromatography eluting with petroleum ether/ethyl acetate 8/2. Yield: 47%. <sup>1</sup>H-NMR (300 MHz-CDCl<sub>3</sub>): δ 0.89 (d, J = 9 Hz, 6H); 1.90-2.03 (m; 1H); 3.48 (d, J = 6 Hz, 1H); 3.74-3.81 (m, 6H); 6.69-6.80 (m, 3H).

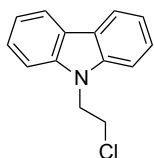
### 2-(Pyridin-3-yl)ethyl 4-methylbenzenesulfonate (128)



A solution of 2-(2-hydroethyl)pyridine (457 μl; 4.06 mmol), triethylamine (848 μl; 6.09 mmol) and p-toluenesulfonyl chloride (851 mg; 4.46 mmol) in dichloromethane (5 ml/mmol) was stirred at room temperature, until consumption of the starting material according to TLC (20 h). Dichloromethane (25 ml) was added to reaction mixture and it was washed with water (3 × 10 ml). The crude material was purified through flash column chromatography eluting with petroleum ether/ethyl acetate 7/3, yielding the title compound as yellow oil. Yield: 75%.

$^1\text{H-NMR}$ (300 MHz- $\text{CDCl}_3$ ):  $\delta$  2.32-2.44 (m, 3H); 3.02-3.16 (m, 2H); 4.37-4.7 (m, 2H); 7.05-7.31 (m, 4H); 7.48-7.71 (m, 3H); 8.33-8.45 (m, 1H).

### 9-(2-Chloroethyl)-9H-carbazole (130)

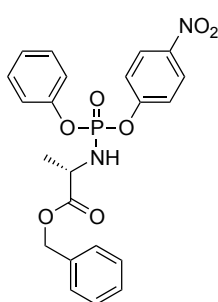


A suspension of carbazole (500 mg, 2.99 mmol), potassium hydroxide (1.68 g, 29.9 mmol), potassium carbonate (4.132 g, 29.9 mmol) and tetrabutylammonium fluoride (94 mg, 0.29 mmol) in 1,2-dichloroethane (0.15 ml/mmol) was stirred at 60 °C overnight. After cooling, water (25 ml) was added to reaction mixture and the mixture was extracted with ethyl acetate (3 × 10 ml). The combined organic layers were washed with water and brine, dried over anhydrous  $\text{Na}_2\text{SO}_4$  and concentrated under reduced pressure. The crude material was purified through flash column chromatography eluting with petroleum ether/ethyl acetate 95/5, yielding the title compound as a white solid. Yield: 40%.

$^1\text{H-NMR}$ (300 MHz-  $\text{CDCl}_3$ ):  $\delta$  3.87 (t, J = 9 Hz, 2H); 4.62 (t, J = 9 Hz, 2H); 7.36-8.2 (m, 8H).

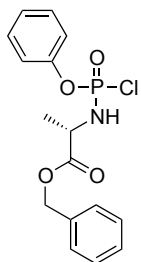
### 5.1.4 Microwave-assisted synthesis of nucleotide phosphoroamidates

#### (2S)-benzyl 2-(((4-nitrophenoxy)(phenoxy)phosphoryl)amino)propanoate



the procedure and the analytical data are already reported elsewhere.<sup>136</sup>

#### (2S)-benzyl 2-((chloro(phenoxy)phosphoryl)amino)propanoate



The procedure and the analytical data are already reported elsewhere.<sup>136</sup>

#### General procedure for Grignard methodology

A solution of nucleoside (1 eq) in THF (5.71 mL/mmol) and NMP (1.96 mL/mmol) was stirred for 10 minutes at room temperature then t-BuMgCl 1M in THF (2 eq) was added and the mixture was stirred at the same temperature for 10 minutes.

In a different round bottomed flask was prepared a solution of the chlorophosphoroamidate or aryloxyphosphoroamidate (2 eq) in THF (1.78 mL/mmol) and it was slowly added to the reaction mixture.

The mixture was heated at conventional heating or under microwave irradiation for different time and temperature as described in the chapter 4. After quenching with H<sub>2</sub>O (2 mL) a saturated solution of NH<sub>4</sub>Cl (10 mL) was added and the aqueous layer was extracted with CH<sub>2</sub>Cl<sub>2</sub> (3\*10 mL).

The HPLC sample was prepared with 15µL of the mixture (after quenching with H<sub>2</sub>O before the addition of NH<sub>4</sub>Cl) diluted in 2.5 mL of H<sub>2</sub>O and 2.5 mL of MeOH.

The crude material was then purified by flash column chromatography with the opportune eluent.

### **General procedure for the NMI methodology**

A solution of nucleoside (1 eq) in THF (7.14 mL/mmol) was stirred for 10 minutes at room temperature then N-methylimidazole (6.3 eq) was added and the mixture was stirred at the same temperature for 30 minutes.

In a different round bottomed flask was prepared a solution of the chlorophosphoramidate (3 eq) in THF (1.19 mL/mmol) and it was slowly added to the reaction mixture.

The mixture was heated at conventional heating or under microwave irradiation for different time and temperature as described in the chapter 4. After quenching with H<sub>2</sub>O (2 mL) a saturated solution of NH<sub>4</sub>Cl (10 mL) was added and the aqueous layer was extracted with CH<sub>2</sub>Cl<sub>2</sub> (3\*10 mL).

The HPLC sample was prepared with 15µL of the mixture (after quenching with H<sub>2</sub>O before the addition of NH<sub>4</sub>Cl) diluted in 2.5 mL of H<sub>2</sub>O and 2.5 mL of MeOH.

The crude material was then purified by flash column chromatography with the opportune eluent.

## 5.2 Biology

Thioridazine (TDZ), verapamil (VER), isoniazid (INH), rifampicin (RIF), amikacin (AMK), ofloxacin (OFX), EtBr, phosphate buffered saline (PBS), and glucose were purchased from Sigma-Aldrich (St. Louis, MO, USA). All solutions were prepared in deionized water except rifampicin and the TDZ analogues which were prepared in DMSO. All solutions were prepared on the day of the experiment. Middlebrook 7H9 (MB7H9) and the OADC supplement (oleic acid/albumin/dextrose/catalase) were purchased from Difco (Madrid, Spain) and Becton and Dickinson (Sparks, MD, USA) respectively. The mycobacterial reference strains *M. smegmatis* mc2155 ATCC700084 and *M. tuberculosis* H37Rv ATCC27294T were used to evaluate the biologic activity of TDZ analogues.

### 5.2.1 Evolution of a series of 2-aminothiazoles

The experimental work was carried out by **Prof Gyanu Lamichhane**, **Dr Amit Kaushik** (John Hopkins University, Baltimore, Maryland), **Prof Miguel Viveiros**, **Dr Diana Machado**, **Dr Sofia Santos Costa**, **Dr Isabel Couto**, (Instituto de Higiene e Medicina Tropical, Universidade Nova de Lisboa, Lisbon) and **Prof Federica Vacondio** (University of Parma, Parma)

### Determination of the Minimum Inhibitory Concentration (MIC)

Minimum inhibitory concentration (MIC<sub>90</sub>) for Mtb was determined using standard broth macrodilution in 15-ml sterile conical tubes containing 2.5 ml of 7H9 broth. Standard broth microdilution method (using 96-well plates) was used for other organisms as per Clinical and Laboratory

Standard Institute (CLSI) recommendations<sup>149</sup>. Middlebrook 7H9 broth was used for Mtb growth as per CLSI guidelines<sup>150</sup>. In summary,  $10^5$  bacilli grown to exponential phase in liquid medium were inoculated into each well containing drug at two fold dilutions ranging from 64  $\mu\text{g}/\text{ml}$  to 0.03  $\mu\text{g}/\text{ml}$ . Growth medium alone and without drug but inoculated with  $10^5$  bacilli were included as negative and positive controls, respectively. Appropriate drugs (INF and RIF) were included as positive control for growth inhibition. Growth was evaluated by visual inspection for presence of bacterial pellet following incubation for fourteen days at 37 °C. The first well in which bacterial pellet is absent and therefore growth is not observable is considered the MIC<sub>90</sub> as per the standard CLSI guidelines. MIC<sub>90</sub> is expressed as a range spanning two concentrations: the higher concentration represents the lowest concentration at which bacterial growth could not be observed.

### **Cytotoxicity evaluation of selected compounds**

*In vitro* cytotoxicity assays were evaluated against human monocyte-derived macrophages. Blood was collected from healthy volunteers and peripheral blood mononuclear cells isolated by Ficoll-Paque Plus (GE Healthcare, Freiburg, Germany) density gradient centrifugation. Monocytes were differentiated into macrophages during seven days in macrophage medium containing RPMI-1640 medium with 10% fetal calf serum (FCS), 1% GlutaMAX<sup>TM</sup>, 1 mM sodium pyruvate, 10 mM HEPES at pH 7.4, 100 IU/ml penicillin and 100  $\mu\text{g}/\text{ml}$  streptomycin (Gibco, Life Technologies), and 20 ng/ml M-CSF (Immunotools, Friesoythe, Germany) and incubated at 37°C in 5% CO<sub>2</sub> atmosphere. Fresh medium was added at day 4 post isolation. The effect of the TDZ analogues was evaluated by using the vital dye

AlamarBlue (Molecular Probes, Life Technologies) following the manufacturer's indications. Briefly, 5x10<sup>4</sup> cells were seeded in 96-well microplates, treated with the compounds and then incubated at 37°C in a 5% CO<sub>2</sub> atmosphere. After 3 days of treatment, cell viability was assessed. Briefly, 10% AlamarBlue was added to each well and incubated during 4 hours at 37°C and 5% CO<sub>2</sub>. Fluorescence was measured with a 540/35 excitation filter and a 590/20 emission filter in a Synergy HT multi-mode microplate reader (BioTek® Instruments, Inc, Vermont, USA). The IC<sub>50</sub> values correspond to the highest concentration of compound at which 50% of the cells are viable to the control<sup>67</sup>.

### **Stability studies in HLM for selected compounds**

Stability of selected compounds in the presence of HLM was assessed by incubation of a 1 µM concentration for 60 min in the presence of HLM (1 mg protein mL<sup>-1</sup>), at 37 °C, in the presence of a NADPH-regenerating system (2 mM NADP<sup>+</sup>, 10 mM glucose-6-phosphate, 0.4 U mL<sup>-1</sup> glucose-6-phosphate dehydrogenase, 5 mM MgCl<sub>2</sub>) in 100 mM PBS buffer solution pH 7.4. The reaction mixtures were preheated (37 °C) for 5 min before adding the parent compound. At fixed time points (t = 0; 15; 30; 60; min), aliquots of samples were withdrawn, deproteinized with two volumes of acetonitrile, centrifuged (9,000 g, 4 °C, 10 min) and the supernatant analysed by injection in HPLC-MS/MS system. The chromatographic separation was performed employing a gradient elution starting from 70% water+0.1% formic acid (solvent A):30% methanol (solvent B) to 90%B:10%A in 10 min; 90%B:10%A was kept for further 5 min; then back to 70%A:30%B and further 5-min of reconditioning time. HPLC-MS analysis employed a Thermo Quantum Access Max TSQ triple quadrupole mass

spectrometer (Thermo, USA) equipped with a H-ESI (Heated-ElectroSpray Ionization) interface and coupled to an Accela UHPLC system (Thermo, USA) constituted of a quaternary pump, a degasser and a thermostated autosampler. Compounds were analysed in positive ion mode using both total ion monitoring mode, over a mass range from 50 to 500 amu, and single ion monitoring mode. Data were acquired and analysed employing Thermo Excalibur 1.4 software (Thermo, USA).

### **5.2.2 Novel and efficient synthesis of 2-aminooxazoles**

The experimental work was carried out by **Prof. Scott G. Franzblau** and **Dr Rui Ma** (Institute for Tuberculosis Research, Chicago, Illinois)

#### **Microplate Alamar Blue assay (MABA assay)**

Briefly, the test compound MICs against *Mtb* H<sub>37</sub>RV (ATCC# 27294) were assessed by the MABA using rifampin, isoniazid and moxifloxacin as positive controls. Compound stock solutions were prepared in DMSO at a concentration of 12.8 mM, and the final test concentrations ranged from 128  $\mu$ M to 0.5  $\mu$ M. Two fold dilutions of compounds were prepared in Middlebrook 7H12 medium (7H9 broth containing 0.1% w/v casitone, 5.6  $\mu$ g/mL palmitic acid, 5 mg/mL bovine serum albumin, 4 mg/mL catalase, filter-sterilized) in a volume of 100  $\mu$ L in 96-well microplates (BD Optilux™, 96-well Microplates , black/clear flat bottom). TB cultures (100  $\mu$ L inoculum of 2  $\times$ 10<sup>5</sup> cfu/mL) was added, yielding a final testing volume of 200  $\mu$ L. The plates were incubated at 37 °C. On the seventh day of incubation 12.5  $\mu$ L of 20% Tween 80, and 20  $\mu$ L of Alamar Blue (Invitrogen BioSource™) were added to the wells of test plate. After incubation at 37 °C for 16-24 h,



fluorescence of the wells was measured (ex 530, em 590 nm). The MICs were defined as the lowest concentration effecting a reduction in fluorescence of  $\geq 90\%$  relative to the mean of replicate bacteria-only controls.

### **Low-oxygen recovery assay (LORA assay)**

Briefly, a low-oxygen adapted culture of recombinant H<sub>37</sub>Rv (pFCA-luxAB), expressing a *Vibrio harveyi* luciferase gene with an acetamidase promoter, was grown in a BiostatQ fermentor. Cells were collected on ice, washed in PBS, and stored at  $-80\text{ }^{\circ}\text{C}$ . Circa  $10^5$  cfu/mL of thawed NRP cells were exposed to 2-fold serial dilutions of test compound in 7H9 broth in black 96-well plates, which were incubated 10 days anaerobically at  $37\text{ }^{\circ}\text{C}$ . Luminescence readings were obtained following a 28 h recovery in an aerobic environment (5% CO<sub>2</sub>). The data were analysed graphically, and the lowest concentration of test compound preventing metabolic recovery (90% reduction relative to untreated cultures) was determined as described previously.

### **Cytotoxicity assay**

Cytotoxicity was determined by exposing different concentrations of samples to Vero cells. Samples were dissolved at  $12.8\text{ }\mu\text{M}$  in DMSO. Geometric three-fold dilutions were performed in growth medium MEM (Gibco, Grand Island, NY), containing 10% fetal bovine serum (HyClone, Logan, UT), 25 mM *N*-(2-hydroxyethyl)-piperazine-*N'*-2-ethanesulfonic acid (HEPES, Gibco), 0.2% NaHCO<sub>3</sub> (Gibco), and 2 mM glutamine (Irvine Scientific, Santa Ana, CA). Final DMSO concentrations did not exceed 1%

v/v. Drug dilutions were distributed in duplicate in 96-well tissue culture plates (Becton Dickinson Labware, Lincoln Park, NJ) at a volume of 50  $\mu$ L per well. An equal volume containing either  $5 \times 10^5$  log phase Vero cells (CCL-81; American Type Culture Collection, Rockville, MD) was added to each well and the cultures were incubated at 37 °C in an atmosphere containing 5% of CO<sub>2</sub>. After 72 h, cell viability was measured using the CellTiter 96 aqueous non-radioactive cell proliferation assay (Promega Corp., Madison, WI) according to the manufacturer's instructions. Absorbance at 490 nm was read in a Victor<sup>2</sup> multilabel reader (PerkinElmer). The IC<sub>50</sub>s were determined using a curve-fitting program.

### **5.2.3 Rational design and synthesis of Thioridazine analogues as enhancers of the antituberculosis therapy**

The experimental work was carried out by **Prof Miguel Viveiros, Dr Diana Machado, Dr Sofia Santos Costa** and **Dr Isabel Couto** (Instituto de Higiene e Medicina Tropical, Universidade Nova de Lisboa, Lisbon)

#### **Determination of the Minimum Inhibitory Concentration (MIC)**

For *M. smegmatis* the determination of the MICs of TDZ analogues 104-114, the efflux inhibitors TDZ and VER, and the efflux substrate EtBr were conducted by the 96-well broth microdilution method. Briefly, *M. smegmatis* was grown in MB7H9 supplemented with 10% OADC at 37°C with shaking until an OD<sub>600</sub> of 0.8. The inoculum was prepared by adjusting the culture to a density corresponding to 0.5 McFarland standard diluted to 1:100. Aliquots of 0.1 mL were transferred to each well of the 96-well plate

containing 0.1 mL of each compound at concentrations prepared from two-fold serial dilutions in MB7H9. The inoculated plates were sealed in plastic bags, incubated at 37°C and the results registered after three days of incubation. Growth controls with no drug and a sterility control were included in each assay. Two hundred microliters of sterile deionized water was added to all outer-perimeter wells of the 96-well plates to reduce evaporation of the medium during the incubation. The MIC was defined as the lowest concentration of compound that inhibited visible mycobacterial growth. Mtb was grown in MB7H9 plus 10% OADC supplement at 37°C until an OD600 of 0.8, without stirring. The inoculum was prepared by diluting the bacterial cultures in MB7H9/OADC to a final density of approximately 10<sup>5</sup> cells/ml (Eliopoulos and Moellering, 1996). The MICs of TDZ analogues 104, 106, 107 and 108, TDZ, VER, and EtBr, were determined by a tetrazolium microplate-based assay (Caviedes et al., 2002) with slight modifications. Briefly, aliquots of 0.1 ml of inoculum were transferred to each well of the plate that contained 0.1 ml of each compound at concentrations prepared from two-fold serial dilutions in MB7H9/OADC medium. Growth controls and a sterility control were included in each assay. The outer perimeter wells of the plates were filled with two hundred microliters of sterile deionized water to reduce evaporation of the medium during the incubation. The inoculated plates were sealed in plastic bags and incubated at 37°C during seven days. After the seven days of incubation, MTT was added to each well to a final concentration of 2.5% and the plates incubated overnight. The bacterial viability was registered for each well based on the MTT colour change and the MIC was defined as the lowest

concentration of compound that totally inhibited bacterial growth (no colour change)<sup>117</sup>. The assays were performed in triplicate.

### **Evaluation of the synergistic effect of TDZ analogues 104, 106, 107 and 108 with selected antibiotics and ethidium bromide by broth microdilution checkerboard assay**

The synergistic effect of TDZ analogues 104, 106, 107 and 108 and that of the efflux inhibitors TDZ and VER in combination with INH, OFX, AMK, RIF and EtBr was evaluated by two dimensional checkerboard assays<sup>124</sup>. *M. Tuberculosis* was grown in MB7H9 medium supplemented with 10% OADC at 37°C, until an OD600 of 0.8. Briefly, the 96-well microdilution plates were inoculated with a suspension of the strain diluted to yield a density of 10<sup>5</sup> CFU/ml. Ethidium bromide or the antibiotics were two-fold serial diluted in MB7H9 supplemented with OADC from column 3 to column 11 of each plate assay. Twofold dilutions of compounds 104, 106, 107, 108, TDZ or VER were then added to rows 2 to 6 of each plate. Column 1 and 2 contains the negative and positive control, respectively. Two hundred microliters of sterile deionized water was added to the outer-perimeter wells of the plates to decrease evaporation of the medium during incubation. The plates were sealed and incubated at 37°C for seven days. After this period, MTT was added, the plates were re-incubated overnight, and the results interpreted as described above. The synergistic effect of TDZ analogues and efflux inhibitors on each antibiotic and ethidium bromide was evaluated through the determination of fractional inhibitory concentrations (FIC), according to the formula:  $FIC_{\text{compound}} = \frac{MIC_{\text{compound in the presence the antibiotic/EtBr}}}{MIC_{\text{compound alone}}}$ . The FIC were interpreted adapting the criteria established

by Pillai et al. (2005) to one variable as follows:  $FIC \leq 0.25$ , synergism;  $FIC > 0.25 < 2$ , indifference and  $FIC \geq 2$ , antagonism.<sup>101</sup> The FIC values were classified as ND (non-determinable) when the MICs of the compounds alone were greater than the highest, less than, or equal to the lowest concentration tested (Moody, 1992). Isobolograms were constructed, by plotting changes in the MIC of antibiotics as a function of the concentration of the compounds, using GraphPad Prism V5.01 software (La Jolla, USA). Synergy is illustrated by a concave isobol and antagonism, by a convex isobol. All assays were carried out in triplicate.

### **Evaluation of efflux inhibitory activity of compounds by real-time fluorometry**

The EtBr accumulation and efflux by the mycobacterial strains was assessed on a real-time basis using a fluorometric method, as previously described.<sup>123,151</sup> *M. smegmatis* and *M. tuberculosis* were grown as described above, with the addition of 0.05% Tween 80 to the growth medium.

(i) Accumulation assays. After reaching an OD<sub>600</sub> of 0.8, the cells were collected by centrifugation at 2940 x g for three minutes, the pellet washed in PBS, and the OD<sub>600</sub> of the suspension adjusted to 0.8 with PBS. To determine the concentration of EtBr at which there is an equilibrium between the influx and efflux of EtBr the assays were performed in the presence of increasing concentrations of EtBr. The assays were prepared to a final volume of 0.1 mL containing 0.05 mL of the cellular suspension (final OD<sub>600</sub> of 0.4) plus 0.05 mL of EtBr solutions to final concentrations of 0.125, 0.25, 0.5, 1, 2, and 3 mg/L. To assess the effect of TDZ analogues

104-114 and that of the efflux inhibitors TDZ and VER on EtBr accumulation, the assays were performed in a final volume of 0.1 mL containing 0.05 mL of the cellular suspension (final OD600 of 0.4) and 0.05 mL of a solution containing the EtBr concentration previously selected (0.25 mg/L for *M. smegmatis* and 0.5 mg/L for *M. tuberculosis*) and the compound to be tested to a final concentration of 1/2 their MIC, in order to not compromise the cellular viability. In all assays, was included a control containing solely EtBr at the equilibrium concentration selected previously. The assays were conducted in a Rotor-Gene 3000TM (Corbett Research, Sydney, Australia) at 37°C, and the fluorescence acquired at 530/585 nm at the end of every 60 seconds, during 60 minutes<sup>52</sup>. The activity of the TDZ analogues, TDZ, and VER on the accumulation of EtBr was evaluated by the relative final fluorescence (RFF) index according to the formula:  $RFF = (RF_{treated} - RF_{untreated}) / RF_{untreated}$ , where  $RF_{treated}$  corresponds to the fluorescence at the last time point of the EtBr accumulation curve (minute 60) in the presence of a compound; and the  $RF_{untreated}$  corresponds to the fluorescence at the last time point of the EtBr accumulation curve of the control tube containing only EtBr.

(ii) Efflux assays. After reaching an OD600 of 0.8, the cells were collected by centrifugation at 2940 x g for three minutes, the pellet washed in PBS, and the OD600 of the suspension adjusted to 0.4 with PBS. Cell suspensions were then exposed to conditions that promote maximum EtBr accumulation, i.e. EtBr at the equilibrium concentration; presence of the efflux inhibitor that caused maximum accumulation (VER for both strains) at 1/2 of the MIC; and incubation at 25°C during one hour. Following, EtBr loaded cells were centrifuged at 4860 x g during five minutes and

resuspended in PBS to a final OD600 of 0.8. Efflux assays were prepared to a final volume of 0.1 mL containing 0.05 mL of the cellular suspension (final OD600 of 0.4) plus 0.05 mL of selected TDZ analogues, TDZ, and VER at 1/2 of their MIC with and without glucose at a final concentration of 0.4%, to energize the cells. In all assays, control conditions containing only cellular suspension and cellular suspension plus glucose (condition of maximum efflux) were included. Fluorescence was measured in the Rotor- Gene™ 3000 at 37°C, at the end of every 30 seconds during 30 minutes. Efflux activity was quantified by comparing the fluorescence data obtained under conditions that promote efflux (presence of glucose and absence of efflux inhibitor) with the data from the control in which the mycobacteria are under conditions of no efflux (presence of an inhibitor and no energy source). Thus, the relative fluorescence corresponds to the ratio of fluorescence that remains per unit of time, relatively to the EtBr-loaded cells (cells plus VER).<sup>123</sup> Statistical analysis of the data was carried out using Student's t- test. A P value <0.05 was considered statistically significant (two-tailed tested).

### **Cytotoxicity evaluation of compounds 104, 106, 107, 108 and 109**

*In vitro* cytotoxicity assays were evaluated against human monocyte-derived macrophages. Blood was collected from healthy volunteers and peripheral blood mononuclear cells isolated by Ficoll-Paque Plus (GE Healthcare, Freiburg, Germany) density gradient centrifugation. Monocytes were differentiated into macrophages during seven days in macrophage medium containing RPMI-1640 medium with 10% fetal calf serum (FCS), 1% GlutaMAX™, 1 mM sodium pyruvate, 10 mM HEPES at pH 7.4, 100 IU/ml

penicillin and 100 µg/ml streptomycin (Gibco, Life Technologies), and 20 ng/ml M-CSF (Immunotools, Friesoythe, Germany) and incubated at 37°C in 5% CO<sub>2</sub> atmosphere. Fresh medium was added at day 4 post isolation. The effect of the TDZ analogues was evaluated by using the vital dye AlamarBlue (Molecular Probes, Life Technologies) following the manufacturer's indications. Briefly, 5x10<sup>4</sup> cells were seeded in 96-well microplates, treated with the compounds and then incubated at 37°C in a 5% CO<sub>2</sub> atmosphere. After 3 days of treatment, cell viability was assessed. Briefly, 10% AlamarBlue was added to each well and incubated during 4 hours at 37°C and 5% CO<sub>2</sub>. Fluorescence was measured with a 540/35 excitation filter and a 590/20 emission filter in a Synergy HT multi-mode microplate reader (BioTek® Instruments, Inc, Vermont, USA). The IC<sub>50</sub> values correspond to the highest concentration of compound at which 50% of the cells are viable to the control.

### **Intracellular synergy assays**

Human monocyte-derived macrophages were infected with *M. tuberculosis* H37Rv at a multiplicity of infection (MOI) 1:1 and were allowed to uptake the bacteria for three hours. After, the cells were washed three times with PBS to remove all non-internalized bacteria. Afterwards, the compounds were added to the infected macrophages at the desired concentrations in combination with INH or RIF. At day three post-infection, cells were lysed with 0.05% Igepal (Sigma-Aldrich). Serial dilutions of the lysate were placed on MB7H11/10% OADC medium. Colony forming units were counted upon three weeks of incubation at 37°C. Compounds were used at concentrations that were shown to be non-toxic for the macrophages: compound 104, 16



µg/ml, 106, 0.078 µg/ml; 107, 1.25 µg/ml, and 108, 40 µg/ml. INH and RIF were used at 1/2 of its MIC (0.05 and 0.5 µg/ml, respectively).

## **6. Acknowledgements**

**Prof Miguel Viveiros, Dr Diana Machado, Dr Sofia Santos Costa and Dr Isabel Couto**, Instituto de Higiene e Medicina Tropical, Universidade Nova de Lisboa (IHMT, UNL), Lisbon

**Prof Gyanu Lamichhane and Dr Amit Kaushik**, John Hopkins University, Baltimore, Maryland

**Prof. Scott G. Franzblau and Dr Rui Ma**, Institute for Tuberculosis Research, Chicago, Illinois

**Prof Federica Vacondio**, University of Parma, Parma

**Dr Andrea Brancale, Dr Cinzia Bordoni and Dr Cecilia Maria Cima**, Cardiff University, Cardiff

P4T group:

**Prof Gabriele Costantino and Dr Marco Pieroni**

**Prof Marco Radi, Dr Agostino Bruno, Dr Claudia Beato, Dr Paolo Vincetti, Dr Giannamaria Annunziato, Dr Sabrina Tassini, Dr Joana Magalhães, Dr Maria Laura Pavone and Dr Miriam Girardini.**

## 7. References

- (1) Martínez, A.; Torello, S.; Kolter, R. Sliding Motility in Mycobacteria. *J. Bacteriol.* **1999**, *181* (23), 7331–7338.
- (2) *Sherris Medical Microbiology: An Introduction to Infectious Diseases*, 4th ed.; Ryan, K. J., Ray, C. G., Sherris, J. C., Eds.; McGraw-Hill: New York, 2004.
- (3) James H. Kerr and Terry L. Barrett, "Atypical Mycobacterial Diseases", *Military Dermatology Textbook*; 401.
- (4) Fu, L. M.; Fu-Liu, C. S. Is Mycobacterium Tuberculosis a Closer Relative to Gram-Positive or Gram-Negative Bacterial Pathogens? *Tuberc. Edinb. Scotl.* **2002**, *82* (2–3), 85–90.
- (5) "Tuberculosis fact sheet N° 104"; WHO; October 2015
- (6) Global Tuberculosis Report 2016
- (7) Pawlowski, A.; Jansson, M.; Sköld, M.; Rottenberg, M. E.; Källenius, G. Tuberculosis and HIV Co-Infection. *PLoS Pathog.* **2012**, *8* (2), e1002464.
- (8) Caminero, J. A.; Sotgiu, G.; Zumla, A.; Migliori, G. B. Best Drug Treatment for Multidrug-Resistant and Extensively Drug-Resistant Tuberculosis. *Lancet Infect. Dis.* **2010**, *10* (9), 621–629.
- (9) Rieder, H. L.; Lauritsen, J. M.; Naranbat, N.; Katamba, A.; Laticevschi, D.; Mabaera, B. Quantitative Differences in Sputum Smear Microscopy Results for Acid-Fast Bacilli by Age and Sex in Four Countries. *Int. J. Tuberc. Lung Dis. Off. J. Int. Union Tuberc. Lung Dis.* **2009**, *13* (11), 1393–1398.

- (10) Corbett, E. L.; Watt, C. J.; Walker, N.; Maher, D.; Williams, B. G.; Raviglione, M. C.; Dye, C. The Growing Burden of Tuberculosis: Global Trends and Interactions with the HIV Epidemic. *Arch. Intern. Med.* **2003**, *163* (9), 1009–1021.
- (11) Boshoff, H. I. M.; Barry, C. E. Tuberculosis - Metabolism and Respiration in the Absence of Growth. *Nat. Rev. Microbiol.* **2005**, *3* (1), 70–80.
- (12) Russell, D. G. Mycobacterium Tuberculosis: Here Today, and Here Tomorrow. *Nat. Rev. Mol. Cell Biol.* **2001**, *2* (8), 569–577.
- (13) Wayne, L. G.; Hayes, L. G. An in Vitro Model for Sequential Study of Shiftdown of Mycobacterium Tuberculosis through Two Stages of Nonreplicating Persistence. *Infect. Immun.* **1996**, *64* (6), 2062–2069.
- (14) Wayne, L. G.; Sohaskey, C. D. Nonreplicating Persistence of Mycobacterium Tuberculosis. *Annu. Rev. Microbiol.* **2001**, *55*, 139–163.
- (15) <http://www.who.int/tb/dots/whatisdots/en/>
- (16) Zhang, Y.; Yew, W. W.; Barer, M. R. Targeting Persisters for Tuberculosis Control. *Antimicrob. Agents Chemother.* **2012**, *56* (5), 2223–2230.
- (17) Chang, K. C.; Leung, C. C.; Yew, W. W.; Chan, S. L.; Tam, C. M. Dosing Schedules of 6-Month Regimens and Relapse for Pulmonary Tuberculosis. *Am. J. Respir. Crit. Care Med.* **2006**, *174* (10), 1153–1158.
- (18) Spigelman, M.K.; *The Journal of Infectious Diseases*; **2007**; 196; 28-34.

- (19) Dorman, S. E.; Chaisson, R. E. From Magic Bullets back to the Magic Mountain: The Rise of Extensively Drug-Resistant Tuberculosis. *Nat. Med.* **2007**, *13* (3), 295–298.
- (20) “Tuberculosis-TB Guidelines-Treatment” Centers for Disease Control. Retrieved 22 February 2016
- (21) Lei, B.; Wei, C. J.; Tu, S. C. Action Mechanism of Antitubercular Isoniazid. Activation by Mycobacterium Tuberculosis KatG, Isolation, and Characterization of Inha Inhibitor. *J. Biol. Chem.* **2000**, *275* (4), 2520–2526.
- (22) “Rifampin” The American Society of Health-System Pharmacists Retrieved 1 August 2015.
- (23) McHugh, T.D.; Wallingford, Oxfordshire; 2010; 219.
- (24) Calvori, C.; Frontali, L.; Leoni, L.; Tecce, G. Effect of Rifamycin on Protein Synthesis. *Nature* **1965**, *207* (995), 417–418.
- (25) Zhang, Y.; Mitchison, D. The Curious Characteristics of Pyrazinamide: A Review. *Int. J. Tuberc. Lung Dis. Off. J. Int. Union Tuberc. Lung Dis.* **2003**, *7* (1), 6–21.
- (26) Zimhony, O.; Cox, J. S.; Welch, J. T.; Vilchèze, C.; Jacobs, W. R. Pyrazinamide Inhibits the Eukaryotic-like Fatty Acid Synthetase I (FASI) of Mycobacterium Tuberculosis. *Nat. Med.* **2000**, *6* (9), 1043–1047.
- (27) Zimhony, O.; Vilchèze, C.; Arai, M.; Welch, J. T.; Jacobs, W. R. Pyrazinoic Acid and Its N-Propyl Ester Inhibit Fatty Acid Synthase Type I in Replicating Tubercle Bacilli. *Antimicrob. Agents Chemother.* **2007**, *51* (2), 752–754.
- (28) Lim, S.-A. Ethambutol-Associated Optic Neuropathy. *Ann. Acad. Med. Singapore* **2006**, *35* (4), 274–278.

- (29) Singh, B.; Mitchison, D. A. Bactericidal Activity of Streptomycin and Isoniazid against Tubercle Bacilli. *Br. Med. J.* **1954**, *1* (4854), 130–132.
- (30) Syal, K.; Srinivasan, A.; Banerjee, D. Streptomycin Interference in Jaffe Reaction - Possible False Positive Creatinine Estimation in Excessive Dose Exposure. *Clin. Biochem.* **2013**, *46* (1–2), 177–179.
- (31) Sharma, D.; Cukras, A. R.; Rogers, E. J.; Southworth, D. R.; Green, R. Mutational Analysis of S12 Protein and Implications for the Accuracy of Decoding by the Ribosome. *J. Mol. Biol.* **2007**, *374* (4), 1065–1076.
- (32) <http://www.medical-reference.net/2012/11/what-is-treatment-of-tuberculosis.html>
- (33) <http://www.who.int/tb/MDRTBguidelines2016.pdf>
- (34) Mingeot-Leclercq, M. P.; Glupczynski, Y.; Tulkens, P. M. Aminoglycosides: Activity and Resistance. *Antimicrob. Agents Chemother.* **1999**, *43* (4), 727–737.
- (35) Barkei, J. J.; Kevany, B. M.; Felnagle, E. A.; Thomas, M. G. Investigations into Viomycin Biosynthesis by Using Heterologous Production in *Streptomyces lividans*. *Chembiochem Eur. J. Chem. Biol.* **2009**, *10* (2), 366–376.
- (36) *Organic Chemistry: Breakthroughs and Perspectives*; Ding, K., Dai, L.-X., Eds.; Wiley-VCH: Weinheim, Germany, 2012.
- (37) Ginsburg, A. S.; Grosset, J. H.; Bishai, W. R. Fluoroquinolones, Tuberculosis, and Resistance. *Lancet Infect. Dis.* **2003**, *3* (7), 432–442.
- (38) Zheng, J.; Rubin, E. J.; Bifani, P.; Mathys, V.; Lim, V.; Au, M.; Jang, J.; Nam, J.; Dick, T.; Walker, J. R.; Pethe, K.; Camacho, L. R. Para-Aminosalicylic Acid Is a Prodrug Targeting Dihydrofolate Reductase in

- Mycobacterium Tuberculosis. *J. Biol. Chem.* **2013**, *288* (32), 23447–23456.
- (39) Pethe, K.; Bifani, P.; Jang, J.; Kang, S.; Park, S.; Ahn, S.; Jiricek, J.; Jung, J.; Jeon, H. K.; Cechetto, J.; Christophe, T.; Lee, H.; Kempf, M.; Jackson, M.; Lenaerts, A. J.; Pham, H.; Jones, V.; Seo, M. J.; Kim, Y. M.; Seo, M.; Seo, J. J.; Park, D.; Ko, Y.; Choi, I.; Kim, R.; Kim, S. Y.; Lim, S.; Yim, S.-A.; Nam, J.; Kang, H.; Kwon, H.; Oh, C.-T.; Cho, Y.; Jang, Y.; Kim, J.; Chua, A.; Tan, B. H.; Nanjundappa, M. B.; Rao, S. P. S.; Barnes, W. S.; Wintjens, R.; Walker, J. R.; Alonso, S.; Lee, S.; Kim, J.; Oh, S.; Oh, T.; Nehrbass, U.; Han, S.-J.; No, Z.; Lee, J.; Brodin, P.; Cho, S.-N.; Nam, K.; Kim, J. Discovery of Q203, a Potent Clinical Candidate for the Treatment of Tuberculosis. *Nat. Med.* **2013**, *19* (9), 1157–1160.
- (40) Barbachyn, M. R.; Hutchinson, D. K.; Brickner, S. J.; Cynamon, M. H.; Kilburn, J. O.; Klemens, S. P.; Glickman, S. E.; Grega, K. C.; Hedges, S. K.; Toops, D. S.; Ford, C. W.; Zurenko, G. E. Identification of a Novel Oxazolidinone (U-100480) with Potent Antimycobacterial Activity. *J. Med. Chem.* **1996**, *39* (3), 680–685.
- (41) Cynamon, M. H.; Klemens, S. P.; Sharpe, C. A.; Chase, S. Activities of Several Novel Oxazolidinones against Mycobacterium Tuberculosis in a Murine Model. *Antimicrob. Agents Chemother.* **1999**, *43* (5), 1189–1191.
- (42) Alffenaar, J. W. C.; van der Laan, T.; Simons, S.; van der Werf, T. S.; van de Kastele, P. J.; de Neeling, H.; van Soolingen, D. Susceptibility of Clinical Mycobacterium Tuberculosis Isolates to a Potentially Less Toxic Derivate of Linezolid, PNU-100480. *Antimicrob. Agents Chemother.* **2011**, *55* (3), 1287–1289.

- (43) Alffenaar, J. W. C.; van der Laan, T.; Simons, S.; van der Werf, T. S.; van de Kastele, P. J.; de Neeling, H.; van Soolingen, D. Susceptibility of Clinical Mycobacterium Tuberculosis Isolates to a Potentially Less Toxic Derivate of Linezolid, PNU-100480. *Antimicrob. Agents Chemother.* **2011**, *55* (3), 1287–1289.
- (44) <http://www.tballiance.org/portfolio/compound/pretomanid>
- (45) Blair, H. A.; Scott, L. J. Delamanid: A Review of Its Use in Patients with Multidrug-Resistant Tuberculosis. *Drugs* **2015**, *75* (1), 91–100.
- (46) Ma, Z.; Lienhardt, C.; McIlleron, H.; Nunn, A. J.; Wang, X. Global Tuberculosis Drug Development Pipeline: The Need and the Reality. *Lancet Lond. Engl.* **2010**, *375* (9731), 2100–2109.
- (47) <http://www.newtbdrugs.org/pipeline.php>
- (48) Li, D.; Sheng, L.; Liu, X.; Yang, S.; Liu, Z.; Li, Y.; Chromatographia; **2014**; *77*; 1697-1703.
- (49) Ishizaki, Y.; Hayashi, C.; Inoue, K.; Igarashi, M.; Takahashi, Y.; Pujari, V.; Crick, D. C.; Brennan, P. J.; Nomoto, A. Inhibition of the First Step in Synthesis of the Mycobacterial Cell Wall Core, Catalyzed by the GlcNAc-1-Phosphate Transferase WecA, by the Novel Caprazamycin Derivative CPZEN-45. *J. Biol. Chem.* **2013**, *288* (42), 30309–30319.
- (50) Hanif, S. N. M.; Hickey, A. J.; Garcia-Contreras, L. Liquid Chromatographic Determination of CPZEN-45, a Novel Anti-Tubercular Drug, in Biological Samples. *J. Pharm. Biomed. Anal.* **2014**, *88*, 370–376.



- (51) Bogatcheva, E.; Hanrahan, C.; Chen, P.; Gearhart, J.; Sacksteder, K.; Einck, L.; Nacy, C.; Protopopova, M. Discovery of Dipiperidines as New Antitubercular Agents. *Bioorg. Med. Chem. Lett.* **2010**, *20* (1), 201–205.
- (52) Bogatcheva, E.; Hanrahan, C.; Nikonenko, B.; de los Santos, G.; Reddy, V.; Chen, P.; Barbosa, F.; Einck, L.; Nacy, C.; Protopopova, M. Identification of SQ609 as a Lead Compound from a Library of Dipiperidines. *Bioorg. Med. Chem. Lett.* **2011**, *21* (18), 5353–5357.
- (53)  
<http://www.sequella.com/docs/SQ609%20TB%20product%20summary.pdf>
- (54) Lee, R. E.; Hurdle, J. G.; Liu, J.; Bruhn, D. F.; Matt, T.; Scherman, M. S.; Vaddady, P. K.; Zheng, Z.; Qi, J.; Akbergenov, R.; Das, S.; Madhura, D. B.; Rathi, C.; Trivedi, A.; Villellas, C.; Lee, R. B.; Rakesh, null; Waidyarachchi, S. L.; Sun, D.; McNeil, M. R.; Ainsa, J. A.; Boshoff, H. I.; Gonzalez-Juarrero, M.; Meibohm, B.; Böttger, E. C.; Lenaerts, A. J. Spectinamides: A New Class of Semisynthetic Antituberculosis Agents That Overcome Native Drug Efflux. *Nat. Med.* **2014**, *20* (2), 152–158.
- (55) Viveiros, M.; Pieroni, M. Spectinamides: A Challenge, a Proof, and a Suggestion. *Trends Microbiol.* **2014**, *22* (4), 170–171.
- (56) Makarov, V.; Manina, G.; Mikusova, K.; Möllmann, U.; Ryabova, O.; Saint-Joanis, B.; Dhar, N.; Pasca, M. R.; Buroni, S.; Lucarelli, A. P.; Milano, A.; De Rossi, E.; Belanova, M.; Bobovska, A.; Dianiskova, P.; Kordulakova, J.; Sala, C.; Fullam, E.; Schneider, P.; McKinney, J. D.; Brodin, P.; Christophe, T.; Waddell, S.; Butcher, P.; Albrethsen, J.; Rosenkrands, I.; Brosch, R.; Nandi, V.; Bharath, S.; Gaonkar, S.; Shandil, R. K.; Balasubramanian, V.; Balganesh, T.; Tyagi, S.; Grosset, J. J.

- Riccardi, G.; Cole, S. T. Benzothiazinones Kill Mycobacterium Tuberculosis by Blocking Arabinan Synthesis. *Science* **2009**, *324* (5928), 801–804.
- (57) Tiwari, R.; Möllmann, U.; Cho, S.; Franzblau, S. G.; Miller, P. A.; Miller, M. J. Design and Syntheses of Anti-Tuberculosis Agents Inspired by BTZ043 Using a Scaffold Simplification Strategy. *ACS Med. Chem. Lett.* **2014**, *5* (5), 587–591.
- (58) Makarov, V.; Lechartier, B.; Zhang, M.; Neres, J.; van der Sar, A. M.; Raadsen, S. A.; Hartkoorn, R. C.; Ryabova, O. B.; Vocat, A.; Decosterd, L. A.; Widmer, N.; Buclin, T.; Bitter, W.; Andries, K.; Pojer, F.; Dyson, P. J.; Cole, S. T. Towards a New Combination Therapy for Tuberculosis with next Generation Benzothiazinones. *EMBO Mol. Med.* **2014**, *6* (3), 372–383.
- (59) Onajole, O. K.; Pieroni, M.; Tipparaju, S. K.; Lun, S.; Stec, J.; Chen, G.; Gunosewoyo, H.; Guo, H.; Ammerman, N. C.; Bishai, W. R.; Kozikowski, A. P. Preliminary Structure-Activity Relationships and Biological Evaluation of Novel Antitubercular Indolecarboxamide Derivatives against Drug-Susceptible and Drug-Resistant Mycobacterium Tuberculosis Strains. *J. Med. Chem.* **2013**, *56* (10), 4093–4103.
- (60) Rao, S. P. S.; Lakshminarayana, S. B.; Kondreddi, R. R.; Herve, M.; Camacho, L. R.; Bifani, P.; Kalapala, S. K.; Jiricek, J.; Ma, N. L.; Tan, B. H.; Ng, S. H.; Nanjundappa, M.; Ravindran, S.; Seah, P. G.; Thayalan, P.; Lim, S. H.; Lee, B. H.; Goh, A.; Barnes, W. S.; Chen, Z.; Gagaring, K.; Chatterjee, A. K.; Pethe, K.; Kuhen, K.; Walker, J.; Feng, G.; Babu, S.; Zhang, L.; Blasco, F.; Beer, D.; Weaver, M.; Dartois, V.; Glynne, R.; Dick, T.; Smith, P. W.; Diagana, T. T.; Manjunatha, U. H. Indolcarboxamide Is

- a Preclinical Candidate for Treating Multidrug-Resistant Tuberculosis. *Sci. Transl. Med.* **2013**, *5* (214), 214ra168.
- (61) Manjunatha, U. H.; Boshoff, H.; Dowd, C. S.; Zhang, L.; Albert, T. J.; Norton, J. E.; Daniels, L.; Dick, T.; Pang, S. S.; Barry, C. E. Identification of a Nitroimidazo-Oxazine-Specific Protein Involved in PA-824 Resistance in Mycobacterium Tuberculosis. *Proc. Natl. Acad. Sci. U. S. A.* **2006**, *103* (2), 431–436.
- (62) Andries, K.; Verhasselt, P.; Guillemont, J.; Göhlmann, H. W. H.; Neefs, J.-M.; Winkler, H.; Van Gestel, J.; Timmerman, P.; Zhu, M.; Lee, E.; Williams, P.; de Chaffoy, D.; Huitric, E.; Hoffner, S.; Cambau, E.; Truffot-Pernot, C.; Lounis, N.; Jarlier, V. A Diarylquinoline Drug Active on the ATP Synthase of Mycobacterium Tuberculosis. *Science* **2005**, *307* (5707), 223–227.
- (63) Lorenzo, D.; Mousa, S. A. Mechanisms of Drug Resistance in Mycobacterium Tuberculosis and Current Status of Rapid Molecular Diagnostic Testing. *Acta Trop.* **2011**, *119* (1), 5–10.
- (64) Spratt, B. G. Resistance to Antibiotics Mediated by Target Alterations. *Science* **1994**, *264* (5157), 388–393.
- (65) Wright, G. D. Bacterial Resistance to Antibiotics: Enzymatic Degradation and Modification. *Adv. Drug Deliv. Rev.* **2005**, *57* (10), 1451–1470.
- (66) Donadio, S.; Staver, M. J.; McAlpine, J. B.; Swanson, S. J.; Katz, L. Modular Organization of Genes Required for Complex Polyketide Biosynthesis. *Science* **1991**, *252* (5006), 675–679.
- (67) Viveiros, M.; Martins, M.; Rodrigues, L.; Machado, D.; Couto, I.; Ainsa, J.; Amaral, L. Inhibitors of Mycobacterial Efflux Pumps as Potential

- Boosters for Anti-Tubercular Drugs. *Expert Rev. Anti Infect. Ther.* **2012**, *10* (9), 983–998.
- (68) Piddock, L. J. V. Clinically Relevant Chromosomally Encoded Multidrug Resistance Efflux Pumps in Bacteria. *Clin. Microbiol. Rev.* **2006**, *19* (2), 382–402.
- (69) Machado, D.; Couto, I.; Perdigão, J.; Rodrigues, L.; Portugal, I.; Baptista, P.; Veigas, B.; Amaral, L.; Viveiros, M. Contribution of Efflux to the Emergence of Isoniazid and Multidrug Resistance in Mycobacterium Tuberculosis. *PLoS One* **2012**, *7* (4), e34538.
- (70) Maggi, N.; Pasqualucci, C. R.; Ballotta, R.; Sensi, P. Rifampicin: A New Orally Active Rifamycin. *Chemotherapy* **1966**, *11* (5), 285–292.
- (71) Lenaerts, A. J.; Gruppo, V.; Marietta, K. S.; Johnson, C. M.; Driscoll, D. K.; Tompkins, N. M.; Rose, J. D.; Reynolds, R. C.; Orme, I. M. Preclinical Testing of the Nitroimidazopyran PA-824 for Activity against Mycobacterium Tuberculosis in a Series of in Vitro and in Vivo Models. *Antimicrob. Agents Chemother.* **2005**, *49* (6), 2294–2301.
- (72) Pieroni, M.; Wan, B.; Cho, S.; Franzblau, S. G.; Costantino, G. Design, Synthesis and Investigation on the Structure-Activity Relationships of N-Substituted 2-Aminothiazole Derivatives as Antitubercular Agents. *Eur. J. Med. Chem.* **2014**, *72*, 26–34.
- (73) Roy, K. K.; Singh, S.; Sharma, S. K.; Srivastava, R.; Chaturvedi, V.; Saxena, A. K. Synthesis and Biological Evaluation of Substituted 4-Arylthiazol-2-Amino Derivatives as Potent Growth Inhibitors of Replicating Mycobacterium Tuberculosis H<sub>37</sub>Rv. *Bioorg. Med. Chem. Lett.* **2011**, *21* (18), 5589–5593.

- (74) Zuliani, V.; Rivara, M.; Fantini, M.; Costantino, G. Sodium Channel Blockers for Neuropathic Pain. *Expert Opin. Ther. Pat.* **2010**, *20* (6), 755–779.
- (75) Rivara, M.; Baheti, A. R.; Fantini, M.; Cocconcelli, G.; Ghiron, C.; Kalmar, C. L.; Singh, N.; Merrick, E. C.; Patel, M. K.; Zuliani, V. 2,4(5)-Diarylimidazoles: Synthesis and Biological Evaluation of a New Class of Sodium Channel Blockers against hNa(v)1.2. *Bioorg. Med. Chem. Lett.* **2008**, *18* (20), 5460–5462.
- (76) Kawai, M.; Sakurada, I.; Morita, A.; Iwamuro, Y.; Ando, K.; Omura, H.; Sakakibara, S.; Masuda, T.; Koike, H.; Honma, T.; Hattori, K.; Takashima, T.; Mizuno, K.; Mizutani, M.; Kawamura, M. Structure-Activity Relationship Study of Novel NR2B-Selective Antagonists with Arylamides to Avoid Reactive Metabolites Formation. *Bioorg. Med. Chem. Lett.* **2007**, *17* (20), 5537–5542.
- (77) Lilienkamp, A.; Pieroni, M.; Franzblau, S. G.; Bishai, W. R.; Kozikowski, A. P. Derivatives of 3-Isoxazolecarboxylic Acid Esters: A Potent and Selective Compound Class against Replicating and Nonreplicating Mycobacterium Tuberculosis. *Curr. Top. Med. Chem.* **2012**, *12* (7), 729–734.
- (78) Lilienkamp, A.; Pieroni, M.; Wan, B.; Wang, Y.; Franzblau, S. G.; Kozikowski, A. P. Rational Design of 5-Phenyl-3-Isoxazolecarboxylic Acid Ethyl Esters as Growth Inhibitors of Mycobacterium Tuberculosis. a Potent and Selective Series for Further Drug Development. *J. Med. Chem.* **2010**, *53* (2), 678–688.
- (79) Mao, J.; Yuan, H.; Wang, Y.; Wan, B.; Pieroni, M.; Huang, Q.; van Breemen, R. B.; Kozikowski, A. P.; Franzblau, S. G. From Serendipity to

- Rational Antituberculosis Drug Discovery of Mefloquine-Isoxazole Carboxylic Acid Esters. *J. Med. Chem.* **2009**, *52* (22), 6966–6978.
- (80) Pieroni, M.; Lilienkamp, A.; Wan, B.; Wang, Y.; Franzblau, S. G.; Kozikowski, A. P. Synthesis, Biological Evaluation, and Structure-Activity Relationships for 5-[(E)-2-Arylethenyl]-3-Isoxazolecarboxylic Acid Alkyl Ester Derivatives as Valuable Antitubercular Chemotypes. *J. Med. Chem.* **2009**, *52* (20), 6287–6296.
- (81) Chiarino, D.; Grancini, G.; Frigeni, V.; Biasini, I.; Carezzi, A. N-(4-Isoxazolylthiazol-2-yl)oxamic Acid Derivatives as Potent Orally Active Antianaphylactic Agents. *J. Med. Chem.* **1991**, *34* (2), 600–605.
- (82) Gong, C.-J.; Gao, A.-H.; Zhang, Y.-M.; Su, M.-B.; Chen, F.; Sheng, L.; Zhou, Y.-B.; Li, J.-Y.; Li, J.; Nan, F.-J. Design, Synthesis and Biological Evaluation of Bisthiazole-Based Trifluoromethyl Ketone Derivatives as Potent HDAC Inhibitors with Improved Cellular Efficacy. *Eur. J. Med. Chem.* **2016**, *112*, 81–90.
- (83) Fairhurst, R. A.; Imbach-Weese, P.; Gerspacher, M.; Caravatti, G.; Furet, P.; Zoller, T.; Fritsch, C.; Haasen, D.; Trappe, J.; Guthy, D. A.; Arz, D.; Wirth, J. Identification and Optimisation of a 4',5-Bisthiazole Series of Selective Phosphatidylinositol-3 Kinase Alpha Inhibitors. *Bioorg. Med. Chem. Lett.* **2015**, *25* (17), 3569–3574.
- (84) Álvarez, G.; Martínez, J.; Varela, J.; Birriel, E.; Cruces, E.; Gabay, M.; Leal, S. M.; Escobar, P.; Aguirre-López, B.; Cabrera, N.; Tuena de Gómez-Puyou, M.; Gómez Puyou, A.; Pérez-Montfort, R.; Yaluff, G.; Torres, S.; Serna, E.; Vera de Bilbao, N.; González, M.; Cerecetto, H. Development of Bis-Thiazoles as Inhibitors of Triosephosphate Isomerase from *Trypanosoma Cruzi*. Identification of New Non-

- Mutagenic Agents That Are Active in Vivo. *Eur. J. Med. Chem.* **2015**, *100*, 246–256.
- (85) Chen, F.; Chai, H.; Su, M.-B.; Zhang, Y.-M.; Li, J.; Xie, X.; Nan, F.-J. Potent and Orally Efficacious Bisthiazole-Based Histone Deacetylase Inhibitors. *ACS Med. Chem. Lett.* **2014**, *5* (6), 628–633.
- (86) Dadiboyena, S.; Xu, J.; Hamme, A. T. Isoxazoles from 1,1-Disubstituted Bromoalkenes. *Tetrahedron Lett.* **2007**, *48* (7), 1295–1298.
- (87) Leivers, M.; Miller, J. F.; Chan, S. A.; Lauchli, R.; Liehr, S.; Mo, W.; Ton, T.; Turner, E. M.; Youngman, M.; Falls, J. G.; Long, S.; Mathis, A.; Walker, J. Imidazopyridazine Hepatitis C Virus Polymerase Inhibitors. Structure–Activity Relationship Studies and the Discovery of a Novel, Traceless Prodrug Mechanism. *J. Med. Chem.* **2014**, *57* (5), 1964–1975.
- (88) Lemerrier, B. C.; Pierce, J. G. Synthesis of Thiohydroxamic Acids and Thiohydroxamic Acid Derivatives. *J. Org. Chem.* **2014**, *79* (5), 2321–2330.
- (89) Oh, L. M.; Wang, H.; Shilcrat, S. C.; Herrmann, R. E.; Patience, D. B.; Spoons, P. G.; Sisko, J. Development of a Scalable Synthesis of GSK183390A, a PPAR  $\alpha/\gamma$  Agonist. *Org. Process Res. Dev.* **2007**, *11* (6), 1032–1042.
- (90) Donald, M. B.; Rodriguez, K. X.; Shay, H.; Phuan, P.-W.; Verkman, A. S.; Kurth, M. J. Click-Based Synthesis of Triazolobithiazole  $\Delta$ F508-CFTR Correctors for Cystic Fibrosis. *Bioorg. Med. Chem.* **2012**, *20* (17), 5247–5253.
- (91) Pieroni, M.; Annunziato, G.; Azzali, E.; Dessanti, P.; Mercurio, C.; Meroni, G.; Trifiró, P.; Vianello, P.; Villa, M.; Beato, C.; Varasi, M.; Costantino, G. Further Insights into the SAR of  $\alpha$ -Substituted

- Cyclopropylamine Derivatives as Inhibitors of Histone Demethylase KDM1A. *Eur. J. Med. Chem.* **2015**, *92*, 377–386.
- (92) Wang, C.; Zhao, Q.; Vargas, M.; Jones, J. O.; White, K. L.; Shackelford, D. M.; Chen, G.; Saunders, J.; Ng, A. C. F.; Chiu, F. C. K.; Dong, Y.; Charman, S. A.; Keiser, J.; Vennerstrom, J. L. Revisiting the SAR of the Antischistosomal Aryl Hydantoin (Ro 13-3978). *J. Med. Chem.* **2016**.
- (93) PCT/IB2005/003085
- (94) Xiang, J.; Ipek, M.; Suri, V.; Masefski, W.; Pan, N.; Ge, Y.; Tam, M.; Xing, Y.; Tobin, J. F.; Xu, X.; Tam, S. Synthesis and Biological Evaluation of Sulfonamidooxazoles and Beta-Keto Sulfones: Selective Inhibitors of 11beta-Hydroxysteroid Dehydrogenase Type I. *Bioorg. Med. Chem. Lett.* **2005**, *15* (11), 2865–2869.
- (95) Gokhale, M.;, Wagal, O.; Kanitkar, A.; Synthesis of Di and Trisubstituted Oxazoles in Nonionic Liquid Under Catalyst Free Conditions; *Int. J. of Pharm Phytopharmacol. Res.*; **2012**; 1(4); 156-160.
- (96) Venkat Narsaiah, A.; Ghogare, R.; and Biradar, D.; Glycerin as alternative solvent for the synthesis of Thiazoles; *Org. Commun.*; **2011**; 4(3); 75-81.
- (97) PCT/US2004/015239
- (98) Guram, A. S.; Buchwald, S. L. Palladium-Catalyzed Aromatic Aminations with in Situ Generated Aminostannanes. *J. Am. Chem. Soc.* **1994**, *116* (17), 7901–7902.
- (99) Paul, F.; Patt, J.; Hartwig, J. F. Palladium-Catalyzed Formation of Carbon-Nitrogen Bonds. Reaction Intermediates and Catalyst



- Improvements in the Hetero Cross-Coupling of Aryl Halides and Tin Amides. *J. Am. Chem. Soc.* **1994**, *116* (13), 5969–5970.
- (100)McGowan, M. A.; Henderson, J. L.; Buchwald, S. L. Palladium-Catalyzed N-Arylation of 2-Aminothiazoles. *Org. Lett.* **2012**, *14* (6), 1432–1435.
- (101)Coelho, T.; Machado, D.; Couto, I.; Maschmann, R.; Ramos, D.; von Groll, A.; Rossetti, M. L.; Silva, P. A.; Viveiros, M. Enhancement of Antibiotic Activity by Efflux Inhibitors against Multidrug Resistant Mycobacterium Tuberculosis Clinical Isolates from Brazil. *Front. Microbiol.* **2015**, *6*, 330.
- (102)Adams, K. N.; Takaki, K.; Connolly, L. E.; Wiedenhoft, H.; Winglee, K.; Humbert, O.; Edelstein, P. H.; Cosma, C. L.; Ramakrishnan, L. Drug Tolerance in Replicating Mycobacteria Mediated by a Macrophage-Induced Efflux Mechanism. *Cell* **2011**, *145* (1), 39–53.
- (103)Adams, K. N.; Szumowski, J. D.; Ramakrishnan, L. Verapamil, and Its Metabolite Norverapamil, Inhibit Macrophage-Induced, Bacterial Efflux Pump-Mediated Tolerance to Multiple Anti-Tubercular Drugs. *J. Infect. Dis.* **2014**, *210* (3), 456–466.
- (104)Rodrigues, L.; Wagner, D.; Viveiros, M.; Sampaio, D.; Couto, I.; Vavra, M.; Kern, W. V.; Amaral, L. Thioridazine and Chlorpromazine Inhibition of Ethidium Bromide Efflux in Mycobacterium Avium and Mycobacterium Smegmatis. *J. Antimicrob. Chemother.* **2008**, *61* (5), 1076–1082.
- (105)Martins, M.; Viveiros, M.; Kristiansen, J. E.; Molnar, J.; Amaral, L. The Curative Activity of Thioridazine on Mice Infected with Mycobacterium Tuberculosis. *Vivo Athens Greece* **2007**, *21* (5), 771–775.

- (106) Abbate, E.; Vescovo, M.; Natiello, M.; Cufre, M.; Garcia, A.; Gonzalez Montaner, P.; Ambroggi, M.; Ritacco, V.; van Soolingen, D. Successful Alternative Treatment of Extensively Drug-Resistant Tuberculosis in Argentina with a Combination of Linezolid, Moxifloxacin and Thioridazine. *J. Antimicrob. Chemother.* **2012**, *67* (2), 473–477.
- (107) Amaral, L.; Martins, M.; Viveiros, M. Enhanced Killing of Intracellular Multidrug-Resistant Mycobacterium Tuberculosis by Compounds That Affect the Activity of Efflux Pumps. *J. Antimicrob. Chemother.* **2007**, *59* (6), 1237–1246.
- (108) Amaral, L.; Viveiros, M. Why Thioridazine in Combination with Antibiotics Cures Extensively Drug-Resistant Mycobacterium Tuberculosis Infections. *Int. J. Antimicrob. Agents* **2012**, *39* (5), 376–380.
- (109) Martins, M.; Viveiros, M.; Couto, I.; Amaral, L. Targeting Human Macrophages for Enhanced Killing of Intracellular XDR-TB and MDR-TB. *Int. J. Tuberc. Lung Dis. Off. J. Int. Union Tuberc. Lung Dis.* **2009**, *13* (5), 569–573.
- (110) Kigundu, E. M.; Njoroge, M.; Singh, K.; Njuguna, N.; Warner, D. F.; Chibale, K. Synthesis and Synergistic Antimycobacterial Screening of Chlorpromazine and Its Metabolites. *MedChemComm* **2014**, *5* (4), 502.
- (111) Singh, M.; Jadaun, G. P. S.; Ramdas, null; Srivastava, K.; Chauhan, V.; Mishra, R.; Gupta, K.; Nair, S.; Chauhan, D. S.; Sharma, V. D.; Venkatesan, K.; Katoch, V. M. Effect of Efflux Pump Inhibitors on Drug Susceptibility of Ofloxacin Resistant Mycobacterium Tuberculosis Isolates. *Indian J. Med. Res.* **2011**, *133*, 535–540.

- (112) Martins, M.; Schelz, Z.; Martins, A.; Molnar, J.; Hajös, G.; Riedl, Z.; Viveiros, M.; Yalcin, I.; Aki-Sener, E.; Amaral, L. In Vitro and Ex Vivo Activity of Thioridazine Derivatives against Mycobacterium Tuberculosis. *Int. J. Antimicrob. Agents* **2007**, *29* (3), 338–340.
- (113) Kumar, M.; Singh, K.; Naran, K.; Hamzabegovic, F.; Hoft, D. F.; Warner, D. F.; Ruminski, P.; Abate, G.; Chibale, K. Design, Synthesis, and Evaluation of Novel Hybrid Efflux Pump Inhibitors for Use against Mycobacterium Tuberculosis. *ACS Infect. Dis.* **2016**, *2* (10), 714–725.
- (114) Aftab, D. T.; Ballas, L. M.; Loomis, C. R.; Hait, W. N. Structure-Activity Relationships of Phenothiazines and Related Drugs for Inhibition of Protein Kinase C. *Mol. Pharmacol.* **1991**, *40* (5), 798–805.
- (115) Salie, S.; Hsu, N.-J.; Semenyá, D.; Jardine, A.; Jacobs, M. Novel Non-Neuroleptic Phenothiazines Inhibit Mycobacterium Tuberculosis Replication. *J. Antimicrob. Chemother.* **2014**, *69* (6), 1551–1558.
- (116) Takács, D.; Cerca, P.; Martins, A.; Riedl, Z.; Hajós, G.; Molnár, J.; Viveiros, M.; Couto, I.; Amaral, L. Evaluation of Forty New Phenothiazine Derivatives for Activity against Intrinsic Efflux Pump Systems of Reference Escherichia Coli, Salmonella Enteritidis, Enterococcus Faecalis and Staphylococcus Aureus Strains. *Vivo Athens Greece* **2011**, *25* (5), 719–724.
- (117) Gupta, S.; Tyagi, S.; Almeida, D. V.; Maiga, M. C.; Ammerman, N. C.; Bishai, W. R. Acceleration of Tuberculosis Treatment by Adjunctive Therapy with Verapamil as an Efflux Inhibitor. *Am. J. Respir. Crit. Care Med.* **2013**, *188* (5), 600–607.

- (118)Gupta, S.; Tyagi, S.; Bishai, W. R. Verapamil Increases the Bactericidal Activity of Bedaquiline against Mycobacterium Tuberculosis in a Mouse Model. *Antimicrob. Agents Chemother.* **2015**, *59* (1), 673–676.
- (119)Kumar, H. M. S.; Reddy, B. V. S.; Anjaneyulu, S.; Yadav, J. S. A Novel and Efficient Approach to Mono-N-Alkyl Anilines via Addition of Grignard Reagents to Aryl Azides. *Tetrahedron Lett.* **1999**, *40* (47), 8305–8306.
- (120)Verbeek, J.; Syvänen, S.; Schuit, R. C.; Eriksson, J.; de Lange, E. C.; Windhorst, A. D.; Luurtsema, G.; Lammertsma, A. A. Synthesis and Preclinical Evaluation of [11C]D617, a Metabolite of (R)-[11C]verapamil. *Nucl. Med. Biol.* **2012**, *39* (4), 530–539.
- (121)Cheng, K.; Kim, I. J.; Lee, M.-J.; Adah, S. A.; Raymond, T. J.; Bilsky, E. J.; Aceto, M. D.; May, E. L.; Harris, L. S.; Coop, A.; Dersch, C. M.; Rothman, R. B.; Jacobson, A. E.; Rice, K. C. Opioid Ligands with Mixed Properties from Substituted Enantiomeric N-Phenethyl-5-Phenylmorphans. Synthesis of a Micro-Agonist Delta-Antagonist and Delta-Inverse Agonists. *Org. Biomol. Chem.* **2007**, *5* (8), 1177–1190.
- (122)Bogdal, D.; Matras, K.; Sanetra, J.; Pokladko, M. Synthesis of Polymethacrylates with Carbazole and Benzofuran Pendant Groups for Photovoltaic Applications. *Macromol. Symp.* **2008**, *268* (1), 48–52.
- (123)Ramón-García, S.; Ng, C.; Anderson, H.; Chao, J. D.; Zheng, X.; Pfeifer, T.; Av-Gay, Y.; Roberge, M.; Thompson, C. J. Synergistic Drug Combinations for Tuberculosis Therapy Identified by a Novel High-Throughput Screen. *Antimicrob. Agents Chemother.* **2011**, *55* (8), 3861–3869.

- (124)Viveiros, M.; Rodrigues, L.; Martins, M.; Couto, I.; Spengler, G.; Martins, A.; Amaral, L. Evaluation of Efflux Activity of Bacteria by a Semi-Automated Fluorometric System. *Methods Mol. Biol. Clifton NJ* **2010**, *642*, 159–172.
- (125)Machado, D.; Couto, I.; Perdigão, J.; Rodrigues, L.; Portugal, I.; Baptista, P.; Veigas, B.; Amaral, L.; Viveiros, M. Contribution of Efflux to the Emergence of Isoniazid and Multidrug Resistance in Mycobacterium Tuberculosis. *PLoS One* **2012**, *7* (4), e34538.
- (126)Rodrigues, L.; Ramos, J.; Couto, I.; Amaral, L.; Viveiros, M. Ethidium Bromide Transport across Mycobacterium Smegmatis Cell-Wall: Correlation with Antibiotic Resistance. *BMC Microbiol.* **2011**, *11* (1), 35.
- (127)da Silva, P. E. A.; Von Groll, A.; Martin, A.; Palomino, J. C. Efflux as a Mechanism for Drug Resistance in Mycobacterium Tuberculosis. *FEMS Immunol. Med. Microbiol.* **2011**, *63* (1), 1–9.
- (128)Costa, S. S.; Lopes, E.; Azzali, E.; Machado, D.; Coelho, T.; da Silva, P. E. A.; Viveiros, M.; Pieroni, M.; Couto, I. An Experimental Model for the Rapid Screening of Compounds with Potential Use Against Mycobacteria. *Assay Drug Dev. Technol.* **2016**, *14* (9), 524–534.
- (129)Efflux-Mediated Antimicrobial Resistance in Bacteria Mechanisms, Regulation and Clinical Implications.; Adis, 2016.
- (130)De Clercq, E. Antiviral Drugs in Current Clinical Use. *J. Clin. Virol. Off. Publ. Pan Am. Soc. Clin. Virol.* **2004**, *30* (2), 115–133.
- (131)Wagner, C. R.; Iyer, V. V.; McIntee, E. J. Pronucleotides: Toward the in Vivo Delivery of Antiviral and Anticancer Nucleotides. *Med. Res. Rev.* **2000**, *20* (6), 417–451.

- (132)De Clercq, E.; Neyts, J. Antiviral Agents Acting as DNA or RNA Chain Terminators. *Handb. Exp. Pharmacol.* **2009**, No. 189, 53–84.
- (133)Faletto, M. B.; Miller, W. H.; Garvey, E. P.; St Clair, M. H.; Daluge, S. M.; Good, S. S. Unique Intracellular Activation of the Potent Anti-Human Immunodeficiency Virus Agent 1592U89. *Antimicrob. Agents Chemother.* **1997**, *41* (5), 1099–1107.
- (134)Rashidi, M. R.; Smith, J. A.; Clarke, S. E.; Beedham, C. In Vitro Oxidation of Famciclovir and 6-Deoxypenciclovir by Aldehyde Oxidase from Human, Guinea Pig, Rabbit, and Rat Liver. *Drug Metab. Dispos. Biol. Fate Chem.* **1997**, *25* (7), 805–813.
- (135)Furman, P. A.; Fyfe, J. A.; St Clair, M. H.; Weinhold, K.; Rideout, J. L.; Freeman, G. A.; Lehrman, S. N.; Bolognesi, D. P.; Broder, S.; Mitsuya, H. Phosphorylation of 3'-azido-3'-deoxythymidine and Selective Interaction of the 5'-triphosphate with Human Immunodeficiency Virus Reverse Transcriptase. *Proc. Natl. Acad. Sci. U. S. A.* **1986**, *83* (21), 8333–8337.
- (136)Serpi, M.; Madela, K.; Pertusati, F.; Slusarczyk, M. Synthesis of Phosphoramidate Prodrugs: ProTide Approach. *Curr. Protoc. Nucleic Acid Chem.* **2013**, *Chapter 15*, Unit15.5.
- (137)Hecker, S. J.; Erion, M. D. Prodrugs of Phosphates and Phosphonates. *J. Med. Chem.* **2008**, *51* (8), 2328–2345.
- (138)Mehellou, Y.; Balzarini, J.; McGuigan, C. Aryloxy Phosphoramidate Triesters: A Technology for Delivering Monophosphorylated Nucleosides and Sugars into Cells. *ChemMedChem* **2009**, *4* (11), 1779–1791.

- (139)Devine, K. G.; McGuigan, C.; O'Connor, T. J.; Nicholls, S. R.; Kinchington, D. Novel Phosphate Derivatives of Zidovudine as Anti-HIV Compounds. *AIDS Lond. Engl.* **1990**, *4* (4), 371–373.
- (140)Mehellou, Y. The ProTides Boom. *ChemMedChem* **2016**, *11* (11), 1114–1116.
- (141)Balzarini, J.; Karlsson, A.; Aquaro, S.; Perno, C. F.; Cahard, D.; Naesens, L.; De Clercq, E.; McGuigan, C. Mechanism of Anti-HIV Action of Masked Alaninyl d4T-MP Derivatives. *Proc. Natl. Acad. Sci. U. S. A.* **1996**, *93* (14), 7295–7299.
- (142)McGuigan, C.; Sutton, P. W.; Cahard, D.; Turner, K.; O'Leary, G.; Wang, Y.; Gumbleton, M.; De Clercq, E.; Balzarini, J. Synthesis, Anti-Human Immunodeficiency Virus Activity and Esterase Lability of Some Novel Carboxylic Ester-Modified Phosphoramidate Derivatives of Stavudine (d4T). *Antivir. Chem. Chemother.* **1998**, *9* (6), 473–479.
- (143)Birkus, G.; Wang, R.; Liu, X.; Kutty, N.; MacArthur, H.; Cihlar, T.; Gibbs, C.; Swaminathan, S.; Lee, W.; McDermott, M. Cathepsin A Is the Major Hydrolase Catalyzing the Intracellular Hydrolysis of the Antiretroviral Nucleotide Phosphonoamidate Prodrugs GS-7340 and GS-9131. *Antimicrob. Agents Chemother.* **2007**, *51* (2), 543–550.
- (144)Pradere, U.; Garnier-Amblard, E. C.; Coats, S. J.; Amblard, F.; Schinazi, R. F. Synthesis of Nucleoside Phosphate and Phosphonate Prodrugs. *Chem. Rev.* **2014**, *114* (18), 9154–9218.
- (145)van Boom, J. H.; Burgers, P. M. J.; Crea, R.; Luyten, W. C. M. M.; Vink, A. B. J.; Reese, C. B. Phosphorylation of Nucleoside Derivatives with Aryl Phosphoramidochloridates. *Tetrahedron* **1975**, *31* (23), 2953–2959.

- (146)McGuigan, C.; Madela, K.; Aljarah, M.; Gilles, A.; Battina, S. K.; Ramamurty, C. V. S.; Srinivas Rao, C.; Vernachio, J.; Hutchins, J.; Hall, A.; Kolykhalov, A.; Henson, G.; Chamberlain, S. Dual pro-Drugs of 2'-C-Methyl Guanosine Monophosphate as Potent and Selective Inhibitors of Hepatitis C Virus. *Bioorg. Med. Chem. Lett.* **2011**, *21* (19), 6007–6012.
- (147)McGuigan, C.; Hassan-Abdallah, A.; Srinivasan, S.; Wang, Y.; Siddiqui, A.; Daluge, S. M.; Gudmundsson, K. S.; Zhou, H.; McLean, E. W.; Peckham, J. P.; Burnette, T. C.; Marr, H.; Hazen, R.; Condreay, L. D.; Johnson, L.; Balzarini, J. Application of Phosphoramidate ProTide Technology Significantly Improves Antiviral Potency of Carbocyclic Adenosine Derivatives. *J. Med. Chem.* **2006**, *49* (24), 7215–7226.
- (148)McGuigan, C.; Perrone, P.; Madela, K.; Neyts, J. The Phosphoramidate ProTide Approach Greatly Enhances the Activity of Beta-2'-C-Methylguanosine against Hepatitis C Virus. *Bioorg. Med. Chem. Lett.* **2009**, *19* (15), 4316–4320.
- (149)Gavan, T. L.; Town, M. A. A Microdilution Method for Antibiotic Susceptibility Testing: An Evaluation. *Am. J. Clin. Pathol.* **1970**, *53* (6), 880–885.
- (150)Woods, G. L.; Clinical and Laboratory Standards Institute. *Susceptibility Testing of Mycobacteria, Nocardiae and Other Aerobic Actinomycetes: Approved Standard*; 2011.
- (151)Louw, G. E.; Warren, R. M.; Gey van Pittius, N. C.; McEvoy, C. R. E.; Van Helden, P. D.; Victor, T. C. A Balancing Act: Efflux/Influx in Mycobacterial Drug Resistance. *Antimicrob. Agents Chemother.* **2009**, *53* (8), 3181–3189.



(152)Pieroni, M., Machado, D., Azzali, E., Santos Costa, S., Couto, I., Costantino, G., Viveiros, M. Rational Design and Synthesis of Thioridazine Analogues as Enhancers of the Antituberculosis Therapy *J. Med. Chem.* 2015, 58 (15), 5842-5853.